

Investigating the ‘osmorepiratory compromise’ during  
hypoxia in freshwater fish

**The 'osmorepiratory compromise' during hypoxia in  
freshwater fish**

By:

FATHIMA I. IFTIKAR, B.Sc.

A Thesis

Submitted to the School of Graduate Studies

in Partial Fulfillment of the Requirements

for the Degree

Master of Science

McMaster University

© Copyright by Fathima I. Iftikar, September 2009.

MASTER OF SCIENCE (2008)

McMaster University

(Biology)

Hamilton, Ontario

TITLE: The 'osmorepiratory compromise' during hypoxia in  
freshwater fish

AUTHOR: Fathima I. Iftikar, B. Sc. (McMaster University)

SUPERVISOR: Professor C. M. Wood

NUMBER OF PAGES: xxii, 201

## Abstract

To understand the ‘osmorepiratory compromise’ (the trade-off in gill function between ion and respiratory gas exchange) during hypoxia in freshwater fish, a species-specific approach was utilized where general ionoregulatory responses to hypoxia were compared in rainbow trout (*Oncorhynchus mykiss*, a hypoxia-intolerant freshwater fish), and in two hypoxia-tolerant species (the goldfish *Carassius auratus* and the Amazonian oscar *Astronotus ocellatus*). In the latter two species, the dual stress situation of hypoxia plus feeding was also explored. Measurements included unidirectional and net  $\text{Na}^+$  flux rates, ammonia excretion rates, net  $\text{K}^+$  loss rates, branchial  $\text{Na}^+/\text{K}^+$ -ATPase and  $\text{H}^+$ -ATPase activities, and branchial morphology by scanning electron microscopy (trout and oscar only). In trout, environmental hypoxia induced complex changes in gill ionoregulatory function, where the direction and magnitude varied with both the extent and duration of the hypoxia regime. The changes in ion-regulation observed in trout in response to hypoxia indicated that the osmorepiratory compromise in this hypoxia-intolerant species was different and more complex compared to its manifestation in oscar and goldfish. This could be attributed to the adaptive physiology of the trout to oxygen-rich environments and its intolerance to low environmental oxygen availability. In both of the hypoxia-tolerant species (oscar and goldfish), there was a general reduction in gill permeability in response to severe hypoxia regardless of feeding regime, rather different from the complex patterns seen in the hypoxia-intolerant trout. However, the effects of feeding on this phenomenon differed between these species. Fed goldfish had elevated

branchial fluxes that were effectively turned down during hypoxia compared to baseline flux rates maintained by starved goldfish. In contrast, fed oscars had lower fluxes compared to starved fish. Although both fed and starved fish suppressed their branchial fluxes with severe hypoxia, fed oscars delayed the turning down of fluxes. Overall, our results indicate that feeding exerts opposite effects on gill ionoregulatory function in these two hypoxia-tolerant species, and thereby differentially modulates the responses to hypoxia. These differences may relate to differences in water chemistry. Furthermore, the manifestation of the osmorepiratory compromise during hypoxia appears to be rather different from the phenomenon during exercise.

### **Acknowledgements:**

Finally, I'm done! First and foremost I would like to sincerely thank my supervisor Dr. Chris Wood for his continuous guidance and tireless effort throughout this project. He had the utmost patience and understanding in editing, revising and in most cases interpreting this thesis. Chris was a fabulous mentor and more importantly taught me a valuable lesson: the importance of having a passion for what you do and enjoying your work. I started at the Wood lab being generally afraid of fish; and I leave it now with complete confidence in fish handling, the ability to work and think independently and excellent socializing skills. A big thank you to my committee members; Drs. Colin Nurse and Mike O' Donnell, for their constant support, patience and always keeping their door open for any help right throughout my thesis.

Data in this thesis was produced with collaborations. Specially, Dr. Gudrun De Boeck for letting me work with her on her project in Manaus, Brazil. I would also like to thank Dr. Katherine Sloman, Dr. Vera F. Almeida-Val, Dr. Adalberto Val and Graham Scott for their support during my work in Manaus, Brazil. A significant (albeit beautiful) part of this thesis is due to Dr. Victoria Matey at SDU, her brilliant microscopy skills and interpretation provided me with SEM scans of gills under time constraints.

I would not be doing my thesis if not for my introduction to research by Monika Patel – my undergrad mentor. A big thank you to the past and present Wood lab members – your support is much appreciated. Specially, Linda Diao, for your calm and smile through all the assays you've helped me with. Dr. Richard Smith, Michele Nawata and

Sunita Nadella have provided constant advice and guidance throughout my project. John Fitzpatrick and Carol Bucking were inspiring housemates and lab mates who taught me to work hard and play even harder.

I would also like to thank team GBM – Dr. Grant McClelland, Paul Craig, Marie-Pierre Schippers and Jacqueline Beaudry for support outside the lab, especially with teaching. My work and life during grad school was made memorable due to Andrea Morash. A sincere thank you for having the patience to edit my thesis, always making sure I was well fed and for constantly being there as a good friend and co-worker. My gratitude also extends to Indi and Priya Dhanoa, Freddie Chain for always lending an ear when I needed to talk and Naveed Hussain for your constant banter that kept me awake throughout those long experiments over the distance. My siblings, Ijaz and Shabna always made sure that I was grounded and did not let me get too ahead of myself.

A sincere thank you to Muiz, for his patience, understanding, humour and unending love across the miles throughout the latter part of this project. You were my dose of calm whenever I needed it. Finally, to my parents, Iftikhar and Shahnaz. You are my pillars of strength. Thank you for believing in me and encouraging me to follow and fulfil my dreams. It was your love and life-changing decision to move countries that provided me this opportunity where I now do what I enjoy.

Fathima I. Iftikar

## Thesis Format

This thesis is organized into four Chapters. Chapter one provides background information and a general overview of the rationale for this research. The second and third chapters describe the experimental work and have been written as manuscripts for submission to scientific journals. The fourth chapter describes the findings of this study and the conclusions of this work. Literature cited follows chapter two and three respectively and general references from chapter one and four follow chapter four.

### Chapter 1: General Introduction

### Chapter 2:

Title: The Osmorespiratory Compromise during Hypoxia in the Freshwater Rainbow Trout *Oncorhynchus mykiss*.

Authors: F. I. Iftikar, V. Matey and C. M. Wood.

Comments: Whole animal and cellular experiments performed by F. I. I. under the supervision of C. M. W. Scanning electron micrographs and analysis by V. M. This paper has been submitted to *Physiol. Biochem. Zool.*

### Chapter 3:

Title: Investigating the effects of feeding on the osmorespiratory compromise during severe hypoxia in two hypoxia-tolerant freshwater species .

Authors: F. I. Iftikar, V. Matey, G. DeBoeck, G. Scott, K. Sloman, A. L. Val,

V. Almeida-Val, and C. M. Wood.

Comments: Whole animal and cellular experiments on goldfish performed by F. I.

I. under the supervision of C. M. W. Whole animal and cellular

experiments on oscar performed by G. D. and C. M. W. with F. I. I.

analyzed samples. Scanning electron micrographs and analysis by V.

M. This paper will be submitted in the near future.

#### Chapter 4: General Conclusions

## Table of Contents

Abstract	iv
Acknowledgements	vi
Thesis Format	viii
Table of Contents	x
List of Tables	xiii
List of Figures	xiv
Chapter 1: General Introduction.	
A Background on ion-regulation in freshwater fish	1
The importance of oxygen to fish	2
The osmorepiratory compromise at the freshwater gill epithelium	6
Objectives of the Present Study	9
Chapter 2: The osmorepiratory compromise during hypoxia in the freshwater rainbow trout <i>Oncorhynchus mykiss</i> .	
Abstract	13
Introduction	15
Materials and Methods	21
Animals	21
Exposure Regimes	21
Analytical methods for fluxes and flux calculations	27
Gill ATPase activity	31
Morphological Analyses	33

Statistical Analyses	34
Results	35
Discussion	42
Acknowledgements	53
Literature Cited	54
Tables	67
Figures	69
Chapter 2: Investigating the effects of feeding on the osmorepiratory compromise during severe hypoxia in two hypoxa-tolerant freshwater species.	
Abstract	95
Introduction	97
Materials and Methods	103
Animals	103
Exposure Regimes (goldfish)	104
Exposure Regimes (oscar)	107
Analytical methods for fluxes and flux calculations	110
Gill ATPase activity	112
Analysis of dietary ions	115
Morphological analyses for oscar gills	116
Statistical Analyses	117
Results:	118
For goldfish	118

For oscar	121
Discussion	127
Literature Cited	142
Tables	154
Figures	162
Chapter 4: General summary and conclusions	185
The osmorepiratory compromise during hypoxia	185
The effects of feeding on the compromise	186
The impact of hypoxia at the gill ionocytes	187
Hypoxia-induced changes in gill morphology	189
Ammonia excretion during hypoxia	191
Conclusion	192
Literature Cited	194

List of Tables:

**Table 2.1.** Group net flux rates of  $K^+$  and ammonia (n = 8-10 fish per group) to the water by juvenile rainbow trout acutely exposed to various levels of hypoxia for 4 h in experiment 1.

**Table 3.1.** Group net flux rates of  $K^+$  and ammonia (n = 10 fish per group) to the water by goldfish acutely exposed to various levels of hypoxia for 4 h in experiment 1.

**Table 3.2.** Ion levels found in goldfish food (mM/kg) and estimated dietary uptake rates based on a 2% daily ration.

**Table 3.3.** Ion levels found in oscar food (mM/kg) and estimated dietary uptake rates based on a 1% daily ration.

**Table 3.4.** Density and apical surface area of the mitochondria-rich cells in fed and starved oscar gills in during normoxia and severe hypoxia (10-20 mmHg).

### List of Figures:

**Figure 2.1:** Mean  $\text{Na}^+$  uptake ( $J^{\text{Na}}_{\text{influx}}$ ) in separate groups of juvenile rainbow trout subjected to increasing severity of hypoxia (4 h) in experiment 1. Values are expressed as means  $\pm$  SEM. Means sharing the same letter are not significantly different from one another at  $P \geq 0.05$ .

**Figure 2.2:** Mean  $\text{Na}^+$  flux rates of adult rainbow trout (N=6) to a progressive induction of hypoxia (down to  $\sim 110$  mmHg) for 4 h followed by an acute restoration of normoxia in experiment 2;  $\text{Na}^+$  unidirectional influx ( $J^{\text{Na}}_{\text{influx}}$ , upward bars),  $\text{Na}^+$  efflux ( $J^{\text{Na}}_{\text{efflux}}$ , downward bars),  $\text{Na}^+$  net flux rates ( $J^{\text{Na}}_{\text{net}}$  striped bars) and water  $\text{O}_2$  tension (black line). Values are expressed as means  $\pm$  SEM. Means values of  $J^{\text{Na}}_{\text{influx}}$  sharing the same letter are not significantly different from one another at  $P \geq 0.05$ . There are no significant differences among time periods in mean values of  $J^{\text{Na}}_{\text{efflux}}$  and  $J^{\text{Na}}_{\text{net}}$  respectively.

**Figure 2.3:** Mean ammonia excretion rates of rainbow trout (N=6) subjected to a progressive induction of hypoxia (down to  $\sim 110$  mmHg) for 4 h followed by an acute restoration of normoxia; water  $\text{O}_2$  tension (black line) in experiment 3. Values are expressed as means  $\pm$  SEM. There are no significant differences present at  $P \leq 0.05$ .

**Figure 2.4:** Mean  $\text{Na}^+$  flux rates of rainbow trout (N=8) subjected to an acute induction of hypoxia ( $\sim 80$  mmHg) prolonged for 8 h subsequent to a 3-h normoxic control period in experiment 3;  $\text{Na}^+$  unidirectional influx ( $J^{\text{Na}}_{\text{influx}}$ , upward bars),  $\text{Na}^+$  efflux ( $J^{\text{Na}}_{\text{efflux}}$ , downward bars),  $\text{Na}^+$  net flux rates ( $J^{\text{Na}}_{\text{net}}$  striped bars) and water  $\text{O}_2$  tension (black line). Values are expressed as means  $\pm$  SEM. Means sharing the same letter are not significantly different from one another at  $P \geq 0.05$ .

**Figure 2.5:** Mean ammonia excretion rates of rainbow trout (N=8) subjected to acute induction of hypoxia (~80 mmHg) prolonged for 8 h subsequent to a 3-h normoxic control period in experiment 3; water O<sub>2</sub> tension (black line). Values are expressed as means ± SEM. There are no significant differences present at  $P \leq 0.05$ .

**Figure 2.6:** Mean potassium (K<sup>+</sup>) net flux rates of rainbow trout (N=8) subjected to an acute induction of hypoxia (~80 mmHg) prolonged for 8 h subsequent to a normoxic 3 h control period in experiment 3; water O<sub>2</sub> tension (black line). Values are expressed as means ± SEM. The asterisks denote a significant difference between overall mean values of control and hypoxic exposures ( $P \leq 0.05$ ).

**Figure 2.7:** Diffusive water exchange rates (k) of rainbow trout (N=8) to acute induction of hypoxia (~80 mmHg) for 4 h followed by an acute restoration of normoxia in experiment 4. Values are expressed as means ± SEM. Means sharing the same letter of the same case are not significantly different from one another at  $P \geq 0.05$ .

**Figure 2.8:** Gill Na<sup>+</sup>/K<sup>+</sup>-ATPase and H<sup>+</sup>-ATPase activity changes in adult rainbow trout (N=8 per sampling time) in response to acute induction of hypoxia (~80 mmHg) for 4 h followed by normoxic recovery in experiment 5. Values are expressed as means ± SEM. Means sharing the same letter of the same case are not significantly different from one another at  $P \geq 0.05$ .

**Figure 2.9:** Trailing edge of gill filament of adult rainbow trout from experiment 5. Normoxia (control), SEM.

- A. Filament epithelium below respiratory lamellae. Note clusters of mitochondria-rich cells, MRCs, (asterisks) and solitary MRCs bearing long microvilli (whitehead arrows).
  - B. Interlamellar region of filament epithelium. Clusters of 3-5 MRCs with apical surfaces ornamented with short microvilli (asterisks). Note MRCs with long microvilli located below interlamellar regions (whitehead arrows).
  - C. Cluster of four MRCs with slightly convex apical surfaces bearing long and straight microvilli.
  - D. Clusters of two MRCs with short microvilli. Note presence of small concave apical crypts
- L- lamella; PVC- pavement cell. Scale bars: A, B- 10 $\mu$ m; C, D- 5 $\mu$ m.

**Figure 2.10:** Surface structure of filament epithelium of the gills of adult rainbow trout exposed to 1 h hypoxia in experiment 5. Trailing edge of filament, SEM

- A. Huge clusters of MRCs in the interlamellar regions (asterisks), 2-cell clusters of MRCs below this area (asterisks). Large solitary MRCs with convex apical surfaces with knob-like or completely reduced microvilli (blackhead arrows) and MRCs with “carpet-like” appearance due to highly interdigitated microvilli (white arrow)
- B. MRCs indicated by blackhead arrow
- C. Two MRCs indicated by white arrow

MC- mucous cell. Scale bars: A- 10  $\mu$ m; B, C- 5  $\mu$ m.

**Figure 2.11:** Surface structure of filament epithelium of the gills of adult rainbow trout exposed to 4h hypoxia in experiment 5. Trailing edge of filament, SEM

- A, B. Lesser number of MRCs, no cell clusters. Solitary MRCs in the interlamellar area and below have either convex surfaces with knob-like microvilli (blackhead arrow) or flat carpet-like appearance (white arrows).

Huge globs of mucus produced by MCs (B). Scale bars: A, B – 10  $\mu\text{m}$ .

**Figure 2.12:** Surface structure of filament epithelium of the gills of adult rainbow trout exposed to hypoxia and a 6h recovery period in normoxic water in experiment 5. Trailing edge of filament, SEM:

- A. Clusters of MRCs with extended microvilli (whitehead arrows). Solitary MRCs with convex surfaces and knob-like microvilli (blackhead arrows). Note presence of mucous cells.
- B. Cluster of 3 MRCs. Note knob-like microvilli in middle and lower cells and longer microvilli in upper cell.
- C. MRCs with carpet-like apical surface.

Scale bars: A- 10  $\mu\text{m}$ ; B, C- 5 $\mu\text{m}$ .

**Figure 2.13:** Quantitative morphometric analysis of changes in mitochondria rich cells (MRCs) of the gill filament epithelium in adult rainbow trout (N=8 per sampling time) of experiment 5 in response to acute induction of hypoxia (~80 mmHg) for 4 h followed by normoxic recovery in experiment 4. (A) MRC density in the filament epithelium, (B) Surface area of apical crypts ( $\mu\text{m}^2$ ) and (C) Surface area occupied by MRC/ $\text{mm}^2$  in the filament epithelium, %. Values are expressed as means  $\pm$  SEM. Means sharing the same letter are not significantly different from one another at  $P \geq 0.05$ .

**Figure 3.1:** Mean  $\text{Na}^+$  uptake rates ( $J_{\text{influx}}^{\text{Na}}$ ) in separate groups of goldfish (n=10) subjected to different levels of hypoxia for 4 h in experiment 1. Values are expressed as means  $\pm$  SEM. Means sharing the same letter are not significantly different from one another at  $P \geq 0.05$ .

**Figure 3.2:** Mean  $\text{Na}^+$  flux rates of goldfish (N=10 for fed and starved groups) in normoxia or when subjected to an acute induction of either moderate

hypoxia (~100 mmHg) or severe hypoxia (~40 mmHg) for 4 h in experiment 2;  $\text{Na}^+$  unidirectional influx ( $J_{\text{influx}}^{\text{Na}}$ , upward bars, clear bars; starved fish, gray bars; fed fish),  $\text{Na}^+$  efflux ( $J_{\text{efflux}}^{\text{Na}}$ , downward bars, clear bars; starved fish, gray bars; fed fish), and  $\text{Na}^+$  net flux rates ( $J_{\text{net}}^{\text{Na}}$ , black bars; starved fish, striped bars; fed fish). Values are expressed as means  $\pm$  SEM. Means sharing the same letter are not significantly different from one another at  $P \geq 0.05$ . The plus sign denotes a significant difference between  $\text{Na}^+$  influx/efflux/netflux values for fed and starved fish in a given  $\text{PO}_2$  exposure at  $P \leq 0.05$ .

**Figure 3.3:** Mean ammonia excretion rates of goldfish (N=10) in normoxia or when subjected to an acute induction of either moderate hypoxia (~100 mmHg) or severe hypoxia (~40 mmHg) for 4 h in experiment 2; Starved fish, clear bars; Fed fish, gray bars. Values are expressed as means  $\pm$  SEM. Means sharing the same letter are not significantly different from one another at  $P \geq 0.05$ . The plus sign denotes a significant difference between ammonia excretion values for fed and starved fish in a given  $\text{PO}_2$  exposure at  $P \leq 0.05$ .

**Figure 3.4:** Mean potassium ( $\text{K}^+$ ) net flux rates of goldfish (N=10) in normoxia or when subjected to an acute induction of either moderate hypoxia (~100 mmHg) or severe hypoxia (~40 mmHg) for 4 h in experiment 2; Starved fish, clear bars; Fed fish, gray bars. Values are expressed as means  $\pm$  SEM. Means sharing the same letter are not significantly different from one another at  $P \geq 0.05$ . The plus sign denotes a significant difference between ammonia excretion values for fed and starved fish in a given  $\text{PO}_2$  exposure at  $P \leq 0.05$ .

**Figure 3.5:** Gill  $\text{Na}^+/\text{K}^+$ -ATPase and  $\text{H}^+$ -ATPase activity changes in goldfish (N=6 per sampling time) in response to acute induction of hypoxia (~40 mmHg) for either 1 h or 4 h followed by normoxic recovery for either 1 h or 3 h in

experiment 3. Values are expressed as means  $\pm$  SEM. Means sharing the same letter of the same case are not significantly different from one another at  $P \geq 0.05$ .

**Figure 3.6:** Mean  $\text{Na}^+$  flux rates of Amazonian oscar (N=10) subjected to an acute induction of hypoxia (~10-20 mmHg) prolonged for 4 h subsequent to a 3-h normoxic control period in experiment 1 for oscar;  $\text{Na}^+$  unidirectional influx ( $J_{\text{influx}}^{\text{Na}}$ , upward bars, clear bars; starved fish, gray bars; fed fish),  $\text{Na}^+$  efflux ( $J_{\text{efflux}}^{\text{Na}}$ , downward bars, clear bars; starved fish, gray bars; fed fish), and  $\text{Na}^+$  net flux rates ( $J_{\text{net}}^{\text{Na}}$ , black bars; starved fish, striped bars; fed fish). Values are expressed as means  $\pm$  SEM. Means sharing the same letter are not significantly different from one another and the plus sign denote a significant difference between overall mean values of fed and starved treatments at  $P \leq 0.05$ .

**Figure 3.7:** Mean ammonia excretion rates of Amazonian oscar (N=10) subjected to acute induction of hypoxia (~10-20 mmHg) prolonged for 4 h subsequent to a 3-h normoxic control period in experiment 1 for oscar; Starved fish, clear bars; Fed fish, gray bars. Values are expressed as means  $\pm$  SEM. Means sharing the same letter are not significantly different from one another and the plus sign denote a significant difference between overall mean values of fed and starved treatments under normoxia at  $P \leq 0.05$ .

**Figure 3.8:** Mean potassium ( $\text{K}^+$ ) net flux rates of Amazonian oscar (N=10) subjected to acute induction of hypoxia (~10-20 mmHg) prolonged for 4 h subsequent to a 3-h normoxic control period in experiment 1 for oscar; Starved fish, clear bars; Fed fish, gray bars. Values are expressed as means  $\pm$  SEM. Means sharing the same letter are not significantly different from one another and the plus sign denote a significant difference between overall mean values of

fed and starved treatments at  $P \leq 0.05$ .

**Figure 3.9:** Gill  $\text{Na}^+/\text{K}^+$ -ATPase and  $\text{H}^+$ -ATPase activity changes in fed and starved oscar (N=6 per sampling time) in response to normoxia and acute induction of severe hypoxia (~10-20 mmHg) for 3h in experiment 2 for oscar. Values are expressed as means  $\pm$  SEM. Means sharing the same letter of the same case are not significantly different from one another at  $P \geq 0.05$ .

**Figure 3.10:** Scanning electron micrographs of oscar gills exposed to normoxic conditions.

- A. Fed fish: Low resolution of the gill filament and lamellae. Note numerous crypts of mitochondria-rich cells in the filament epithelium and lamellar epithelium.
  - B. Fed fish. Higher resolution of lamellae displays a large population of mitochondria rich cells with huge apical crypts (arrows) distributed along lamellae and few mucous cells.
  - C. Starved fish (10 d of starvation). Low resolution of the filament and lamellae. Filament epithelium shows few apical crypts of mitochondria-rich cells (arrows) that remain abundant in the lamellae surface.
  - D. Starved fish (10 d of starvation). Higher resolution of lamellae shows small apical crypts of mitochondria-rich cells on the surface of lamellar epithelium.
- MC-mucous cell. Scale bars: A, C- 50  $\mu\text{m}$ ; B, D- 30  $\mu\text{m}$ .

**Figure 3.11:** Scanning electron micrographs of filament epithelium in fed oscars (A-D) and starved oscars (E-F) exposed to normoxic conditions, control.

- A. Fed fish. Trailing edge of filament. Large pavement cells, mucous cells releasing huge globs of secretion and mitochondria-rich cells (arrows) with large apical crypts present in filament epithelium surface.

- B- C. Fed fish. Large roughly circular and flat apical crypts of MRCs with a fence-like surface structure composing of interdigitated and fused microplicae.
- D. Cluster of MRCs, common in the interlamellar areas of filament epithelium.
- E. Starved fish. Trailing edge of filament. Note alterations in the PVCs surface pattern, small crypts of MRCs and few MCs.
- F. Starved fish. Slightly concave apical crypt of the MRC. Note its irregular shape, smaller size compare to C-D, and more simple arrangement of "fence"-like surface structure.
- PVC- pavement cells. Scale bars: A, E- 10  $\mu\text{m}$ ; B-D,F- 2  $\mu\text{m}$ .

**Figure 3.12 :** Scanning electron micrographs of oscar gills exposed to 3h hypoxia.

- A. Fed fish. Low resolution of filament and lamellae. Note small apical crypts of MRCs in filament epithelium surface and no visible MRCs in the lamellar epithelium.
- B. Starved fish. Trailing edge of filament. Low resolution of filament and lamellae. Few small MRC apical crypts in filament epithelium, mostly at the lamellae base. No MRCs found on the surface of lamellar epithelium.
- C-D. High magnification of filament epithelium in fed and starved fish, respectively. Note characteristic topology of PVCs and shape and size of apical crypts of MRCs.
- E-F. Fed fish. Highly concave MRC apical crypt masked by mucus. Note reduction of MRC surface area compare to control.
- G. Starved fish. Deeply invaginated apical crypt of MRC. Note irregular

shape of the crypt and dramatic reduction of its surface compare to control.

Scale bars: A, B- 25  $\mu\text{m}$ ; C, D- 10  $\mu\text{m}$ ; E- G- 2  $\mu\text{m}$ .

## CHAPTER 1

### GENERAL INTRODUCTION

#### **I. A background on ion-regulation in freshwater fish**

Almost half of the vertebrate species are fishes (Ali, 1980). The majority of species of fish live either in freshwater or the oceans. Interestingly, freshwater covers only about 1% of the earth's surface but has about 6,850 species of fish while saltwater covers about 70% of the globe and has only about 11,650 species (Ali, 1980). Since Canada has the largest amount of freshwater per capita in the world, there is a great importance placed on studying and understanding the physiology of aquatic vertebrates that live in these systems. Freshwater fish differ greatly from their saltwater counterparts in terms of their inherent physiology, fine-scale morphology and ecology. Additionally, the varying concentrations of salts in freshwater systems across the world further create entirely different adaptations in the freshwater fish living in these systems.

Osmoregulation refers to the control of water and salt levels in the blood. It is a homeostatic mechanism employed by all species to sustain life. Osmoregulation for fish is very important due to the diverse environments in which they live, and primarily occurs at the gill (Isaia, 1984). One of the first theories about osmoregulatory function of fish was suggested by the physiologist Homer W. Smith in the early 1930s. Smith (1932) theorized that in fresh water, organisms osmoregulate by *hypotonic excretion* as the salt content of their body is superior to their surroundings and there is a tendency for water to be taken into the body and salt to be lost. So he proposed that in order to prevent 'dilution' of the internal composition, freshwater fish should excrete from their body a

dilute solution, possibly via urine (Smith, 1932). Smith (1932) was correct in his theory about the homeostatic mechanisms taking place for freshwater vertebrates to live in their environment. However, what is currently realized is the importance of the gill as the main osmoregulatory organ in freshwater teleosts in maintaining homeostatic balance compared to the kidney that was initially proposed by Smith (1932).

Freshwater fish are *hyper-osmoregulators* where their plasma is regulated at an osmotic concentration higher than their dilute environment (Evans et al., 2005). These animals face constant diffusive ion loss and osmotic water gain across the large surface area of their gill epithelium, and to counteract this they actively uptake ions from the water and excrete dilute urine. [Ions are also taken up from the diet (Smith et al., 1989), although this pathway is often overlooked by osmoregulatory physiologists.] Consequently, the freshwater gill epithelium is an example of a multifunctional structure that is involved in complex osmoregulatory and excretory roles, in addition to its well-known functions in respiration and acid-base balance.

## **II. The importance of oxygen to fish:**

### **a. Oxygen in the aquatic environment.**

Water as a respiratory medium poses severe constraints on the vertebrates living in it compared to air as a respiratory medium. This is due to the inherent properties of water, in combination with the variation in the availability of oxygen content in the aquatic environment. In a given volume of water at a particular  $PO_2$ , there is only about 1/30th of the amount of oxygen as contained in the same volume of air. Furthermore, the

rate of oxygen diffusion in water is 10,000 times slower than the rate in air (Dejours, 1975). Water is also much denser, more viscous, and has higher heat capacity and conductivity than air. In addition to these physical properties that make water a challenging respiratory medium, freshwater aquatic habitats tend to have large gradients in oxygen availability determined by environmental factors such as temperature, high acidity and the respiration of other organisms. Even minute levels of oxygen consumption by biological or nonbiological processes can swiftly reduce the amount of oxygen available to vertebrates that live in the aquatic environment. Therefore, the chances of freshwater fish encountering episodic hypoxia or low environmental oxygen, are very high in these systems (Nikinmaa and Rees, 2005).

b. Oxygen uptake in freshwater fish.

The gills are the primary respiratory organ in freshwater teleost fish, where allometric scaling and habitat effects on gill surface area lead to a host of adaptations according to environmental conditions (Graham, 2006). The movement of oxygen across the gill epithelium is driven by diffusion according to the Fick principle and is based on the partial pressure ( $PO_2$ ) gradient across lamellae, the permeation coefficient for oxygen, lamellar surface area and the distance between the water and capillary beds of the gill epithelium (Graham, 2006).

Under hypoxia, several physiological systems respond to maintain oxygen transport in freshwater fish. Increased ventilation during hypoxia maintains delivery of oxygen to the gills by an increase in breathing rate and the depth of each breath (Holeton and Randall 1967 b). Gill diffusion capacity also increases due to re-organization of

blood flow in both the respiratory and systemic circulations in fish during hypoxia. An increased vascular resistance in the gills is associated with a shunting of blood through an alternate pathway which decreases the diffusion distance between the blood and water and increases the gill surface area for oxygen uptake (Holeton and Randall, 1967a; Isaia, 1984; Sundin and Nilsson, 1997). Furthermore, fish facing hypoxia can increase the functional respiratory surface area of their gill by increasing their blood pressure to open up more of the lamellar vasculature (lamellar recruitment) by constricting the efferent (outgoing) side of the gill vasculature and/or by dilating afferent (incoming) lamellar arterioles (Booth, 1979; Soivio and Tuurala, 1981). Additionally, hypoxia leads to an increased haemoglobin affinity to oxygen in fish blood by a variety of mechanisms. Exposure to hypoxia leads to an increase in the erythrocytic volume due to an increase in the intraerythrocytic pH leading to an increased blood oxygen affinity (Wood and Johansen, 1973 *b*; Nikinmaa and Soivio, 1982). The hypoxic shift in the blood dissociation curve leftward and steeper, increases oxygen loading at the gills and amplifies oxygen saturation of the blood with only small oxygen tension changes at the gills (Nikinmaa and Soivio, 1982). In addition to alterations in cardiovascular and respiratory function during hypoxia, fish also secrete catecholamines (epinephrine and/or norepinephrine) and corticosteroids (e.g. cortisol) into the blood (Perry and Reid, 1992; Reid and Perry, 2003). These stress hormones play significant roles in minimizing the decrease in blood oxygen content during exposure to hypoxia. These multiple physiological mechanisms serve to optimize gas transfer across the gills, better enabling freshwater teleosts to extract oxygen from the water to maintain blood oxygen content

and provide adequate oxygen delivery to metabolically active tissues under hypoxic conditions.

c. Cellular impacts of hypoxia at the gill.

At the cellular level, the primary cause of hypoxia-induced death in mammals is the loss of ionic integrity of the cell membrane (Boutilier, 2001). In contrast to mammals, water-breathing animals encounter environmental hypoxia regularly, so maintaining ionic integrity across the gills is of utmost importance to freshwater fish. Maintenance of a homeostatic intracellular environment requires the redistribution of ions through ATP-dependent pumping systems such as the  $\text{Na}^+/\text{K}^+$ -ATPase and  $\text{H}^+$ -ATPase, which can consume 20–80% of the cell's resting metabolic rate (Boutilier, 2001). A hypoxic cell has reduced oxygen delivery for the oxidative metabolism needed to supply the energy needs of the cell. So severe oxygen deprivation is indicated by a) a rapid depletion of cellular ATP and b) a loss of intracellular  $\text{K}^+$  as the  $\text{Na}^+/\text{K}^+$  pump begins to fail (Boutilier and St-Pierre, 2000). Hypoxic cell death occurs when ATP production fails to meet the energetic maintenance demands of ionic and osmotic equilibrium (Boutilier, 2001). Several theories have been suggested of mechanisms to prevent hypoxic cell death, of which the most well-known is the “channel arrest” hypothesis (Hochachka, 1986; Boutilier, 2001). The closure of ion channels leads to a general suppression in  $\text{Na}^+$  and  $\text{K}^+$  leak (passive effluxes), reducing the need for ATPase pump activity to maintain ionic gradients across cell membranes. Therefore the cells of hypoxia-tolerant animals are able to reduce their metabolic rate and thereby reduce cellular ATP demand at times of severe oxygen lack. The overall result is that cell permeability is reduced and therefore the energetic costs of

maintaining ionic integrity across cell membranes is reduced (Hochachka, 1986; Boutilier, 2001).

### **III. The osmorepiratory compromise at the freshwater gill epithelium**

#### **a. Background.**

During hypoxia there would appear to be a basic conflict between the requirements for gas exchange and the demands of ion regulation in the gills of freshwater fish (Randall et al., 1972). Changes at the gill that may take place to increase gas transfer could also affect ion exchange across the gills. When gill membranes are effectively “thicker” (i.e. reduced in functional surface area and/or increased in blood-to-water diffusion distance), they limit diffusive ion movement and reduce the cost of ion regulation. However, the accompanying reduction in permeability to ions and water may compromise respiratory gas exchange. This phenomenon has also been termed the “osmorepiratory compromise” (Nilsson, 1986; Gonzalez and McDonald 1992, 1994).

At resting conditions when oxygen demand is low, teleost fish solve this compromise by using only a fraction of their total gill surface area therefore minimizing the area available for diffusive ion loss (Gonzalez and McDonald, 1992). Furthermore, by only partially perfusing secondary lamellae during normoxia (Booth, 1978) and shunting the blood flow in the perfused lamellae through non-exchange pathways, they are able to further minimize diffusive ion loss (Farrell et al., 1980). The ‘osmorepiratory compromise’ has been studied extensively under severe exercise in freshwater fish

(Randall et al. 1972; Wood et al., 1973a,b,c; Gonzalez and McDonald 1992, 1994) to better understand ion loss versus gas exchange at the gill epithelium.

b. The osmorepiratory compromise during aerobic exercise

Exercise demands increased oxygen consumption and therefore the functional surface area of the gill epithelium is elevated to meet these demands (Booth, 1979). Consequently this results in an elevated diffusive efflux of  $\text{Na}^+$  (Randall et al., 1972; Wood and Randall, 1973a, b) and osmotic gain of water (Wood and Randall, 1973c). During exercise,  $\text{Na}^+$  loss across the gills increased with an increase in oxygen consumption where the increase in  $\text{Na}^+$  loss was usually greater than the increase in oxygen consumption due to factors that control their respective diffusion gradients (Gonzalez and McDonald, 1992). Oxygen diffusion across gills relies on many factors which were described previously. With exercise, an increase in oxygen consumption mainly results from an increase in the functional surface area and the  $\text{PO}_2$  gradient; however a reduction in diffusion distance through lamellar thinning may also contribute to this increase (Gonzalez and McDonald, 1992). The functional surface area is thought to increase via lamellar recruitment where closed lamellae are opened and opened lamellae are increasingly perfused (Nilsson, 1986). Since simple diffusion of  $\text{Na}^+$  across the membrane is a function of the same factors that affect oxygen uptake, an increase in the functional surface area for oxygen diffusion should also increase diffusive  $\text{Na}^+$  loss. Catecholamines mobilized into the blood during exercise are thought to play an important role in this phenomenon. (Gonzalez and McDonald, 1992). Catecholamines progressively

increase intralamellar pressure thereby dilating the lamellae and increasing functional surface area leading to diffusive ion loss. Therefore, to prevent detrimental ion loss during the upper limits of aerobic exercise, freshwater fish exhibit an osmorepiratory compromise at the gill epithelium where the ion/gas ratio (ion loss per unit oxygen diffusion) is increased acutely with exercise but returned to routine levels with continued exercise (Gonzalez and McDonald, 1992).

c. The osmorepiratory compromise during hypoxia.

Until recently there has been little investigation of how the osmorepiratory compromise functions during hypoxia. In one previous study, net branchial  $\text{Na}^+$  and  $\text{Cl}^-$  fluxes under hypoxia were measured in the hypoxia-intolerant rainbow trout (Thomas et al., 1986), but this study focused mainly on acid-base balance changes with deep but short (20 min) hypoxia. A slight stimulation of ionic losses was shown, but results were confounded due to faecal contamination of the water (Thomas et al., 1986). Close to two decades later, a recent study of the osmorepiratory compromise in a very hypoxia-tolerant species, the Amazonian Oscar, *Astronotus ocellatus*, has revived attention in this area (Wood et al., 2007). Contrary to the osmorepiratory compromise observed during exercise in other species (Wood and Randall 1973a,b; Gonzalez and McDonald, 1992, 1994), the oscar exhibited a quick albeit profound reduction of both unidirectional  $\text{Na}^+$  uptake and unidirectional  $\text{Na}^+$  efflux during acute severe hypoxia, so that net  $\text{Na}^+$  flux was not altered, suggesting that a general reduction in both gill permeability and active transport occurred. This would appear to be an adaptive strategy, because in the Amazon,

individuals often cannot escape hypoxic conditions in their natural environment (Muusze et al., 1998; Almeida-Val et al., 2000).

#### **IV. Objectives of the Present Study:**

The primary goal of this thesis was to understand the effects of hypoxia on unidirectional and net  $\text{Na}^+$  fluxes, as well as other indices of gill transport and permeability functions, in the hypoxia-intolerant rainbow trout (Chapter 2) and in two hypoxia-tolerant species, the previously studied Amazonian oscar *Astronotus ocellatus* and the common goldfish *Carassius auratus* (Chapter 3). Due to inherent inter-species divergence in responding to hypoxia, we expected ion fluxes during hypoxia to be regulated differently in trout versus goldfish and oscar. Since ionoregulation in response to hypoxia has been examined in the oscar (Wood et al., 2007), we predicted that the hypoxia-tolerant goldfish would also exhibit similar depressions in ion fluxes however to a lesser extent due to differences in water chemistry of the environments between these species. The ionoregulatory patterns of the rainbow trout were expected to be relatively different from both oscar and goldfish due to its inherent intolerance to hypoxia.

In general, we wanted to understand how unidirectional  $\text{Na}^+$  influx ( $J_{\text{influx}}^{\text{Na}}$ ) and unidirectional  $\text{Na}^+$  efflux ( $J_{\text{efflux}}^{\text{Na}}$ ) rates changed in response to acute hypoxia (4-h), prolonged hypoxia (8-h) and also if fluxes were restored back to control conditions after hypoxia (normoxic recovery). This was carried out by adding radiolabelled  $^{22}\text{Na}$  to the external water and examining its disappearance into the fish over time. Together with measurements of changes in net  $\text{Na}^+$  concentrations in the external water, this allowed calculation of rates of  $J_{\text{influx}}^{\text{Na}}$ ,  $J_{\text{efflux}}^{\text{Na}}$ , and  $J_{\text{net}}^{\text{Na}}$ . We further measured branchial  $\text{Na}^+/\text{K}^+$

ATPase, H<sup>+</sup> ATPase activity, whole animal rates of K<sup>+</sup> loss, and gill morphology through scanning electron microscopy to better understand the cellular and structural mechanisms underlying hypoxic effects on ionoregulation at the gills. Ammonia excretion was also measured to elucidate if hypoxia affected nitrogenous waste excretion.

In Chapter 3, an additional goal was to determine how dietary ion load affected unidirectional ion fluxes under severe hypoxia in the two hypoxia-tolerant species, the common goldfish and the Amazonian oscar. Although gills are considered to be the major site of active ionic uptake in freshwater fish, dietary ions may also make an important contribution to overall ion uptake, and therefore to osmoregulation (Smith et al., 1989). Therefore, our objectives were to understand if there were significant differences in  $J_{\text{influx}}^{\text{Na}}$ ,  $J_{\text{efflux}}^{\text{Na}}$ ,  $J_{\text{net}}^{\text{Na}}$ , ammonia excretion rates, branchial Na<sup>+</sup>/K<sup>+</sup> ATPase, H<sup>+</sup> ATPase activity and whole animal rates of K<sup>+</sup> loss between starved versus fed fish firstly during normoxia and then with severe hypoxic exposure. Finally, gill morphology in the oscar was examined using scanning electron microscopy to understand if structural changes of the gill epithelium occurred during hypoxia and if feeding affected this change.

Our results indicated that environmental hypoxia induces complex changes in gill ionoregulatory function in the rainbow trout, the direction and magnitude of which vary with both the extent and duration of the hypoxia regime. Therefore, we did not see a tightly regulated compromise between ion loss and gas exchange as observed for this species during exercise (Gonzalez and McDonald, 1992). We suggest that during hypoxia, a host of competing physiological factors may have complex influences on the osmorepiratory compromise. This difference in regulation was attributed to the adaption

of the physiology of trout to exercise performance, in contrast to its intolerance to low environmental oxygen availability.

In both goldfish and oscar, there were clear reductions in gill permeability in response to severe hypoxia regardless of feeding regime, rather different from the complex patterns seen in the hypoxia-intolerant trout. However, the effects of feeding on this phenomenon differed between these species. Fed goldfish had elevated unidirectional fluxes that were effectively turned down during hypoxia compared to baseline flux rates maintained by starved goldfish. In contrast, fed oscars exhibited lower fluxes compared to starved fish. Although both fed and starved fish suppressed their ion loss to the water with severe hypoxia, fed oscars delayed the turning down of fluxes. These differences due to feeding/starvation between oscars and goldfish may reflect differences in ion concentrations in the waters (ion-poor Amazonian water versus ion-rich hardwater) in which these species live.

Overall, this study has made significant contributions to the understanding of the physiological, biochemical, and structural responses of the gills with respect to ionoregulation and N-waste handling during exposure to low environmental oxygen conditions in freshwater fish. As such, it is one of the first to examine the working of the osmorepiratory compromise during hypoxia, and has shown that the compromise differs considerably from the phenomenon previously documented during exercise. Furthermore the nature of the trade-off differs according to the innate hypoxia tolerance or intolerance of the species, with important interactive effects of feeding/starvation. This study

therefore sets the stage for much further research in this important but relatively sparsely investigated area.

## CHAPTER 2

### **The Osmorespiratory Compromise during Hypoxia in the Freshwater Rainbow Trout *Oncorhynchus mykiss*.**

#### **Abstract:**

The trade-off between ion and gas exchange at the gills has been well-studied during exercise, but not during environmental hypoxia. We utilized a freshwater model teleost, *Oncorhynchus mykiss*, to examine the “osmorespiratory compromise” at the gills during hypoxia. Unidirectional flux measurements with  $^{22}\text{Na}^+$  showed that progressive mild hypoxia led first to a significant elevation in  $J_{\text{influx}}^{\text{Na}}$  but at 4 h hypoxia when  $\text{PO}_2$  reached  $\sim 110$  mmHg, there was a substantial 79% depression in  $J_{\text{influx}}^{\text{Na}}$ . Influx remained depressed during the first hour of normoxic recovery but was restored back to control rates thereafter. Changes in  $J_{\text{efflux}}^{\text{Na}}$  tended to mirror those in  $J_{\text{influx}}^{\text{Na}}$ , but overall there were no significant change. A more prolonged (8 h) and severe hypoxic ( $\sim 80$  mmHg) exposure induced a tri-phasic response whereby  $J_{\text{influx}}^{\text{Na}}$  was significantly elevated during the first hour, but returned to control rates during the subsequent three hours. Thereafter, rates started to gradually increase and remained significantly elevated for the last three h of hypoxia compared to control rates. A similar tri-phasic trend was observed with  $J_{\text{efflux}}^{\text{Na}}$  but with larger changes than in  $J_{\text{influx}}^{\text{Na}}$ . In both experiments, negative  $\text{Na}^+$  balance was observed during the hypoxic exposure in comparison to the near zero  $\text{Na}^+$  balance in the control normoxic period. Net  $\text{K}^+$  loss rates to the water approximately doubled in response to prolonged hypoxia (8 h). There were no significant alterations in

ammonia excretion rates. An initial significant depression in diffusive water flux was observed with 1 h of hypoxia however this was eliminated with 4 h of hypoxia and normoxic recovery when flux rates were restored back to control levels. Branchial  $\text{Na}^+/\text{K}^+$ -ATPase activity did not change with acute hypoxia (4-h at  $\text{PO}_2 \sim 80$  mmHg) and normoxic recovery. Patterns in branchial  $\text{H}^+$ -ATPase activity were similar but  $\text{H}^+$ -ATPase activity was significantly depressed by  $\sim 75\%$  after 6 h of normoxic restoration.

Examination of gill filament morphology by scanning electron microscopy revealed clusters of 3-5 mitochondria-rich cells (MRCs) with apical surfaces ornamented with short microvilli, and solitary MRCs bearing long microvilli under normoxia. With acute hypoxia ( $\text{PO}_2 \sim 80$  mmHg), exposed MRC numbers initially increased, individual MRC exposed surface area increased, and total MRC surface area tripled. MRC numbers had decreased below control levels by 4 h, but increased surface exposure persisted, albeit to a lesser extent, and no cell clusters were seen. Solitary MRCs exhibited either convex surfaces with knob-like microvilli or flat carpet-like appearance. Globes of mucus were produced by mucus cells. With normoxic recovery (up to 6h), MRC clusters re-appeared with extended microvilli, but solitary MRCs with convex surface and knob-like microvilli were also present, and increased MRC surface exposure persisted. Overall, our results indicate that environmental hypoxia induces complex changes in gill ionoregulatory function in this hypoxia intolerant species, the direction and magnitude of which vary with both the extent and duration of the hypoxia regime.

**Introduction:**

The natural properties of water, in combination with variable rates of oxygen consumption and production by aquatic biota, result in marked temporal and spatial heterogeneity in the oxygen content of the aquatic environment (Nikinmaa and Rees, 2005). Low environmental oxygen availability in water or hypoxia is now recognized as one of the most important environmental problems worldwide (Diaz et al., 2004). The increasing frequency of episodic or chronic hypoxia occurring in marine, estuarine, and freshwater habitats necessitates the study of how this environmental condition affects the physiology of fish that exist in this setting. Furthermore, variation in environmental oxygen availability in water has played an important role in the evolution of fishes, leading to a variety of anatomic, behavioural, and physiological strategies used by fishes to acquire oxygen and deliver it to tissues (Nikinmaa and Rees, 2005). To date, the impact of hypoxia on gill function, specifically, ionoregulation and nitrogenous (N) waste excretion, has received little attention and therefore has been the focus of this study.

Freshwater fish are exposed to markedly variable concentrations of ions in freshwater and are continuously faced with the problem of water influx and ion loss (McDonald and Rogano, 1986). The diffusive loss of ions from body fluids into the dilute external environment, and the osmotic gain of water in the opposite direction occur mainly at the gills because the skin is virtually impermeable. Additional ion loss also occurs via urine (McDonald and Rogano, 1986). During hypoxia there would appear to be a basic conflict between the requirements for gas exchange and the demands of ion

regulation in the gills of freshwater fish (Randall et al., 1972). A highly permeable gill membrane with large surface area is required for efficient gas transfer; however a small, impermeable epithelium is required to minimize diffusive ion losses. So an increase in surface area to promote oxygen consumption under hypoxia would be expected to accelerate a loss of ions to the surrounding water, while reductions of surface area to lower ion loss would be expected to reduce the ability of the gill to take up oxygen. This phenomenon has been termed the “osmorepiratory compromise” (Nilsson, 1986).

In previous studies, the “osmorepiratory compromise” has mainly been investigated with respect to exercise and swimming speed in a variety of freshwater fish (Wood and Randall, 1973a, b; Gonzalez and McDonald, 1992, 1994). With the increase in oxygen consumption during exercise, there is indeed a substantial  $\text{Na}^+$  loss due to an increase in the functional surface area of the freshwater fish gill. Furthermore, this loss of ions is not specific to the movement of just  $\text{Na}^+$ , but seems to apply generally to the movement of all permeable electrolytes across the functional surface area of the gill epithelium (Gonzalez and McDonald, 1992). In contrast, until recently there has been little investigation of how the osmorepiratory compromise functions during hypoxia. Net branchial  $\text{Na}^+$  and  $\text{Cl}^-$  fluxes under hypoxia have been measured in one previous study on the hypoxia-intolerant rainbow trout (Thomas et al., 1986), but this study focused mainly on the changes in acid-base balance with deep but short (20 min) hypoxia. A slight stimulation of ionic losses was reported, but results were confounded by faecal contamination of the water (Thomas et al., 1986).

However, a recent study of the osmorepiratory compromise in a very hypoxia-tolerant species, the Amazonian Oscar, *Astronotus ocellatus*, has rekindled interest in this area (Wood et al., 2007). Contrary to the manifestation of the osmorepiratory compromise during exercise in other species (Wood and Randall 1973a,b; Gonzalez and McDonald, 1992, 1994), the oscar exhibited a rapid and profound reduction of both unidirectional  $\text{Na}^+$  uptake and unidirectional  $\text{Na}^+$  efflux during acute severe hypoxia, so that net  $\text{Na}^+$  flux was not altered. Ammonia-N excretion was also reduced, while plasma ammonia levels increased, suggesting that a general reduction in gill permeability occurred. This would appear to be an adaptive strategy, because in the Amazon, individuals often cannot escape hypoxic conditions in their natural environment. Consequently, they possess the capacity to modify their physiology and biochemistry by down-regulating aerobic metabolic rate (Muusze et al., 1998; Sloman et al., 2006; Scott et al., 2008) and upregulating glycolysis (Almeida-Val., 2000; Richards et al., 2007; Scott et al., 2008) so as to survive low oxygen exposure.

With this background in mind, in the present study we directly examined the ionoregulatory responses of the rainbow trout, a hypoxia-intolerant freshwater fish, for comparison with those of the hypoxia-tolerant oscar. Complex changes in branchial blood perfusion (Holeton and Randall, 1967a; Booth, 1979; Soivio and Tuurula, 1981; Sundin et al., 1997), increased branchial water flow (Holeton and Randall, 1967b), and increased gill  $\text{O}_2$  transfer factor (Randall et al., 1967) have all been observed in rainbow trout subjected to moderate hypoxia, and are considered strategies to maintain  $\text{O}_2$  uptake in the face of declining availability. All these are suggestive of lamellar recruitment, increased

gill surface area, and therefore general increases in gill permeability. Therefore, our first hypothesis was that unidirectional  $\text{Na}^+$  efflux rates to the water should increase in trout under hypoxic conditions.

The freshwater gill is also the major site of diffusional water exchange due to a large surface area, short diffusion distances and countercurrent flow (Loretz, 1979; Rudy, 1967). Net water flux is known to increase during exercise in trout (Wood and Randall, 1973c). Since we expect an increased branchial surface area during hypoxia, our second hypothesis was that diffusional water exchange rates should increase during hypoxia as well.

The gill epithelium is the principal barrier between fish blood and the ambient water and plays a major role in maintaining ionic integrity as well as active  $\text{Na}^+$  uptake powered by  $\text{Na}^+/\text{K}^+$ -ATPase and  $\text{H}^+$ -ATPase (Avella and Bornancin, 1989; Evans et al., 2005). Maintenance of a homeostatic intracellular environment requires the redistribution of ions through ATP-dependent pumping systems such as the  $\text{Na}^+/\text{K}^+$ -ATPase, which can consume 20–80% of the cell's resting metabolic rate (Boutilier, 2001). When a cell becomes hypoxic, the rate of oxygen delivery is less than that which is required for oxidative metabolism to supply the energy needs of the cell. So the two key indicators of severe oxygen deprivation are a rapid depletion of cellular ATP and a loss of intracellular  $\text{K}^+$  as the  $\text{Na}^+/\text{K}^+$  pump begins to fail (Boutilier and St-Pierre, 2000). Therefore, we set out to investigate if rainbow trout did face severe oxygen deprivation at the level of the gill cells during hypoxia by measuring the unidirectional uptake of  $\text{Na}^+$  at the gills as well

the activity of gill  $\text{Na}^+/\text{K}^+$  ATPase and  $\text{H}^+$ -ATPase enzymes. Specifically, our third and fourth hypotheses were that  $\text{Na}^+$  influx rates from the water would fall during hypoxia, together with  $\text{Na}^+/\text{K}^+$ -ATPase and  $\text{H}^+$ -ATPase activities, in order to save metabolic costs. Coupled with these ideas, our fifth hypothesis was that  $\text{K}^+$  leakage rates to the water would increase during hypoxia. In light of recent reports that severe hypoxic exposure can result in rapid, marked remodelling of the gills of hypoxia-tolerant species (Sollid and Nilsson, 2006; Nilsson, 2007; Matey et al., 2008), we examined gill surface morphology using scanning electron microscopy. Our sixth hypothesis was that if this phenomenon occurred at all in the hypoxia-intolerant rainbow trout, it would be far less marked.

We further focused on nitrogen waste excretion at the gill, specifically looking at ammonia excretion under hypoxia. Ammonia is highly toxic, and appears to be excreted across the branchial epithelium mainly via passive diffusion in freshwater fish, though there is some evidence of coupling to active  $\text{Na}^+$  uptake (Wilkie, 2002). During hypoxia, hypoxia-tolerant oscar depress their ammonia excretion to the water, similar to their depression of ion influx and efflux rates (Wood et al., 2007). In trout, increased gill permeability would be expected to increase ammonia excretion, while reductions in  $\text{Na}^+$  uptake and aerobic metabolism would be expected to decrease ammonia excretion. The suppression is believed to be caused by decreased protein catabolism and deamination of amino acids during anaerobic conditions, leading to a reduced production of ammonia-N (van Waarde, 1983). However, as trout generally increase ammonia production and efflux rates at times of stress (Wood, 2001), our final hypothesis was that this hypoxia-

intolerant teleost would likely not reduce ammonia excretion during moderate hypoxia, in contrast to the Amazonian oscar.

Through this hypothesis-driven study, our overall goal was to contribute to the understanding of the physiological and biochemical responses of ionoregulation and N-waste handling to low environmental oxygen conditions in freshwater fish.

## **Methods and Materials:**

### *Experimental Animals:*

Rainbow trout, *Oncorhynchus mykiss*, were obtained from Humber Springs Trout farm in Orangeville and acclimated for at least 2 weeks to  $15 \pm 0.5^\circ\text{C}$  in flowing dechlorinated Hamilton tapwater ( $\text{Na}^+ = 0.6$ ;  $\text{Cl}^- = 0.7$ ;  $\text{K}^+ = 0.05$ ;  $\text{Ca}^{2+} = 1.0 \text{ mmol L}^{-1}$ ,  $\text{pH} = 8.0$ ) under a 12-h light photoperiod. Fish were fed a commercial fish feed every two days until experiments when feeding was suspended 48 h before experimentation. Animals were cared for in accord with the principles of the Canadian Council on Animal Care and protocols were approved by the McMaster Animal Care Committee. All protocols were designed to maximize the accuracy of branchial flux measurements over the critical exposure, and to ensure that the external to internal specific activity ratios remained high for greatest accuracy in radioisotopic flux determinations while ensuring the water ammonia levels remained low. Therefore different sizes of fish, container volumes, and experimental durations were used in different trials.

### *Exposure Regimes:*

- 1. Unidirectional  $\text{Na}^+$  uptake and net  $\text{K}^+$  and ammonia fluxes in response to a range of acute (4 h) hypoxic exposures.***

In an initial range-finding study, juvenile rainbow trout (mass =  $1.61 \pm 0.03$  (58) g; mean  $\pm$  1 SEM ( $n$ )) were transferred in groups of 10 to small plastic aquaria (2 L) covered with duct tape for darkening, and left overnight. Experimental chambers were

continuously supplied ( $0.5 \text{ L min}^{-1}$ ) with temperature-controlled ( $15 \pm 0.5^\circ\text{C}$ ) tapwater and submerged in an external water bath to maintain external temperature. The chambers were well aerated so as to maintain  $\text{PO}_2 \geq 140 \text{ mmHg}$  (normoxia). The experimental design consisted of 4-h exposures, where each randomly selected experimental group of fish were exposed to either normoxia or one of a range of  $\text{PO}_2$  levels of 120, 100, 80, 60 and 40 mmHg. Hypoxia was induced by a  $\text{N}_2$ /air mixture which was empirically adjusted using a gas mixing pump (Wösthoff 301-af) to the desired severity of hypoxia.

During the flux measurement, the aquaria were operated as closed systems at a volume of 1.5 L. Radioisotope ( $^{22}\text{Na}^+$  1.0 $\mu\text{Ci}$ /tank, PerkinElmer®, Boston MA) was added at 0- h. After an initial 10 min mixing period, a water sample (30 ml) was taken and subsequently at 1-h intervals till the end of the experiment for analysis of external  $[\text{Na}^+]$ , external  $[\text{K}^+]$ , total external ammonia ( $[\text{Amm}]$ ), and  $^{22}\text{Na}^+$  radioactivity (cpm). Water  $\text{PO}_2$  was monitored (1-ml samples) at the beginning of each 1-h flux during the 4-h exposure. At the end of the experiment, fish were rapidly anaesthetized with neutralized 0.0075 g.  $\text{L}^{-1}$ MS-222, killed via cephalic concussion, weighed and transferred to 15 ml plastic vials for gamma radioactivity counting to determine whole body uptake of  $^{22}\text{Na}^+$ .

***2. Unidirectional  $\text{Na}^+$  influxes, effluxes, and net fluxes and net ammonia fluxes in response to progressive (4-h) hypoxia and acute normoxic recovery.***

Adult rainbow trout ( $395.4 \pm 12.4$  (6) g) were transferred to separate, darkened, well-aerated acrylic flux boxes (4 L) with flow-through water supply ( $0.5 \text{ L min}^{-1}$ ) and left overnight. Experimental chambers were held under similar conditions as experiment

1. The experimental design consisted of a 3-h control normoxic period, a 4-h experimental hypoxic period, and a subsequent 3-h recovery normoxic period. Environmental hypoxia was induced by bubbling N<sub>2</sub> and air at a low rate in the individual tanks to bring the PO<sub>2</sub> of the holding water gradually down to a desired level of hypoxia over 4 h (PO<sub>2 w</sub> = ~110 mmHg).

During the experiment, flux boxes were operated as closed systems at a volume of 2 L for the control normoxic period and at 2.25 L for the subsequent 4-h hypoxic exposure and 3-h normoxic recovery periods. Water was completely flushed and changed in the flux boxes (without air-exposure of the fish) between the control normoxic period and the subsequent hypoxic exposure. Radioisotope (<sup>22</sup>Na<sup>+</sup>, 2.0μCi/box) was added immediately after the flushes at 0 h of the control normoxic period and prior to the hypoxic exposure. After an initial 10-min mixing period, a water sample (40 ml) was taken and subsequently at 1-h intervals till the end of the experiment for analysis of external [Na<sup>+</sup>], total external ammonia ([Amm]), and <sup>22</sup>Na<sup>+</sup> radioactivity (cpm). Water PO<sub>2</sub> was monitored (1-ml samples) at the beginning of each 1-h flux. At the end of the experiment, the fish were anaesthetized (neutralized MS-222, 0.0075 g. L<sup>-1</sup>) and a blood sample taken by caudal puncture into a heparinized syringe. Plasma was separated by rapid centrifugation (10,000G for 1 min) and frozen for analysis of internal <sup>22</sup>Na<sup>+</sup> radioactivity (cpm) and internal [Na<sup>+</sup>] levels. The fish were then immediately euthanized by an overdose of neutralized MS-222.

***3. Unidirectional Na<sup>+</sup> influxes, effluxes, and net fluxes and net K<sup>+</sup> and ammonia fluxes in response to prolonged acute (8 h) hypoxia.***

Adult rainbow trout ( $188.1 \pm 8.7$  (8) g) were transferred to the same flux boxes as used in experiment 2 and held under similar conditions. Experimental design consisted of a 3-h control normoxic period and a subsequent 8-h hypoxic exposure period. Hypoxia was induced by a N<sub>2</sub>/air mixture which was empirically adjusted using a gas mixing pump (Wösthoff 301-af) to a desired level of hypoxia ( $PO_2_w = \sim 80$  mmHg).

During the experiment, flux boxes were operated as closed systems at a volume of 2.5 L for the control normoxic period and at 3.5 L for the subsequent 8-h hypoxic exposure. Water was completely flushed and changed in the flux boxes between the control normoxic period and the subsequent hypoxic exposure. Radioisotope ( $^{22}\text{Na}^+$  2.0 $\mu\text{Ci}/\text{box}$ ) was added immediately after the flushes at 0 h of the control normoxic period and ( $^{22}\text{Na}^+$  4.0 $\mu\text{Ci}/\text{box}$ ) prior to the hypoxic exposure. The external radioisotope concentration was doubled at the beginning of hypoxia so as to raise the external specific activity sufficiently to minimize the need for back-flux correction. After an initial 10 min mixing period, a water sample (30 ml) was taken and subsequently at 1-h intervals till the end of the experiment for analysis of external [ $\text{Na}^+$ ], external [ $\text{K}^+$ ], total external ammonia ([Amm]), and  $^{22}\text{Na}^+$  radioactivity (cpm). Water  $PO_2$  was monitored (1-ml samples) at the beginning of each 1-h flux. At the end of the experiment, the fish were anaesthetized (neutralized MS-222, 0.0075 g. L<sup>-1</sup>) and a blood sample taken by caudal puncture into a heparinized syringe. Plasma was separated for analysis of internal  $^{22}\text{Na}^+$

radioactivity (cpm) and internal [ $\text{Na}^+$ ] levels, and the fish were then euthanized as in experiment 2.

#### ***4. The effect of acute hypoxia (4h) and normoxic recovery on diffusive water exchange***

Juvenile rainbow trout ( $n = 8$  per sampling point, 40 in total, mean (SE) mass  $12.1 \pm 0.3$  g) were transferred to experimental chambers ( $n = 2/\text{chamber}$ ) which were 1-L sealable polyethylene containers with flow-through water supply ( $0.1 \text{ L min}^{-1}$ ) and left overnight. Experimental chambers were maintained under identical conditions as in previous exposures. The experimental design consisted of a 3-h control normoxic period, 4-h hypoxic exposure and a subsequent 4-h normoxic recovery period. Hypoxia was induced by a  $\text{N}_2/\text{air}$  mixture which was empirically adjusted using a gas mixing pump (Wösthoff 301-af) to a desired level of hypoxia ( $\text{PO}_2 \text{ w} = \sim 80 \text{ mmHg}$ ).

During the experiment, experimental chambers were operated as closed systems at a volume of 0.6 L. The experiment was designed to obtain various “snap-shots” of diffusive water flux during normoxia, hypoxic exposure and recovery. Tritiated water ( $^3\text{H}_2\text{O}$ , Sigma®, St. Louis MO) was added to the experimental chambers ( $10 \mu\text{Ci}/0.6 \text{ L}$ ) 20 minutes before sampling. A water sample (5-ml) was taken immediately after adding radioisotope and at the end of the 20-minute sampling time to monitor the radioactivity (cpm) of  $^3\text{H}_2\text{O}$  in the water. Fish were rapidly killed via cephalic concussion after 3 h of normoxic exposure, 1-h and 4 h of hypoxia exposure, and after 1-h and 4-h of normoxic recovery to determine whole body water exchange rate. In each case, the 20-minute flux

period spanned the sampling time. Water PO<sub>2</sub> (1-ml samples) was also measured at each sampling time point. This protocol was designed to maximize the accuracy of water flux measurements over the critical experimental exposures, and was chosen based on preliminary experiments with various flux periods and techniques.

**5. *The effect of acute hypoxia (4h) and normoxic recovery on branchial Na<sup>+</sup>/K<sup>+</sup> - ATPase and H<sup>+</sup> - ATPase activities and gill morphology.***

Adult rainbow trout ( $n = 6$  per sampling point, 30 in total, mass  $193.8 \pm 6.1$  g) were transferred to the same flux boxes as used in experiment 2, with flow-through water supply ( $0.5 \text{ L min}^{-1}$ ), and left overnight. The experimental design consisted of a control normoxic period, 4-h hypoxia exposure and a subsequent 6-h normoxic recovery period. Hypoxia was induced by a N<sub>2</sub>/air mixture which was empirically adjusted using a gas mixing pump (Wösthoff 301-af) to a desired level of hypoxia ( $\text{PO}_{2\text{w}} = \sim 80 \text{ mmHg}$ ).

During the experiment, flux boxes were operated as closed systems at a volume of 3 L. Water was completely flushed and changed in the flux boxes (without air exposure of the fish) between the control normoxic period and the subsequent hypoxic exposure. Fish were rapidly killed with a lethal dose of anaesthetic ( $0.5 \text{ g L}^{-1}$  neutralized MS-222) during normoxia, after 1-h and 4-h of hypoxia, and after 1-h and 6-h of normoxic recovery. Water PO<sub>2</sub> (1-ml samples) was also measured at each sampling time point. Samples of gill filaments were excised. Specifically, the 2<sup>nd</sup> gill arch was snap-frozen in liquid N<sub>2</sub> and stored at  $-80^\circ\text{C}$  for later analysis for Na<sup>+</sup>/K<sup>+</sup> and H<sup>+</sup> - ATPase activities. The 3<sup>rd</sup> gill arch was dissected out, quickly rinsed in water and immediately fixed in cold

Karnovsky's fixative (8% glutaraldehyde and 16% paraformaldehyde in a 0.4 M Sodium phosphate buffer; Karnovsky, 1965). These samples were later transported to San Diego State University, CA, USA for scanning electron microscopy (SEM).

*Analytical Methods for Fluxes and Flux Calculations:*

Water PO<sub>2</sub> was monitored by injecting a 1-ml sample into an O<sub>2</sub> electrode (Radiometer-Copenhagen, Denmark) thermostatted to the experimental temperature and connected to a oxygen meter (A-M Systems polarographic amplifier, Kingston, ON). Water total ammonia (salicylate hypochlorite assay, Verdouw et al., 1978) was determined colorimetrically. Water total Na<sup>+</sup> and K<sup>+</sup> concentrations were measured using flame atomic absorption spectrophotometry (AAAnalyst 800, Perkin Elmer). <sup>22</sup>Na<sup>+</sup> radioactivity was measured using a gamma counter (Minaxi Auto-Gamma 5000 Series, Canberra-Packard, Meriden, CT) where absolute counts were calculated from counts per minute (cpm) values after background correction. <sup>3</sup>H<sub>2</sub>O radioactivity was measured using a QuantaSmart (Tricarb) Liquid Scintillation Analyzer (PerkinElmer, Downer's Grove, IL), with correction for background and internal standardization for quench correction as outlined below.

In experiment 1, unidirectional Na<sup>+</sup> uptake ( $J_{\text{influx}}^{\text{Na}}$ , by convention positive) was measured based on the appearance of radioactivity in the whole body of the fish. Unidirectional Na<sup>+</sup> uptake for this experiment was calculated using the following equations based on Matsuo et al. (2004):

$$SA \text{ (average over 4 h)} = 0.2 \left( \frac{[R1]}{[ion1]} + \frac{[R2]}{[ion2]} + \frac{[R3]}{[ion3]} + \frac{[R4]}{[ion4]} + \frac{[R5]}{[ion5]} \right) \quad (1)$$

$$\text{Radioactivity in fish (R}_F\text{)} = \text{counts per minute} / W \quad (2)$$

$$J_{\text{influx}}^{\text{Na}} = R_F / SA \times T \quad (3)$$

where  $ionN$  are the  $\text{Na}^+$  concentrations in the water ( $\mu\text{mol L}^{-1}$ ) and  $RN$  are the radioactivity values ( $\text{cpm L}^{-1}$ ) of the  $^{22}\text{Na}$  at each of the 5 measurement times over the 4-h flux period,  $W$  is the weight of the fish (kg),  $T$  is the total flux period (4 h),  $SA$  is the mean specific activity of the isotope in  $\text{cpm} \cdot \mu\text{mol}^{-1}$  during the flux time.

In experiments 2 and 3,  $\text{Na}^+$  flux calculations were performed based on equations presented by Wood and Randall (1973a), Kirschner (1970), and Wood (1992). Net  $\text{Na}^+$  flux rates ( $J_{\text{net}}^{\text{Na}}$ ) were calculated from the change in total  $\text{Na}^+$  concentration in the water (factored by time, volume, and fish mass):

$$J_{\text{net}}^{\text{Na}} = \frac{([X_i] - [X_f]) \cdot V_{\text{ext}}}{W \cdot T} \quad (4)$$

where  $[X_i]$  and  $[X_f]$  are total  $\text{Na}^+$  concentrations ( $\mu\text{mol L}^{-1}$ ) in the external water at the start and end of each flux period respectively of each 1-h flux period,  $V_{\text{ext}}$  is the external water volume (L),  $W$  is the weight of the fish (kg), and  $T$  is the time (1 h). Net flux rates of ammonia ( $J^{\text{Amm}}$ ) and  $\text{K}^+$  ( $J^{\text{K}}$ ) in all experiments were calculated as for  $J_{\text{net}}^{\text{Na}}$ .

$\text{Na}^+$  influx rates ( $J_{\text{influx}}^{\text{Na}}$ , by convention positive) were calculated from the mean external specific activity over each 1-h flux period (equation analogous to equation 1 for

averaging over 1 h), and the disappearance of counts from the external water (factored by time, volume, and fish mass). Backflux correction was applied by the end of the experiment when internal specific activity reached about 10 % of external specific activity. Therefore, influx was calculated as:

$$J_{\text{influx}}^{\text{Na}} = \frac{([R_i] - [R_f]) \cdot V_{\text{ext}} - SA_{\text{int}} ([X_i] - [X_f]) \cdot V_{\text{ext}}}{(SA_{\text{ext}} - SA_{\text{int}}) \cdot W \cdot T} \quad (5)$$

where  $[R_i]$ , and  $[R_f]$  represent initial and final  $^{22}\text{Na}^+$  radioactivity (cpm  $\text{L}^{-1}$ ),  $SA_{\text{int}}$  and  $SA_{\text{ext}}$  are the mean internal and external specific activities (in cpm  $\mu\text{mol}^{-1}$ ) over the 1-h flux period, and the other symbols are as in equation 4.  $SA_{\text{int}}$  at each time was estimated as described by Maetz (1956). In the calculation of  $SA_{\text{int}}$ , values of the internal distribution volume of  $\text{Na}^+$  and the exchangeable internal pool of  $\text{Na}^+$  were based on terminal plasma measurements. Unidirectional  $\text{Na}^+$  efflux rates ( $J_{\text{efflux}}^{\text{Na}}$ , by convention negative) were calculated by difference:

$$J_{\text{efflux}}^{\text{Na}} = J_{\text{net}}^{\text{Na}} - J_{\text{influx}}^{\text{Na}} \quad (6)$$

In experiment 4, diffusive water flux was measured by assaying the appearance of  $^3\text{H}_2\text{O}$  radioactivity in the whole body of the fish. Fish were weighed and put into tightly sealed vials (Falcon tubes, to prevent evaporation) with an equal volume of de-ionized water and digested at  $60^\circ\text{C}$  for 6 h. Tissues were vortexed and a 2 ml sample was then centrifuged for 5 min at 5000  $g$  to obtain supernatant. 1 ml of supernatant was diluted with 4 ml of de-ionized water to make a final sample volume of 5 ml. External water samples (5 ml) were also counted. Radioactivity was counted on the QuantaSmart

(Tricarb) Liquid Scintillation Analyzer following the addition of 10 ml scintillation fluid (ACS Amersham, Buckinghamshire, U.K.) to both 5 ml tissue and water samples. For quench correction, all samples were internally standardized by further adding 0.5  $\mu\text{Ci}$  to both water and tissue samples and re-counting. This procedure corrected the counting efficiency of each tissue digest to the same efficiency as that for external water samples. Correction of the cpm data was applied as follows:

$$\text{Correction for quenching} = \frac{\text{initial cpm reading for tissue sample} \times (\text{cpm difference after standardization in water sample} / \text{cpm difference after standardization in tissue sample})}{\text{cpm difference after standardization in water sample}} \quad (7)$$

A multiplication factor was then applied to the total quench-corrected cpm, for the digestion dilution and subsequent sub-sampling of tissue extracts for counting, so as to determine total  $^3\text{H}_2\text{O}$  radioactivity in fish:

$$\text{Multiplication factor} = (A / 1 \text{ ml}) \quad (8)$$

where  $A = \{[\text{weight of fish(g)} \times \text{percentage body water (~80\%)}] + \text{volume of water added (g)}\}$ . Grams and millilitres were considered equivalent in this context. After corrections were made, the rate constant ( $K$ ) of the influx of water into the fish was calculated using a standard formula (Rudy 1967):

$$K = \frac{1}{T} \ln \frac{C_{\infty}}{C_{\infty} - C_t} \quad (9)$$

where  $K$  = rate constant ( $\text{h}^{-1}$ ),  $C_t$  = specific activity in fish tissue fluids (cpm/ml),  $T$  = uptake time period (in this experiment, 20 minutes) and  $C_{\infty}$  was the specific activity (cpm/ml) of the external water.

*Gill Na<sup>+</sup>/K<sup>+</sup>-ATPase Enzyme Activity:*

Gill Na<sup>+</sup>/K<sup>+</sup>-ATPase activity was measured on crude gill homogenates using the methods outlined by McCormick (1993). Homogenate (10 µl aliquots) was assayed for ATPase activity in the absence (solution A) or presence (solution B) of 500 µmol L<sup>-1</sup> ouabain. Each gill sample was run in triplicate and measured at 340 nm in a kinetic microplate reader (SpectraMAX Plus; Molecular Devices, Menlo Park, CA) at 15-s intervals for 30 min. The remaining homogenate was measured for [protein] using the Bradford assay as outlined below. Na<sup>+</sup>/K<sup>+</sup>-ATPase activities were calculated as described below (Richards et al., 2003).

*Gill H<sup>+</sup>-V-ATPase Enzyme Activity:*

Lin and Randall's methodology (1993) with some modifications was employed, using *N*-ethylmaleimide (NEM) as an H<sup>+</sup>-ATPase inhibitor. Sodium azide was used to remove background activity of mitochondrial ATPases. Homogenate (10 µl) from gill samples (as prepared for the Na<sup>+</sup>/K<sup>+</sup>-ATPase activity above) was added to wells in a 96-well plate. Two treatments for each sample C and D [C: ouabain (500 µmol l<sup>-1</sup>) + sodium azide, and D: ouabain (500 µmol l<sup>-1</sup>) + sodium azide + NEM (50 nmol l<sup>-1</sup>)] with triplicate measurements of each treatment were performed. The plate was then measured at 340 nm in the same kinetic microplate reader at 15-s intervals for 30 min. The remaining homogenate was measured for [protein] using the Bradford assay as outlined below. H<sup>+</sup>-ATPase activity was calculated as described below.

*Protein Measurement:*

Protein standards with concentrations ranging from 50 to 600  $\mu\text{g protein/ml}$  were prepared using  $1.0 \text{ mg}\cdot\text{ml}^{-1}$  BSA stock (BioChemika).  $10 \mu\text{l}$  of each protein standard was pipetted in a 96-well microplate in duplicates.  $10 \mu\text{l}$  of diluted homogenized sample (all dilutions in de-ionized water) were dispensed in triplicates into the same plate. To all standards and samples,  $250 \mu\text{l}$  of Bradford Assay Reagent (Sigma) was added, and the plate was read at  $595 \text{ nm}$ .

*Calculation of  $\text{Na}^+/\text{K}^+$ -ATPase and  $\text{H}^+$ -V-ATPase Enzyme Activities:*

Activities of the ATPase enzymes were measured using the linear disappearance of NADH over time. The average rate for each treatment was taken from the stable slope and calculated from an ADP standard curve generated just prior to the assay. ADP standard curves were run from 0 to  $20 \text{ nmol ADP}\cdot\text{well}^{-1}$ . The rate of depletion in NADH stabilized around  $-0.012 \text{ OD unit}\cdot\text{nmol ADP}^{-1}\cdot\text{well}^{-1}$ .  $\text{Na}^+/\text{K}^+$ -ATPase activity was determined by subtracting the difference in ATP hydrolysis between the control wells and the ouabain-treated ones (A vs. B).  $\text{H}^+$ -ATPase activity was obtained by calculating the difference in ATP hydrolysis between wells treated with ouabain + sodium azide and those treated with ouabain + sodium azide + NEM (C vs. D). Calculated activity was then normalized to total protein content (measured as described above) and expressed in  $\mu\text{mol ADP}\cdot\text{mg}^{-1}\cdot\text{protein h}^{-1}$ .

### *Morphological Analyses*

#### Scanning electron microscopy:

At San Diego State University, the middle part of each fixed gill arch (~4 mm long) bearing up to 12 filaments in both anterior and posterior rows were used for scanning electron microscopy. Gill samples were rinsed in 0.1 M phosphate-buffered saline (PBS), and post-fixed in 1% osmium tetroxide for 1 h. Then samples were dehydrated in ascending concentrations of ethanol from 30% to 100%, critical-point dried with liquid CO<sub>2</sub>, mounted on stubs, sputter-coated with gold, and examined with a Hitachi S 2700 scanning electron microscope (Tokyo, Japan) at the accelerating voltage of 20 kV.

#### Morphometry:

Gill parameters measured in control and experimental fish included density of mitochondria-rich cells (number of MRCs per mm<sup>2</sup>) and surface area of individual MRCs. Quantification of MRCs density was done on randomly selected areas of trailing edges of filaments located below respiratory lamellae. SEM microphotographs (magnification 2000x) of 5 randomly selected areas of filament epithelium of 6 fish (total number of measurements = 30) were analyzed and the number of apical crypts of MRCs were counted. The surface area of 30 individual MRCs (5 apical crypts for each of 6 fish examined in control and experiment) was calculated on photographs at 6000x magnification accordingly to the shape of their crypts that varied from circular to oval, triangular and roughly trapezoid.

### *Statistical Analyses*

Data are reported as means  $\pm$  SE (N is the number of fish), unless otherwise stated. Data were normally distributed; therefore parametric statistics were used in all analyses. In experiments 2 and 3, where repeated measurements were made on the same fish, differences within experimental exposures (e.g., control vs. 1 h hypoxia and 4 h hypoxia ) at different time periods were evaluated with a repeated measures analysis of variance (ANOVA) followed by a post hoc test (Dunnett's multiple comparison test for paired data). In instances where ANOVA indicated significant variation, but the post hoc test indicated no specific differences, a paired two-tailed Student's t-test was used to compare the overall mean value for the treatment period with that for the control period. In experiment 1,4 and 5, statistical relationships were assessed by one-way ANOVA followed by Tukey's test for independent data. The level of significance was set at  $P < 0.05$ . All statistical tests were run using SigmaStat<sup>®</sup> version 3.1 (Systat Software, Inc., San Jose, California).

## Results:

### *1. Unidirectional Na<sup>+</sup> uptake and net K<sup>+</sup> and ammonia fluxes in response to a range of acute (4 h) hypoxic exposures.*

To understand the overall effects of hypoxia on branchial ionoregulation, we initially surveyed gill ion fluxes at a range of acute (4 h) hypoxic exposures in juvenile rainbow trout (Fig. 1). There was no significant difference between  $J_{\text{influx}}^{\text{Na}}$  rates at normoxia or 120 mmHg, clearly indicating this level of hypoxia had no effect. However, there was a significant decrease of Na<sup>+</sup> uptake at around 100 mmHg, while at more severe hypoxic exposures (80, 60, and 40 mmHg), flux rates were intermediate, at levels between those of normoxia and those at 100 mmHg. During the normoxic treatment and hypoxic exposures of 120, 100, 80 and 60 mmHg, all 10 fish in each group survived. However, during the PO<sub>2</sub> = 40 mmHg exposure, only 8 of the 10 trout survived the 4 h treatment (Fig. 1).

Group net flux rates of K<sup>+</sup> and ammonia to the water were also measured in these experiments. Interestingly, with increasing severity of hypoxia, loss of K<sup>+</sup> to the water seemed to increase while ammonia excretion was suppressed (Table 1).

### *2. Unidirectional Na<sup>+</sup> influxes, effluxes, and net fluxes and net ammonia fluxes in response to progressive (4 h) hypoxia and normoxic recovery.*

In general, within a species, larger, older individuals are less hypoxia-tolerant than younger, smaller individuals. Therefore, in this series with adult trout (N = 6), which

examined sequential changes in both unidirectional influxes and effluxes of  $\text{Na}^+$  during hypoxia and normoxic recovery, we chose a final target  $\text{PO}_2$  of  $\sim 110$  mmHg, based on the results of experiment 1 with juvenile trout. Progressive hypoxia (4 h) led to a significant change in mean  $J_{\text{influx}}^{\text{Na}}$  starting exactly at the onset of hypoxic exposure when  $\text{PO}_2$  started to fall below 140 mmHg (Fig. 2). During the first 3 h of hypoxia exposure,  $J_{\text{influx}}^{\text{Na}}$  was significantly elevated by about 21% compared to control normoxic rates. However, at 4 h of hypoxia, when  $\text{PO}_2$  reached  $\sim 110$  mmHg, there was a marked and significant depression in  $J_{\text{influx}}^{\text{Na}}$  to about 21% of normoxic values.  $J_{\text{influx}}^{\text{Na}}$  remained depressed during the first hour of normoxic recovery and was restored back to control rates during the second hour of normoxic recovery. Changes in  $J_{\text{efflux}}^{\text{Na}}$  tended to mirror those in  $J_{\text{influx}}^{\text{Na}}$ , but overall there were no significant changes in  $J_{\text{efflux}}^{\text{Na}}$  rates throughout the hypoxic exposure and subsequent normoxic recovery when compared to the control normoxic rates. For  $J_{\text{net}}^{\text{Na}}$  flux rates, a trend towards negative  $\text{Na}^+$  balance was observed during the hypoxic exposure while a positive balance was observed during normoxic recovery, though again, the changes were not significant (Fig. 2).

Overall, there were no significant changes in mass-specific ammonia excretion rates throughout the hypoxic exposure and normoxic recovery (Fig. 3). However, there seemed to be a trend towards depressed ammonia excretion at 4 h of hypoxia which persisted during the first hour of normoxic recovery, and a tendency towards increased excretion near the end of the normoxic recovery when water  $\text{PO}_2$  was fully restored back to control normoxic levels (Fig. 3).

***3. Unidirectional Na<sup>+</sup> influxes, effluxes, and net fluxes and net K<sup>+</sup> and ammonia fluxes in response to prolonged (8 h) hypoxia.***

Since we had observed a significant depression in  $J_{\text{influx}}^{\text{Na}}$  rates at 4 h of hypoxic exposure (~110 mmHg; Fig. 2), a follow-up experiment with adult trout (N=8) was initiated to examine sequential changes in flux rates in response to a more prolonged (8 h) and slightly more severe hypoxic (~80mmHg) exposure (Figs. 4, 5 and 6). In this experiment, water PO<sub>2</sub> was acutely lowered over the first hour. In comparison to the 3 h control normoxic exposure, unidirectional Na<sup>+</sup> fluxes during 8 h of hypoxia displayed a tri-phasic response (Fig. 4).  $J_{\text{influx}}^{\text{Na}}$  was significantly elevated during the first hour of hypoxic exposure similar to the response seen during the first hour in experiment 2 (Fig. 2). During the subsequent three hours (2, 3, and 4 h of hypoxia),  $J_{\text{influx}}^{\text{Na}}$  rates were reduced back to control levels (Fig. 4). Thereafter, rates then started to gradually increase and remained significantly elevated for the last three h of hypoxia (6, 7, and 8 h of hypoxia) compared to control rates. A virtually identical tri-phasic trend was further observed with  $J_{\text{efflux}}^{\text{Na}}$  rates, with increases during early hypoxia, followed by correction and then increases again late in hypoxia (Fig. 4). As in experiment 2 (Fig. 2), a similar trend towards negative Na<sup>+</sup> balance was observed during the hypoxic exposure in comparison to the near zero Na<sup>+</sup> balance in the control normoxic period (Fig. 4). After 2-h of hypoxic exposure there was a significantly increased negative  $J_{\text{net}}^{\text{Na}}$  flux rate compared to the control normoxic period.

Similar to unidirectional  $\text{Na}^+$  flux rates, mass specific ammonia excretion rates also seemed to exhibit a tri-phasic response to hypoxia, although overall as in experiment 2, the changes were not significant (Fig. 5). Net  $\text{K}^+$  loss rates to the water approximately doubled in response to pro-longed hypoxia, and overall there was a significant increase compared to normoxic control levels (Fig. 6).

#### ***4. The effect of acute hypoxia (4h) and normoxic recovery on diffusive water exchange***

Mean fractional diffusive water exchange rates, measured with  $^3\text{H}_2\text{O}$ , for juvenile rainbow trout under normoxic control conditions were  $0.47 \pm 0.06 \text{ h}^{-1}$ ,  $N=8$  (Fig. 7). After 1 h of hypoxic exposure ( $\text{PO}_2 \sim 80 \text{ mmHg}$ ), the rate constant for water exchange ( $k$ ) was significantly depressed to about 5% of this value. However, this depression was completely eliminated at 4 h of hypoxia, when exchange rates were restored back to control levels. Water exchange rates during 1 h and 4 h of normoxic recovery were also comparable to control levels (Fig. 7).

#### ***5. The effect of acute hypoxia (4h) and normoxic recovery on branchial $\text{Na}^+/\text{K}^+$ - ATPase and $\text{H}^+$ - ATPase activity.***

The hypoxia exposure protocol in this terminal sampling experiment essentially duplicated that of experiment 3 for the first 4 h of acute exposure to reduced  $\text{PO}_2$ , but was followed by 6h of normoxic recovery. Branchial  $\text{Na}^+/\text{K}^+$ -ATPase activity did not change with acute hypoxia ( $\text{PO}_2 \sim 80 \text{ mmHg}$ ; Fig. 8). Gill  $\text{Na}^+/\text{K}^+$ -ATPase activity during normoxia was  $2.3 \pm 0.2 \mu\text{molADP. mg protein}^{-1}. \text{h}^{-1}$  and remained at this level after 1 h or

4 h of hypoxia exposure, and after 1 h of normoxic recovery. After 6 h of normoxic restoration, gill  $\text{Na}^+/\text{K}^+$ -ATPase activity was reduced to  $1.2 \pm 0.2 \mu\text{molADP} \cdot \text{mg protein}^{-1} \cdot \text{h}^{-1}$  although this depression was not significant (Fig. 8).

Patterns in branchial  $\text{H}^+$ -ATPase activity were similar (Fig. 8). Gill  $\text{H}^+$ -ATPase activity during normoxia was  $2.4 \pm 0.1 \mu\text{molADP} \cdot \text{mg protein}^{-1} \cdot \text{h}^{-1}$ , and did not change after 1 h or 4 h of hypoxic exposure.  $\text{H}^+$ -ATPase activity remained unchanged after 1 h of normoxic recovery but was significantly depressed after 6 h of normoxic restoration to about 25% of the control activity.

#### ***6. The effect of acute hypoxia (4h) and normoxic recovery on gill morphology.***

Gill morphology was studied in the rainbow trout of experiment 4. Macrostructure of the gills and ultrastructure of the gill epithelium of this fish were typical for salmonids. Pavement cells (PVC), the major component of the gill epithelium, had a complex surface pattern composed of branched microridges (Fig. 9). Numerous mitochondria-rich cells (MRCs) were distributed along the trailing edge of gill filaments, below respiratory lamellae and in the interlamellar regions (Figs. 9 A, B). MRCs in the interlamellar regions of the filament epithelium tended to group in clusters of 3-5 large cells with flat or slightly convex apical surfaces ornamented by short microvilli (Fig. 9 B). MRCs in the epithelial region located below respiratory lamellae were either solitary or gathered into clusters of 2-4 cells (Figs. 9 A, C-D). Commonly, the apical surface of these MRCs was flat and had long and straight microvilli that were raised above the level of the pavement cells (PVCs) surface (Fig. 9 C). Mucous cells (MCs) were present but did not

appear to have specialized activity during normoxia (Fig. 9 A). The lamellar surface was covered by PVCs and exhibited few MRCs located only in the junctional regions between filament and lamellae (Fig 9 B).

After 1 h exposure to hypoxia (~80mmHg), MRCs in the interlamellar regions were still organized into clusters of 2-3, or rarely 5 cells while below the interlamellar spaces MRCs were mostly solitary and only few clusters of 2 cells were seen in this area (Fig. 10 A). Mitochondria- rich cells looked “swollen” and their convex apical surfaces contained either short or stubby “knob-like” microvilli or displayed an almost smooth surface with completely reduced microvilli (Figs. 10 A, B). A limited number of MRCs were ornamented with long microvilli, and a novel "carpet-like" surface pattern of highly interdigitated microvilli was further observed (Fig. 10 C). This surface pattern was not found in normoxic control fish (Fig. 9). In some samples, MCs were found to excrete globs of mucus (Figs. 10 A, B). After 4h exposure to hypoxia, there were definitely fewer MRCs visible by SEM. No MRC clusters were observed, instead solitary MRCs were present (Fig. 11). These cells had either convex surfaces with knob-like microvilli (white arrow) or a flat carpet-like appearance (Fig. 11). Similar to 1 h hypoxic exposure, MCs were found to release secretion (Fig. 11 B). No changes seen by SEM were found in cell composition and surface structure of the lamellar epithelium during exposure to hypoxia.

After fish were transferred from hypoxic to normoxic water, there were definite signs of recovery in the surface structure of the gill filament epithelium. After 6 hours in normoxic water, MRC clusters composed of 2-3 cells re-appeared (Figs. 12 A, B). Cells

joined into clusters had either knob-like or more extended microvilli (Fig. 12 B). Surface structure of the solitary MRCs varied. Cells with knob-like microvilli as well as cells with “carpet like” surface were observed in all regions of the filament epithelium (Figs. 12 A, C). Further, large, actively functioning mucous cells were also evident (Fig. 12 A).

The magnitude of the above described gill morphological changes were then quantified to obtain changes in MRC density in the filament epithelium, surface area of apical crypts and percentage of surface area occupied by MRCs / mm<sup>2</sup> (Fig. 13 A, B, C). After 1-h of hypoxic exposure, the number of MRC's per mm<sup>2</sup> of gill filament epithelium was increased by 31% compared to MRC density during normoxia (Fig. 13 A). Similarly, the exposed surface area of individual MRCs after 1-h hypoxia exposure displayed a dramatic 3-fold increase compared to that in normoxic conditions (Fig. 10 B). This led to a significant increase in the percentage of the surface area occupied by MRCs when comparing to the same parameter in normoxic fish gills (from 6% to 24%) (Fig. 13 C). After 4 h of hypoxia, while the density of MRCs was significantly reduced, the surface area of individual apical crypts remained elevated, though not as high as at 1h of hypoxia. Therefore the percentage of surface area occupied by MRCs declined almost twofold but remained significantly larger than under normoxic conditions (Fig. 13 A-C). During recovery after hypoxia in normoxic water, MRC density came back to its original level (Fig. 13 A). However, exposed surface area of MRCs and percentage of surface area occupied by MRC's remained significantly elevated compared to the same values in normoxic fish gills (Fig. 13 B, C).

## **Discussion:**

### *The Osmorespiratory Compromise during Hypoxia in the Freshwater Rainbow Trout:*

The focus of this study was to examine the relationship between ion and gas exchange at the branchial epithelium of the rainbow trout and its regulatory adaptation under hypoxia. We measured fluxes across the whole animal assuming the gills to be the predominant site of exchange in freshwater fish. While the kidney is known to contribute to ion and ammonia losses via dilute urine, fluxes through this route are typically less than 10% of total losses (McDonald and Wood, 1981; Marshall and Grosell, 2006). We mainly focused on the exchange of  $\text{Na}^+$  across the gill epithelium, but further examined the loss of  $\text{K}^+$ , ammonia excretion and the cellular and morphological alterations of the gill to fully comprehend the osmorespiratory compromise during hypoxia. Experiment 1, with juvenile fish, served to demonstrate that the compromise does occur in this species, and to identify the  $\text{PO}_2$  range of interest (Fig. 1). However, in light of well-known differences in hypoxia tolerance between juvenile and adult teleosts (see Sloman et al., 2006 for discussion), our detailed analysis is largely restricted to the latter. Overall, our results indicate that environmental hypoxia induces changes in gill ionoregulatory function in the freshwater adult rainbow trout, the direction and magnitude of which vary with both the extent and duration of the hypoxia regime. The bidirectional nature of the changes suggests a more complex set of responses in this hypoxia-intolerant species, compared to those seen in the hypoxia-tolerant Amazonian oscar (Wood et al., 2007).

### *Responses in Na<sup>+</sup> Influx:*

Branchial Na<sup>+</sup> influx was clearly very sensitive to even small changes in environmental oxygen levels. In experiment 2, progressive small reductions in PO<sub>2</sub> below 140 mmHg resulted in initial increases in J<sup>Na</sup><sub>influx</sub> (discussed subsequently) followed by significant depression by 4 h exposure, once PO<sub>2</sub> reached 110 mmHg (Fig. 2). This depression, which persisted during the first hour of normoxic recovery (Fig. 2), supports our third hypothesis. Similarly, the Amazonian oscar, *Astronotus ocellatus*, exhibited a rapid and profound reduction of Na<sup>+</sup> uptake during 3 h of much more severe hypoxia (< 20 mmHg) and this suppression of Na<sup>+</sup> influx was also seen during 1 h of normoxic recovery (Wood et al., 2007). While the fall in J<sup>Na</sup><sub>influx</sub> during hypoxia could be due to simple O<sub>2</sub> starvation (i.e. ATP limitation) of the ionocytes, it seems less likely that the continuation of the inhibition during normoxic recovery has the same explanation. A regulated phenomenon for conservation of metabolic energy at the level of transporters or channels, as proposed by Wood et al. (2007) for the oscar, could be involved.

The nature of the J<sup>Na</sup><sub>influx</sub> response appears to depend on the severity and duration of the hypoxic exposure. With acute, slightly deeper hypoxia (80 mmHg) prolonged for 8h in experiment 3, a tri-phasic response in J<sup>Na</sup><sub>influx</sub> was observed (Fig. 4). As in the preceding experiment, there was an initial elevation of J<sup>Na</sup><sub>influx</sub> compared to normoxic levels during the first hour. During the subsequent 2-3 h, this uptake was reduced back to control levels, but there was no reduction in J<sup>Na</sup><sub>influx</sub> below control normoxic levels, in contrast to experiment 1. In turn this was followed by a second significant elevation of

$J_{\text{influx}}^{\text{Na}}$  in the last 3 h of hypoxia (Fig. 4). This is contrary to what we predicted in our hypothesis and what has been previously observed in oscar (Wood et al., 2007). We speculate that several competing factors may come into play here, including blood flow patterns, exchange diffusion, acid-base status, and branchial ionocyte morphology.

An increased perfusion of the lamellae with blood as well as an overall increase in gill vascular resistance have been well documented during severe hypoxia ( $\text{PO}_2 < 50$  mmHg) in trout (Holeton and Randall, 1967a; Booth, 1979; Soivio and Tuurala, 1981; Sundin and Nilsson, 1997), but it is not clear what happens during the more moderate hypoxia studied here. Catecholamine release is triggered with the onset of severe hypoxia in adult trout (Perry and Reid, 1992, 1994; Reid and Perry, 2003); the increase in circulating catecholamines serves to improve lamellar perfusion, thereby increasing the transfer factor of the gills for oxygen (Holeton and Randall, 1967b), an adjustment which is vital in a situation when environmental oxygen content is lacking (Randall et al., 1972). The paradoxical increase in gill vascular resistance appears to be caused by a post-lamellar cholinergic constriction, potentially diverting more blood flow to the central venous sinus which underlies the filamental epithelium (Sundin and Nilsson, 1997). There are more MRCs on the filamental epithelium than on the lamellae but whether the blood-perfused “area” available for active ion uptake actually increases (which could explain increased  $J_{\text{influx}}^{\text{Na}}$ ) is uncertain. Certainly, our morphological data indicate that the available area of filamental MRCs on the epithelium that faces ambient water increases during moderate hypoxia (Fig. 10). Furthermore, *Oncorhynchus mykiss* is a species which shows clear evidence of exchange diffusion in branchial  $\text{Na}^+$  transport, a coupling of a

portion of influx to efflux which results in no net transport (Randall et al., 1972; Wood and Randall, 1973b). If the morphological area available for transport increases on either the blood or water side, it is likely that the exchange diffusion fluxes will also increase, manifested as matching changes in  $J^{\text{Na}}_{\text{influx}}$  and in  $J^{\text{Na}}_{\text{outflux}}$ . This was clearly seen in the experiment 3 (Fig. 4), and to a lesser in the extent milder hypoxic exposure of experiment 2 (Fig. 2).

A study by Thomas et al. (1986), again using a more severe hypoxia (40 mmHg), showed a rapid, biphasic systemic acidosis over 20 min., probably representing catecholamine-driven extrusion of  $\text{H}^+$  ions from gill ionocytes, followed by lactic acid mobilization. Given the more moderate  $\text{PO}_2$  levels used here, which are well above the threshold for catecholamine release in trout (Perry and Reid, 1992; Reid and Perry, 2003), it is unlikely that the former occurred in our experiments. However, lactic acid production may well have taken place in the longer term exposures. This factor would also be expected to raise  $J^{\text{Na}}_{\text{influx}}$  due to the well-known coupling of  $\text{Na}^+$  influx to acidic equivalent excretion, as seen after exhaustive exercise in trout (Wood, 1988).

#### *Responses in $\text{Na}^+$ Efflux:*

With progressive mild hypoxia down to 110 mmHg over 4 h in experiment 2, we did not see any significant changes in  $J^{\text{Na}}_{\text{efflux}}$  rates, though there was a tendency for  $J^{\text{Na}}_{\text{efflux}}$  to co-vary with  $J^{\text{Na}}_{\text{influx}}$ , as might occur with a varying exchange diffusion component (see above), a trend that persisted through normoxic recovery as well (Fig. 2). However, a more pronounced co-variation of  $J^{\text{Na}}_{\text{efflux}}$  with  $J^{\text{Na}}_{\text{influx}}$  occurred with the

acute and prolonged hypoxia (8 h at 80 mmHg) in experiment 3, in the triphasic fashion noted earlier for  $J_{\text{influx}}^{\text{Na}}$  (Fig. 4). More importantly, the changes in  $J_{\text{efflux}}^{\text{Na}}$  resulted in a changeover to significant net  $\text{Na}^+$  loss (negative  $J_{\text{net}}^{\text{Na}}$ ), thereby supporting our first hypothesis. This increased  $J_{\text{efflux}}^{\text{Na}}$  may be explained by a rise in passive diffusion of electrolytes across the gill due to a change in blood flow pattern which increases the area for gas transfer and ionic loss, similar to the situation during exercise (Randall et al., 1972; Wood and Randall, 1973a, b; Gonzalez and McDonald, 1992, 1994). Closed lamellae are opened and open lamellae are increasingly perfused (Nilsson, 1986; Booth, 1979; Soivio and Tuurala, 1981; Sundin and Nilsson, 1997). This, however, is very different from the response of the Amazonian oscar which is able to down-regulate  $\text{Na}^+$  efflux so as to maintain ion balance during hypoxia (Wood et al., 2007), underlining an important difference between a hypoxia tolerant and a hypoxia-intolerant teleost.

*Hypoxic effects on diffusive water exchange:*

Contrary to our second hypothesis, diffusional water exchange rates did not increase during hypoxia. After 1 h of hypoxic exposure, the rate constant for water exchange ( $k$ ) was significantly depressed to about 5% of control normoxic rate constant (Fig. 7). This depression was completely eliminated at 4 h of hypoxia and normoxic recovery, when exchange rates were restored back to control levels. This trend was unexpected as hypoxia is known to increase ventilation rate (Loretz, 1979) and lamellar perfusion (Holeton and Randall, 1967a,b; Booth, 1979). *A priori*, increases in gill surface area and blood perfusion should lead to increased water fluxes. We think the smaller size

of fish used in this study compared to experiment 2 (10-fold smaller) might be a reason for this significantly depressed water flux in light of an established negative relationship between physiological tolerance of hypoxia and size (Burlinson et al., 2001; Robb and Abrahams, 2003; Sloman et al., 2006). Intraspecific size-sensitive variation in tolerance to hypoxic conditions predicts that smaller fish are more tolerant to hypoxia due to differences in ventilation frequencies (Jones, 1971), blood oxygen carrying capacity (Lowe-Jinde & Niimi, 1983; Zanuy & Carrillo, 1985), and gill uptake rates (Sijm et al., 1995) that better adapt them to low oxygen conditions. We might be observing a similar conservation of metabolic energy at the level of transporters or channels, as for the oscar (Wood et al., 2007), that enable these fish to depress their water flux immediately when faced with hypoxia. However with continuing exposure, initial water flux depressions were eliminated possibly because branchial chemoreceptors at the gills of these fish recognized that experimental hypoxic levels were adequate for sufficient oxygen extrusion to maintain metabolic energy supply (Reid and Perry, 2003) and therefore diffusive flux rates return back to control normoxic levels.

*The Impact of Hypoxia at the Gill Ionocytes:*

To elucidate hypoxic effects at the cellular level, we examined the activity of  $\text{Na}^+/\text{K}^+$ -ATPase and  $\text{H}^+$ -ATPase pumps. Note that the measurements were made under optimal conditions *in vitro*, so we are measuring capacity, and not the situation *in vivo* where ATP supply may be limiting. Contrary to our third hypothesis we found no change in the activity of these pumps with 4 h of hypoxic (80 mmHg) exposure (Fig. 8). We

expected a downregulation of these pump activities so as to conserve ATP in a situation where oxidative phosphorylation is slowed down by oxygen limitation during hypoxia (Boutilier and St. Pierre, 2000). In contrast, the Amazonian oscar markedly downregulates branchial  $\text{Na}^+/\text{K}^+$ -ATPase activity after 3-4 h of severe hypoxia (Richards et al, 2007; Wood et al., 2007), so this appears to be another difference between the two species (see Chapter 3). However many previous reviews indicate that absolute downregulation of ATP pumps occurs when animals are subjected to anoxic conditions and/or face very severe oxygen lack (Hochachka, 1986; Boutilier and St. Pierre, 2000; Hochachka and Lutz, 2001) which was not the case in this study.

Interestingly, we saw net  $\text{K}^+$  loss rates to the water approximately double with prolonged hypoxia, a significant increase compared to normoxic levels (Fig. 6), indicating cellular distress, (Boutilier, 2001) and providing support of our fourth hypothesis. Cells are believed to lose intracellular  $\text{K}^+$  when the  $\text{Na}^+/\text{K}^+$ -ATPase pump begins to fail with oxygen deprivation (Boutilier and St. Pierre, 2000). This suggests that *in vivo*, ATP limitation may impact  $\text{Na}^+/\text{K}^+$ -ATPase activity during moderate hypoxia in trout, even though there was no change in enzyme capacity (Fig. 8). This again contrasts with the Amazonian oscar, which loses less, rather than more,  $\text{K}^+$  during severe hypoxia (Chapter 3), and where direct measurements have found no evidence of  $\text{O}_2$  limitation in gill epithelial cells (Scott et al., 2008).

### *Hypoxia-induced Changes in Gill Morphology:*

Environmental conditions that cause respiratory or osmoregulatory demands (eg; hypoxia) are not only accommodated by a host of circulatory and behavioural adaptations, but also involve alterations in the structure of the gills (Sollid and Nilsson, 2006). In light of recent findings on the plasticity of gill morphology in fish exposed to hypoxia (Sollid et al., 2003; Sollid and Nilsson, 2006; Matey et al., 2008), we also examined the trout gill epithelium and its changes with hypoxia utilizing SEM (Figs. 9-13), expecting a less obvious change compared to hypoxia-tolerant species. During normoxia, MRCs on the filament epithelium surface are represented by either clusters or solitary cells with flat or slightly convex surface bearing well-shaped microvilli (Fig. 9). It is known that in teleost fishes, some MRCs are located just beneath the leaf-like PVCs that compose the vast majority of the gill epithelium surface (Wilson and Laurent, 2002). The apical surfaces of these MRCs tend to be covered completely by PVCs and are usually not visible by SEM. With 1 h hypoxic exposure, there were immediate alterations in the cellular composition in the filament epithelium. Density and surface area of MRCs increased (Fig. 13 A-B). The expanded apical surfaces were convex in shape and displayed reduced microvilli probably due to the stretching of the apical membranes of the MRCs (Fig. 10). We postulate that the “hidden” MRCs previously covered by PVCs become dilated and push out the PVCs that covered them, exposing their apical openings to the environment. Therefore, as a first response to hypoxia we see an alteration in MRC surface structure (Fig. 10). As mentioned previously, this structural alteration can be mainly attributed to the opening of closed lamellae by an increase in the intra-lamellar

pressure during hypoxia (Holeton and Randall 1967 *a, b*; Wood and Shelton, 1980a) which in turn causes closed lamellae to distend leading to an increase in volume and surface area (Soivio and Tuurala, 1981). The initial increases observed in  $J_{\text{influx}}^{\text{Na}}$  and  $J_{\text{efflux}}^{\text{Na}}$  we see in experiment 3 can be attributed to this distention.

After a fast response to 1 h of hypoxic exposure, rainbow trout adjusted their gill morphology to minimize the contact of MRCs with the ambient water. After a 4 h hypoxic exposure, MRCs became less numerous and displayed smaller surface areas (Fig. 13 B). We propose that when MRCs decrease their volume and their apices display a more flat appearance, the PVCs become more protracted and are able to cover part of the MRCs on the epithelial surface. During this time, clusters of MRCs also disappeared (Fig. 11). Reduction of the apical surface of MRCs as well as their density has been observed as a gill response in different fish species not only to hypoxia (Matey et al., 2008) but to a number of other environmental stresses such as high salinity (Sardella et al., 2004), low pH (Wendelaar Bonga et al., 1990), hypercapnia (Goss et al., 1994; 1998), and highly diluted water (Fernandes et al., 1998). During exposure to hypoxia, mucous cells (MCs) were found to secrete globs of mucous (Figs. 10, 11). This is a generalized response of fish gills to a range of environmental stressors to which hypoxia can now be added (Matey et al., 2008). During normoxic recovery, we see the re-emergence of MRC clusters that still had an enlarged apical surface. Few of the MRCs had longer microvilli compared to the initial knob-like microvilli we saw during hypoxia (Fig. 12). The gill morphology changes in the Amazonian oscar in response to hypoxia were investigated in chapter 3. The oscar exhibited a different pattern of response in comparison to the trout

gill, highlighting the importance for the oscar of being adapted to low environmental oxygen conditions.

*Ammonia Excretion during Hypoxia:*

Waste excretion in fish are mainly composed of two nitrogenous end products; ammonia-N and urea-N, where ammonia is the major end product composing ~70% of total waste in freshwater species and excreted mainly at the gills (Van Waarde, 1983; Wood, 2001). We observed no significant changes in mass-specific ammonia excretion rates to acute 4-h hypoxic conditions although a trend towards depressed ammonia excretion at the end of 4 h exposure was observed (Fig. 3). Similar to reductions in  $\text{Na}^+$  uptake in experiment 2, we expected a decrease in ammonia excretion. In the Amazonian oscar, ammonia excretion was reduced in a similar fashion to  $J_{\text{influx}}^{\text{Na}}$  and  $J_{\text{efflux}}^{\text{Na}}$ , and this inhibition was pronounced during prolonged hypoxia, usually persisting to the first hour of normoxic restoration (Wood et al., 2007). This decline in excretion during hypoxia was believed to be due to a downregulation in the ammonia production rate (van Waarde, 1983). Further, it was also suggested that the branchial ammonia excretion maybe blocked by a hypoxia-induced mechanism such as down-regulation of a  $\text{Na}^+$ -linked transport system or channel arrest in the oscar (Wood et al., 2007). Similarly, we believe the suppression of ammonia excretion in rainbow trout during acute hypoxia (Fig. 3) maybe caused by anaerobic conditions, leading to a reduced production of ammonia (van Waarde, 1983). Anaerobic metabolism is known to increase during hypoxia and there is an up-regulation of anaerobic enzymes and down-regulation of energy expenditure that is

coupled to this up-regulation of anaerobic metabolic pathways (Randall, 1982; van den Thillart and Kesbeke, 1978). Specifically, protein catabolism (which is directly related to ammonia production) is reduced therefore depressing overall ammonia production.

Contrastingly, during times of stress (eg; exercise) trout are shown to increase ammonia production and efflux rates (Wood, 2001). Compared to the initial 4 h hypoxic exposure, an 8-h prolonged and slightly severe hypoxia was thought to be more stressful and was predicted to elevate ammonia excretion although this observed elevation was not significant (Fig. 5). With hypoxic stress, cortisol elevation is believed to contribute to increased ammonia excretion via free amino acid mobilization (Milligan, 1997). These mobilized amino acids are thought to be deaminated and oxidized for glycogen (to supply ATP to gill ionocytes under hypoxia) and therefore contribute to excess ammonia excretion (Wood, 2001).

In conclusion, we suggest that the osmorepiratory compromise has a different adaptation during hypoxia than its regulation during exercise in the rainbow trout. During exercise, we see a tightly regulated compromise between ion loss and gas exchange (Gonzalez and McDonald, 1992), however, this compromise is not as obvious during hypoxia (present study). There seems to be other factors that have complex influences on the osmorepiratory compromise where several competing aspects such as alterations in blood flow patterns, exchange diffusion, acid-base status, and branchial ionocyte morphology take place during hypoxia. This change in regulation could be attributed to

the inherent physiology of the trout and adaptations to exercise performance, in contrast to its intolerance to low environmental oxygen availability.

### **Acknowledgements**

Funded by an NSERC Canada Discovery grant to CMW, who is supported by the Canada Research Chair Program. We thank Linda Daio, Andrea Morash and John Fitzpatrick for their assistance during experimental set up.

**Literature Cited:**

Almeida-Val, V. M. F., A. L. Val, W. P. Duncan, F. C. A. Souza, M. N. Paula-Silva, S. and Land. 2000. Scaling effects on hypoxia tolerance in the Amazon fish *Astronotus ocellatus* (Perciformes: Cichlidae): contribution of tissue enzyme levels. *Comp Biochem Physiol B* 125:219-226.

Avella, M. and M. Bornancin. 1989. A new analysis of ammonia and sodium transport through the gills of the freshwater rainbow trout (*Salmo gairdneri*). *J Exp Biol* 142:155 - 175.

Booth, J.H. 1979. The effect of oxygen supply, epinephrine, and acetylcholine on the distribution of blood flow in trout gills. *J Exp Biol* 83:31-39.

Boutilier, R. G. and J. St-Pierre. 2000. Surviving hypoxia without really dying. *Comp Phys & Biochem* 126:481-490.

Boutilier, R. G. 2001. Mechanisms of cell survival in hypoxia and hypothermia. *J Exp Biol* 204:3171-3181.

Bradford, M. M. 1976. A rapid and sensitive method for the quantitation of microgram quantities of protein utilizing the principle of protein-dye binding. *Anal Biochem* 72:248-54.

Bucking, C and C. M. Wood. 2006. Gastrointestinal processing of Na<sup>+</sup>, Cl<sup>-</sup>, and K<sup>+</sup> during digestion: implications for homeostatic balance in freshwater rainbow trout. *Am J Physiol Regul Integr Comp Physiol* 291:R1764-R1772.

Burleson, M. L., D. R. Wilhelm, and N.J. Smatresk. 2001. The influence of fish size on the avoidance of hypoxia and oxygen selection by largemouth bass. *J Fish Biol* 59: 1336-1349.

De Boeck, G., C. M. Wood, F. I. Iftikar, K.A. Sloman, G. R. Scott, V. M. F. Almeida-Val, and A. L. Val. 2008. The effect of feeding on the osmorepiratory compromise in the Amazonian oscar, *Astronotus ocellatus*. Unpublished.

Diaz, R. J., J. Nestlerode, and M. L. Diaz. 2004. A global perspective on the effects of eutrophication and hypoxia on aquatic biota. In: *Proceedings of the 7th International Symposium on Fish Physiology, Toxicology, and Water Quality*, pp. 1–33.

Evans, D. H., P. M. Piermarini, and K. P. Choe. 2005. The multifunctional fish gill: dominant site of gas exchange, osmoregulation, acid-base regulation, and excretion of nitrogenous waste. *Physiol Rev* 85:97-177.

Fernandes, M. N., S. A. Perna, and S. F. Moron. 1998. Chloride cell apical surface changes in gill epithelia of the armoured catfish *Hypostomus plecostomus* during exposure to distilled water. *J Fish Biol* 52:844-849.

Gonzalez, R. J. and D. G. McDonald. 1992. The relationship between oxygen consumption and ion loss in a freshwater fish. *J Exp Biol* 163:317–332.

Gonzalez, R. J. and D. G. McDonald. 1994. The relationship between oxygen uptake and ion loss in fish from diverse habitats. *J Exp Biol* 190:95-108.

Goss, G. G., P. Laurent, and S. F. Perry. 1994. Gill morphology during hypercapnia in brown bullhead (*Ichthylurus nebulosus*): role of chloride cells and pavement cells in acid-base regulation. *J Fish Biology* 45:705-718.

Goss, G. G., S. F. Perry, J. N. Fryer, and P. Laurent. 1998. Gill morphology and acid-base regulation in freshwater fishes. *Comp Biochem Physiol A* 119:107-115.

Hochachka, P. W. 1986. Defense strategies against hypoxia and hypothermia. *Science* 231:234–241.

Hochachka, P. W. and P. L. Lutz. 2001. Mechanism, origin, and evolution of anoxia tolerance in animals. *Comp Biochem Physiol B* 130:435–459.

Holeton, G. F. and D. J. Randall. 1967*a*. Changes in blood pressure in the rainbow trout during hypoxia. *J Exp Biol* 46:297-305.

Holeton, G. F. and D. J. Randall. 1967*b*. The effect of hypoxia on the partial pressures of gases in the blood and water afferent and efferent to the gills of rainbow trout. *J Exp Biol* 46:317-327.

Hwang, P. P. and T. H. Lee. 2007. New insights into fish ion regulation and mitochondrion-rich cells. *Comp Biochem Physiol A Mol Integr Physiol* 148:479-497.

Jones, D. R. 1971. Theoretical analysis of factors which may limit the maximum oxygen uptake of fish: The oxygen cost of the cardiac and branchial pumps. *J Theor Biol* 32:341–349.

Karnovsky, M. J. 1965. A formaldehyde-glutaraldehyde fixative for high osmolarity for use in electron microscopy. *J Cell Biol A* 27:137.

Kirschner, L. B. 1970. The study of NaCl transport in aquatic animals. *Am. Zool.* 10:365-76.

Lin, H. and D. J. Randall. 1993. H<sup>+</sup>-ATPase activity in crude homogenates of fish gill tissue: inhibitor sensitivity and environmental and hormonal regulation. *J exp Biol* 180:163-174.

Loretz, C. A. 1979. Water exchange across fish gills: the significance of tritiated-water flux measurements. *J Exp Biol* 79: 147-162.

Lowe-Jinde, L. and A. J. Niimi. 1983. Influence of sampling on the interpretation of haematological measurements of rainbow trout, *Salmo gairdneri*. *Can J Zool* 61:396–402.

Maetz, J. 1956. Les changes de sodium chez le poisson *Carassius auratus* L. Action d'un inhibiteur de l'anhydrase carbonique. *J Physiol Paris* 48:1085-1099.

Marshall, W. S. and M. Grosell. 2006. Ion transport and osmoregulation in fish. Pp. 177-230 in D. Evans, eds. *The Physiology of Fishes* Boca Raton, FL: CRC Press.

Matey, V., J. G. Richards, Y. Wang, C. M. Wood, J. Rogers, R. Davies, B. W. Murray, X. Q. Chen, J. Du, and C. J. Brauner. 2008. The effect of hypoxia on gill morphology and ionoregulatory status in the Lake Qinghai scaleless carp, *Gymnocypris przewalskii*. *J Exp Biol* 211:1063-1074.

Matsuo, A. Y., R. C. Playle, A. L. Val, and C. M. Wood. 2004. Physiological action of dissolved organic matter in rainbow trout in the presence and absence of copper: Sodium uptake kinetics and unidirectional flux rates in hard and SW. *Aquat Toxicol* 70:63-81.

McCormick, S. D. 1993. Method for non-lethal hill biopsy and measurement of  $\text{Na}^+$ ,  $\text{K}^+$  ATPase activity. *Can J Fish Aquat Sci* 50:656 -658.

McDonald, D.G. and M.S. Rogano. 1986. Ion regulation by the rainbow trout, *Salmo gairdneri*, in ion poor water. *Physiol Zool* 59:318-331.

McDonald, D. G. and C. M. Wood. 1981. Branchial and renal acid and ion fluxes in the rainbow trout, *Salmo gairdneri*, at low environmental pH. *J exp Biol* 93:101–111.

Milligan, C. L. 1997. The role of cortisol in amino acid mobilization and metabolism following exhaustive exercise in rainbow trout (*Oncorhynchus mykiss* Walbaum). *Fish Physiol Biochem* 16:119-128.

Muusze, B., J. Marcon, G. van den Thillart, and V. M. F. Almeida-Val. 1998. Hypoxia tolerance of Amazon fish. Respirometry and energy metabolism of the cichlid *Astronotus ocellatus*. *Comp Biochem Physiol A* 120:151-156.

Nikinmaa, M. and B. B. Rees. 2005. Oxygen-dependent gene expression in fishes. *Am J Physiol Regul Integr Comp Physiol* 288:R1079-R1090.

Nilsson, G.E. 2007. Gill remodeling in fish – a new fashion or an ancient secret? *J Exp Biol* 210:2403-2409.

Nilsson, S. 1986. Control of gill blood flow. Pp 87-101 in S. Nilsson and S. Holmgren, eds. *Fish Physiology: Recent Advances*. London, Croom Helm.

Perry, S. F. and S. G. Reid, 1992. Relationships between blood oxygen content and catecholamine levels during hypoxia in rainbow trout and American eel. *Am J Physiol* 263:R240–249.

Perry, S. F. and S. G. Reid. 1994. The effects of acclimation temperature on the dynamics of catecholamine release in the rainbow trout (*Oncorhynchus mykiss*). *J Exp Biol* 186:289–307.

Randall, D.J. 1982. The control of respiration and circulation in fish during exercise and hypoxia. *J exp Biol* 100:275-288.

Randall, D. J., G. F. Holeton, and E. D. Stevens. 1967. The exchange of oxygen and carbon dioxide across the gills of rainbow trout. *J Exp Biol* 46:339 – 348.

Randall, D. J., D. Baumgarten, and M. Malyusz. 1972. The relationship between gas and ion transfer across the gills of fishes. *Comp Biochem Physiol A* 41:629-637.

Reid, S. G. and S. F. Perry. 2003. Peripheral O<sub>2</sub> chemoreceptors mediate humoral catecholamine secretion from fish chromaffin cells. *Am J Physiol Regul Integr Comp Physiol* 284: R990–R999.

Richards, J. G., J. W. Semple, J. S. Bystriansky, and P. M. Schulte. 2003. Na<sup>+</sup>/K<sup>+</sup>-ATPase  $\alpha$ -isoform switching in gills of rainbow trout (*Oncorhynchus mykiss*) during salinity transfer. *J Exp Biol* 206:4475-4486.

Richards, J. G., Y. S. Wang, C. J. Brauner, R. J. Gonzalez, M. L. Patrick, P. M. Schulte, A. M. Chippari-Gomes, V. M. F. Almeida-Val, and A. L. Val. 2007. Metabolic and ionoregulatory responses of the Amazonian cichlid, *Astronotus ocellatus*, to severe hypoxia. *J. Comp. Physiol B* 177:361-374.

Robb, T. and M. V. Abrahams. 2003. Variation in the tolerance to hypoxia in a predator and prey species: an ecological advantage of being small? *J Fish Biol* 62:1067-1081.

Rudy, P. P. 1967. Water permeability in selected decapod crustaceans. *Comp Biochem Physiol*. 22:581-589.

Rudy, P. P. 1967. Water permeability in selected decapods crustacean. *Comp. Biochem. Physiol.* 22: 581-589.

Sardella, B. A., V. Matey, J. Cooper, R. J. Gonzalez, and C. J. Brauner. 2004. Physiological, biochemical and morphological indicators of osmoregulatory stress in 'California' Mozambique tilapia (*Oreochromis mossambicus* x *O. urolepis hornorum*) exposed to hypersaline water. *J Exp Biol* 207: 1399-1413.

Scott, G. R., C. M. Wood, K. A. Sloman, F. I. Iftikar, G. De Boeck, V. M. Almeida-Val, V. M., and A. L. Val. 2008. Respiratory responses to progressive hypoxia in the Amazonian oscar, *Astronotus ocellatus*. *Respir Physiol Neurobiol* 162:109-116.

Sijm, D. T. H. M., M. E. Verberne, W. J. DeJonge, P. Pärt, and A. Opperhuizen. 1995. Allometry in the uptake of hydrophobic chemicals determined in vivo and in isolated perfused gills. *Toxic Appl Pharm* 131:130-135.

Sloman, K. A., C. M. Wood, G. R. Scott, S. Wood, K. Kajimura, O. E. Johannsson, V. M. F., Almeida-Val, and A. L. Val. 2006. Tribute to R.G. Boutilier: The effect of size on the physiological and behavioural responses of oscar, *Astronotus ocellatus*, to hypoxia. *J Exp Biol* 209:1197-1205.

Soivio, A. and H. Tuurula. 1981. Structural and circulatory responses to hypoxia in the secondary lamellae of *Salmo gairdneri* gills at two temperatures. J Comp. Phys. 145:37–43.

Sollid, J., P. De Angelis, K., Gundersen, and G. E. Nilsson. 2003. Hypoxia induces adaptive and reversible gross morphological changes in crucian carp gills. J Exp Biol 206:3667-3673.

Sollid, J. and G. E. Nilsson. 2006. Plasticity of respiratory structures – adaptive remodeling of fish gills induced by ambient oxygen and temperature. Respir Physiol Neurobiol. 154:241-251.

Soivio, A. and H. Tuurula. 1981. Structural and circulatory responses to hypoxia in the secondary lamellae of *Salmo gairdneri* gills at two temperatures. J Comp Physiol B 135:37-43.

Sundin, L. and G. E. Nilsson. 1997. Neurochemical mechanisms behind gill microcirculatory responses to hypoxia in trout: in vivo microscopy study. Am J Physiol 272: R576-R585.

Thomas, S., B. Fievet, and R. Motais. 1986. Effect of deep hypoxia on acid-base balance in trout: role of ion transfer processes. *Am J Physiol Regul Integr Comp Physiol* 250:R319–R327.

van den Thillart, G. and F. Kesbeke. 1978. Anaerobic production of carbon dioxide and ammonia by goldfish *Carassius auratus (L.)*. *Comp Biochem Physiol A*. 59:393-400.

van Waarde, A. 1983. Aerobic and anaerobic ammonia production by fish. *Comp Biochem Physiol B*. 74:675-684.

Verdouw, H., C. J. A. van Echteld, and E. M. J. Dekkers. 1978. Ammonia determination based on indophenol formation with sodium salicylate. *Water Res* 12:399–402.

Wendelaar Bonga, S. F., G. Flik, P. H. M. Balm, and J. C. A. van der Meij. 1990. The ultrastructure of chloride cells in the gills of the teleost *Oreochromis mossambicus* during exposure to acidified water. *Cell Tiss Research* 259: 575-585.

Wilkie, M.P. 2002. Ammonia excretion and urea handling by fish gills: present understanding and future research challenges. *J. Exp. Biol.* 293:284 –301.

Wilson, J. M. and P. Laurent. 2002. Fish gill morphology: inside out. *J Exp Zool* 293: 192-213.

Wood, C.M. and D. J. Randall. 1973a. The influence of swimming activity on sodium balance in the rainbow trout (*Salmo gairdneri*). J Comp Physiol 82:207-233.

Wood, C.M. and D. J. Randall. 1973b. Sodium balance in the rainbow trout (*Salmo gairdneri*) during extended exercise. J Comp Physiol 82:235-256.

Wood, C.M. and D. J. Randall. 1973c. The influence of swimming activity on water balance in the rainbow trout (*Salmo gairdneri*). J Comp Physiol 82:257-276.

Wood, C. M. and G. Shelton. 1980b. The reflex control of heart rate and cardiac output in the rainbow trout: interactive influences of hypoxia, haemorrhage and systemic vasomotor tone. J Exp Biol 87:247-270.

Wood, C. M. 1988. Acid-base and ionic exchanges at gills and kidney after exhaustive exercise in the rainbow trout. J Exp Biol 136: 461–481.

Wood, C.M., 1992. Flux measurements as indices of H<sup>+</sup> and metal effects on freshwater fish. Aquat. Toxicol. 22:239–264.

Wood, C. M. 2001. The influence of feeding, exercise, and temperature on nitrogen metabolism and excretion. Pp. 201-238 in P. A. Anderson and P. A. Wright, eds. Fish Physiology. Academic Press, Orlando.

Wood, C. M., M. Kajimura, K. A. Sloman, G. R. Scott, P. J. Walsh, V. M. F. Almeida-Val, and A. L. Val. 2007. Rapid regulation of Na<sup>+</sup> fluxes and ammonia excretion in response to acute environmental hypoxia in the Amazonian oscar, *Astronotus ocellatus*. *Am J Physiol. Regul Integr Comp Physiol.* 292:R2048-R2058.

Zanuy, S. and M. Carrillo. 1985. Annual cycles of growth, feeding rate, gross conversion efficiency and hematocrit levels of sea bass (*Dicentrarchus labrax* L.) adapted to different osmotic media. *Aquaculture* 44:11–25.

**Table 1**

Group net flux rates of  $K^+$  and ammonia (n = 8-10 fish per group) to the water by juvenile rainbow trout acutely exposed to various levels of hypoxia for 4 h in experiment 1.

---

Exposure	K <sup>+</sup> excretion ( $\mu\text{mol. kg}^{-1} \cdot \text{h}^{-1}$ )	Ammonia excretion ( $\mu\text{mol. kg}^{-1} \cdot \text{h}^{-1}$ )
Normoxic Control (n=10)	- 103	- 633
PO <sub>2</sub> = 120 mmHg (n=10)	- 116	- 325
PO <sub>2</sub> = 100 mmHg (n=10)	- 149	- 347
PO <sub>2</sub> = 80 mmHg (n=10)	- 170	- 252
PO <sub>2</sub> = 60 mmHg (n=10)	- 194	- 246
PO <sub>2</sub> = 40 mmHg (n=8)	- 197	- 141

---

**Figure 1:** Mean Na<sup>+</sup> uptake ( $J_{\text{influx}}^{\text{Na}}$ ) in separate groups of juvenile rainbow trout subjected to increasing severity of hypoxia (4 h) in experiment 1. Values are expressed as means  $\pm$  SEM. Means sharing the same letter are not significantly different from one another at  $P \geq 0.05$ .

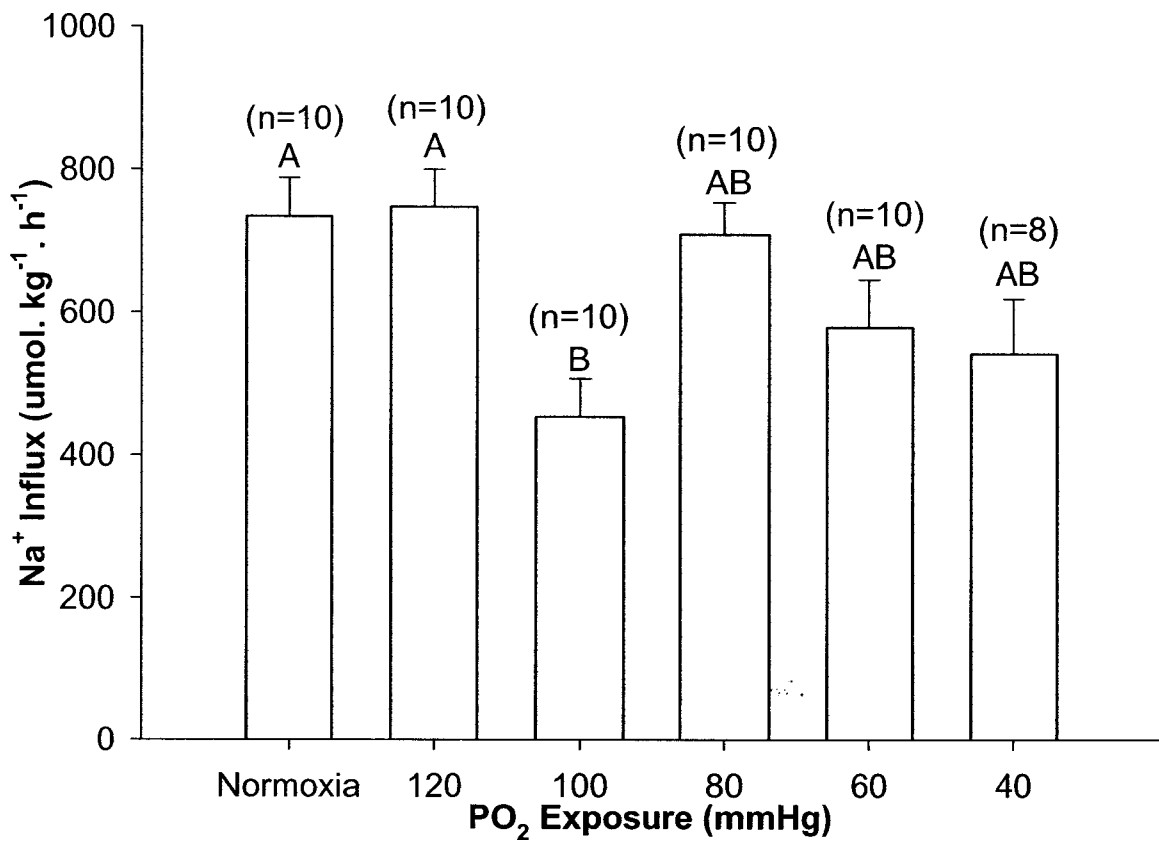


**Figure 2:** Mean Na<sup>+</sup> flux rates of adult rainbow trout (N=6) to a progressive induction of hypoxia (down to ~110 mmHg) for 4 h followed by an acute restoration of normoxia in experiment 2; Na<sup>+</sup> unidirectional influx ( $J_{\text{influx}}^{\text{Na}}$ , upward bars), Na<sup>+</sup> efflux ( $J_{\text{efflux}}^{\text{Na}}$ , downward bars), Na<sup>+</sup> net flux rates ( $J_{\text{net}}^{\text{Na}}$  striped bars) and water O<sub>2</sub> tension (black line). Values are expressed as means  $\pm$  SEM. Means values of  $J_{\text{influx}}^{\text{Na}}$  sharing the same letter are not significantly different from one another at  $P \geq 0.05$ . There are no significant differences among time periods in mean values of  $J_{\text{efflux}}^{\text{Na}}$  and  $J_{\text{net}}^{\text{Na}}$  respectively.

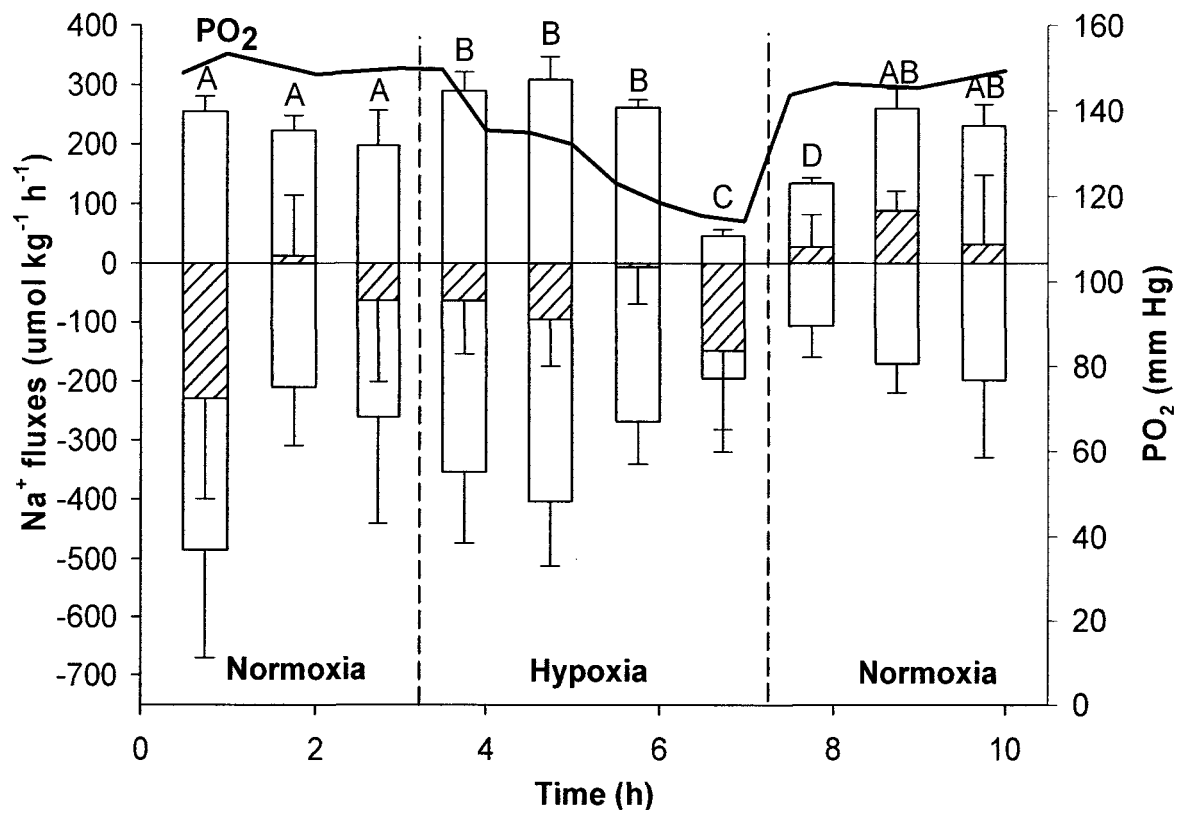


**Figure 3:** Mean ammonia excretion rates of rainbow trout (N=6) subjected to a progressive induction of hypoxia (down to ~110 mmHg) for 4 h followed by an acute restoration of normoxia; water O<sub>2</sub> tension (black line) in experiment 3. Values are expressed as means ± SEM. There are no significant differences present at  $P \leq 0.05$ .

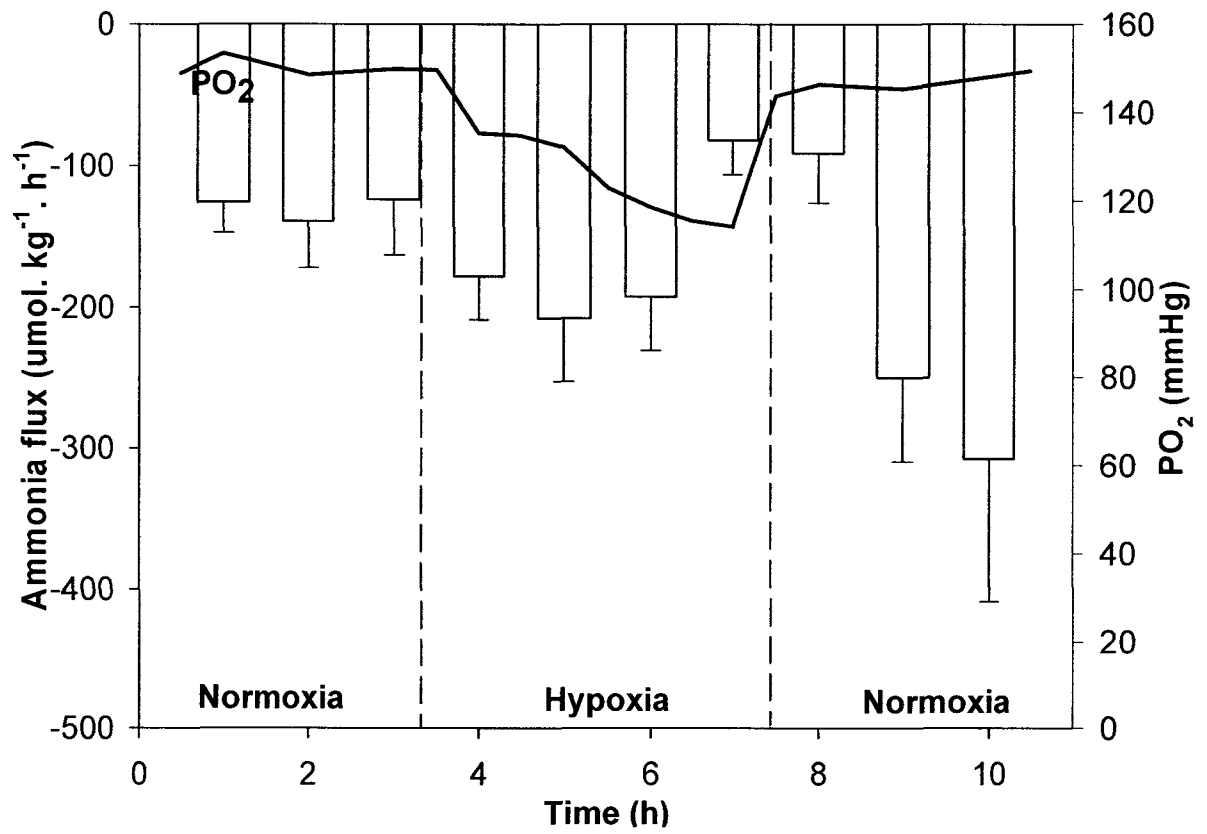


**Figure 4:** Mean Na<sup>+</sup> flux rates of rainbow trout (N=8) subjected to an acute induction of hypoxia (~80 mmHg) prolonged for 8 h subsequent to a 3-h normoxic control period in experiment 3; Na<sup>+</sup> unidirectional influx ( $J_{\text{influx}}^{\text{Na}}$ , upward bars), Na<sup>+</sup> efflux ( $J_{\text{efflux}}^{\text{Na}}$ , downward bars), Na<sup>+</sup> net flux rates ( $J_{\text{net}}^{\text{Na}}$  striped bars) and water O<sub>2</sub> tension (black line). Values are expressed as means ± SEM. Means sharing the same letter are not significantly different from one another at  $P \geq 0.05$ .

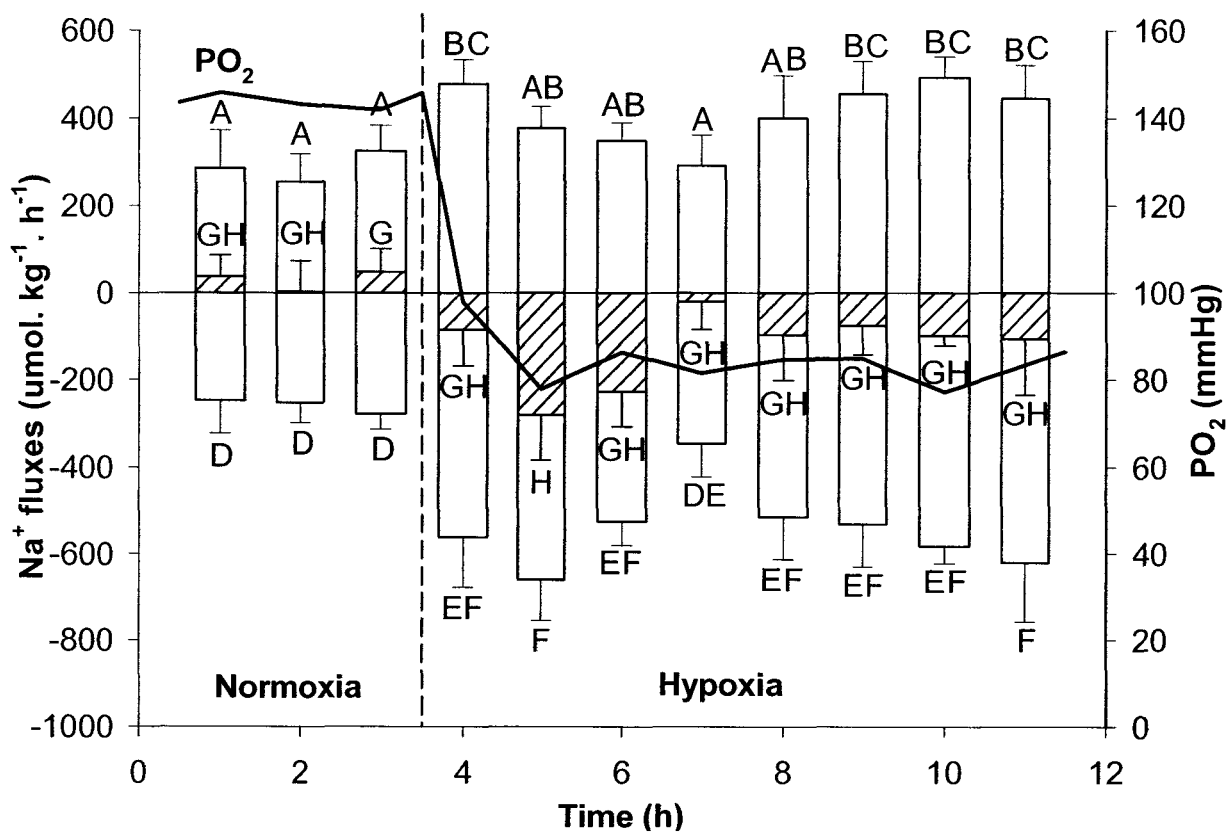


**Figure 5:** Mean ammonia excretion rates of rainbow trout (N=8) subjected to acute induction of hypoxia (~80 mmHg) prolonged for 8 h subsequent to a 3-h normoxic control period in experiment 3; water O<sub>2</sub> tension (black line). Values are expressed as means ± SEM. There are no significant differences present at  $P \leq 0.05$ .

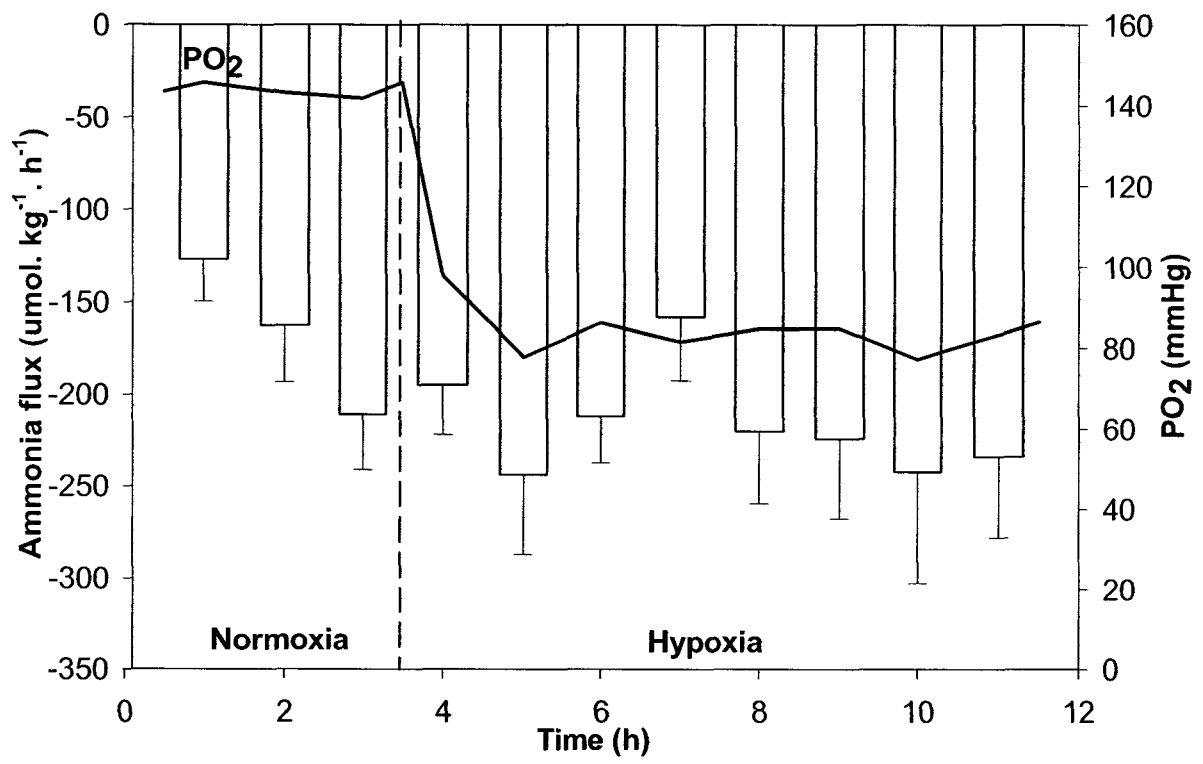


**Figure 6:** Mean potassium ( $K^+$ ) net flux rates of rainbow trout (N=8) subjected to an acute induction of hypoxia (~80 mmHg) prolonged for 8 h subsequent to a normoxic 3 h control period in experiment 3; water  $O_2$  tension (black line). Values are expressed as means  $\pm$  SEM. The asterisks denote a significant difference between overall mean values of control and hypoxic exposures ( $P \leq 0.05$ ).

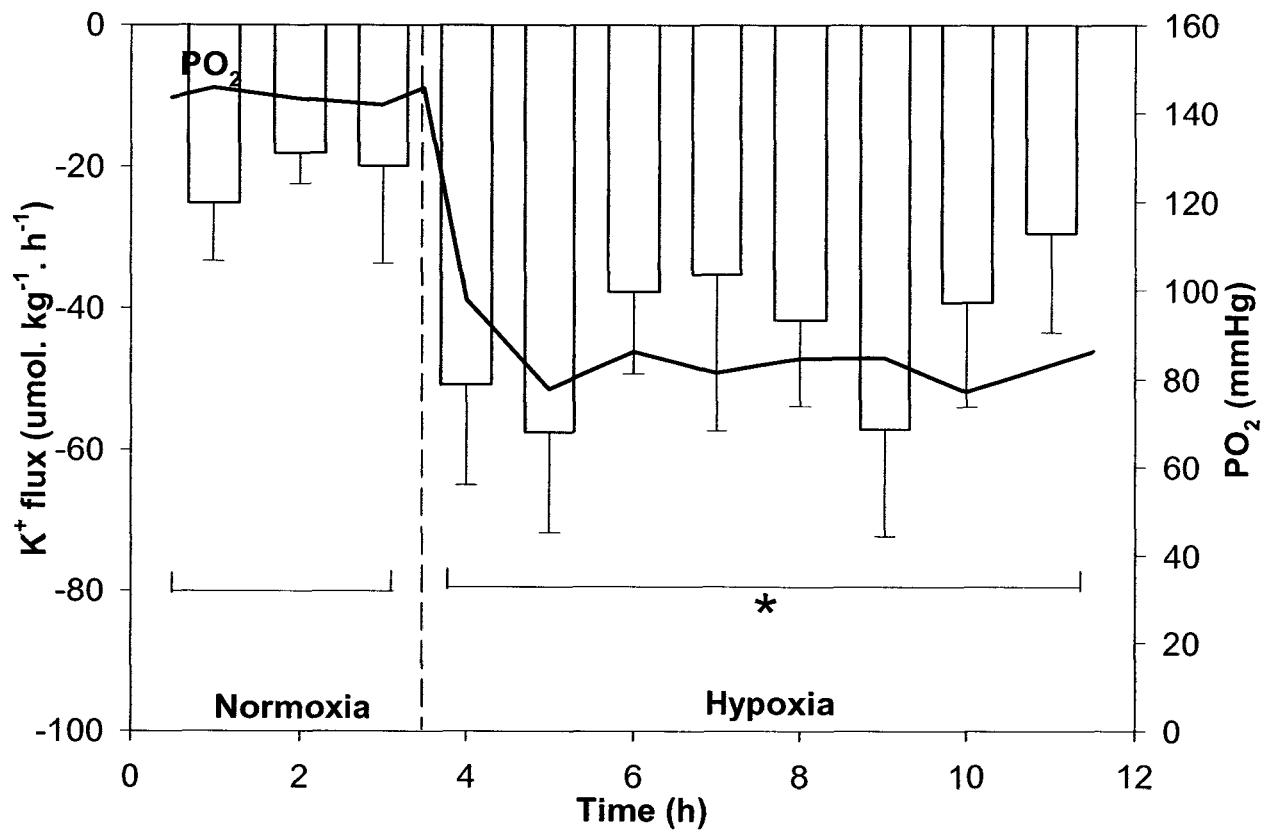


**Figure 7:** Diffusive water exchange rates ( $k$ ) of rainbow trout (N=8) to acute induction of hypoxia (~80 mmHg) for 4 h followed by an acute restoration of normoxia in experiment 4. Values are expressed as means  $\pm$  SEM. Means sharing the same letter of the same case are not significantly different from one another at  $P \geq 0.05$ .

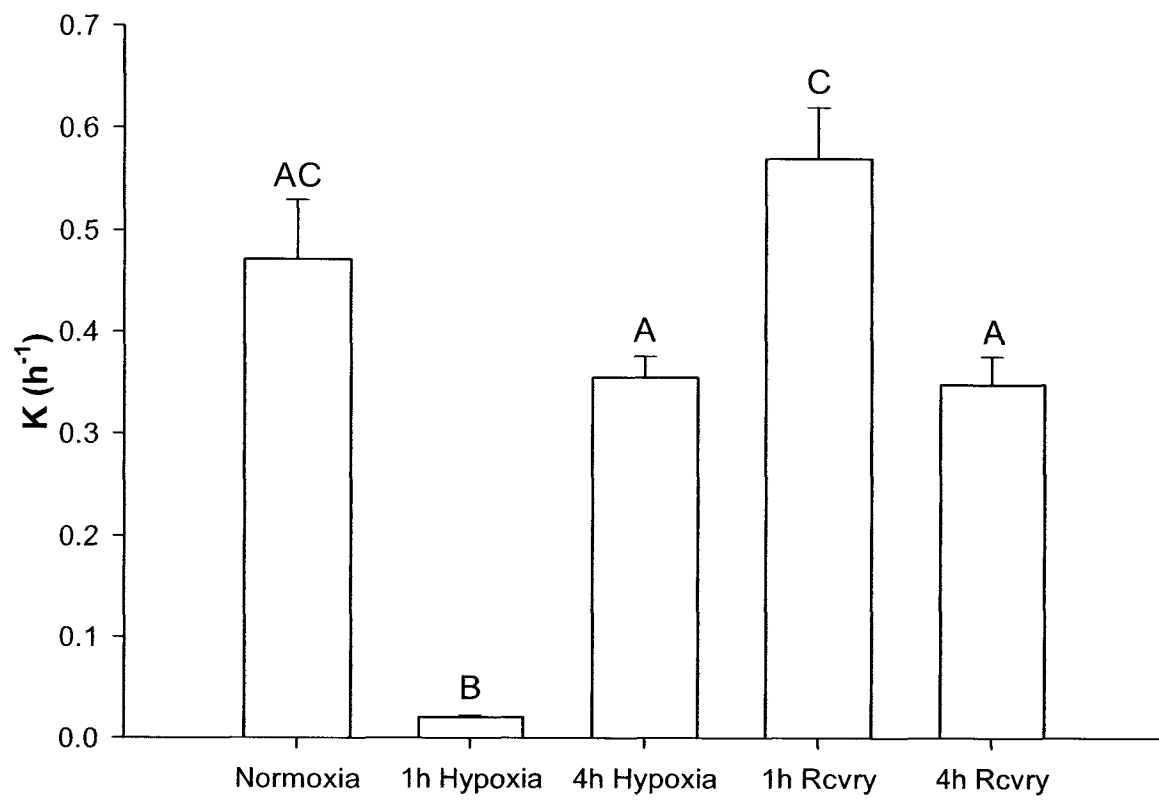


**Figure 8:** Gill Na<sup>+</sup>/K<sup>+</sup>-ATPase and H<sup>+</sup>-ATPase activity changes in adult rainbow trout (N=8 per sampling time) in response to acute induction of hypoxia (~80 mmHg) for 4 h followed by normoxic recovery in experiment 5. Values are expressed as means ± SEM. Means sharing the same letter of the same case are not significantly different from one another at  $P \geq 0.05$ .

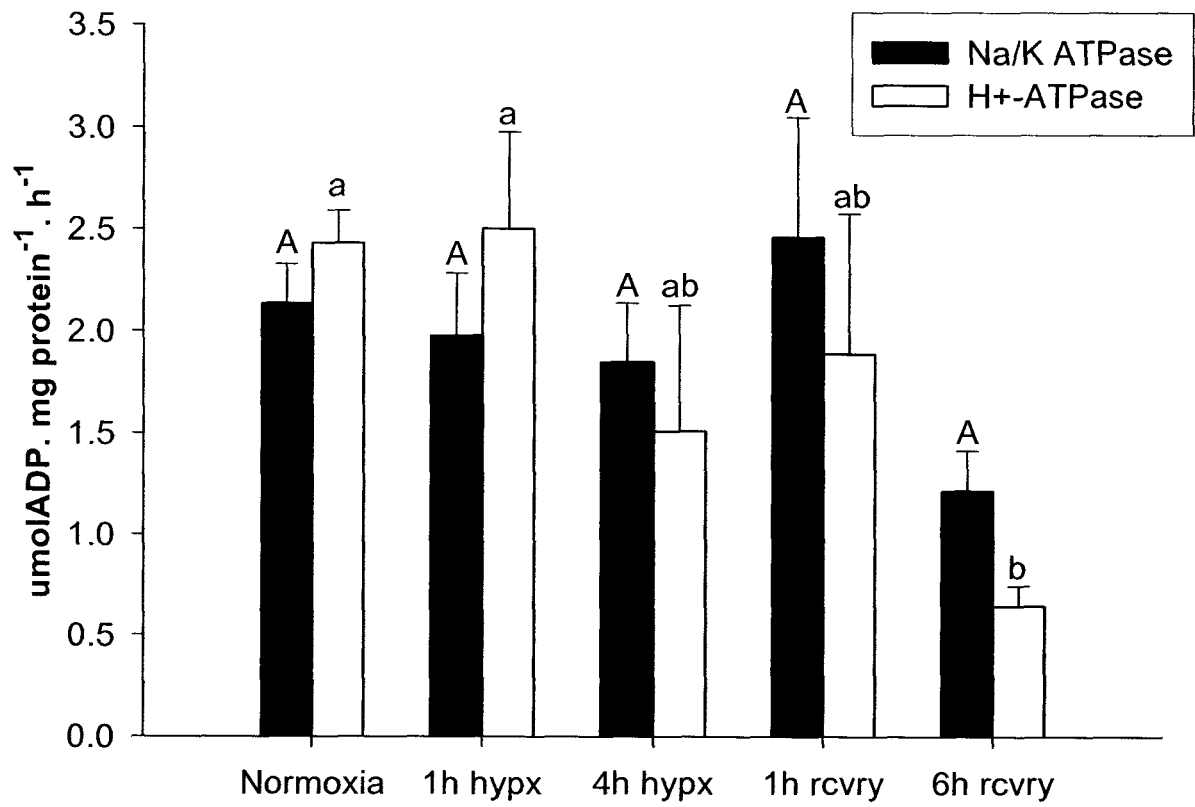


**Figure 9:** Trailing edge of gill filament of adult rainbow trout from experiment 5. Normoxia (control), SEM.

- A.** Filament epithelium below respiratory lamellae. Note clusters of mitochondria-rich cells, MRCs, (asterisks) and solitary MRCs bearing long microvilli (whitehead arrows).
  
- B.** Interlamellar region of filament epithelium. Clusters of 3-5 MRCs with apical surfaces ornamented with short microvilli (asterisks). Note MRCs with long microvilli located below interlamellar regions (whitehead arrows).
  
- C.** Cluster of four MRCs with slightly convex apical surfaces bearing long and straight microvilli.
  
- D.** Clusters of two MRCs with short microvilli. Note presence of small concave apical crypts

L- lamella; PVC- pavement cell.

Scale bars: A, B- 10 $\mu$ m; C, D- 5 $\mu$ m.

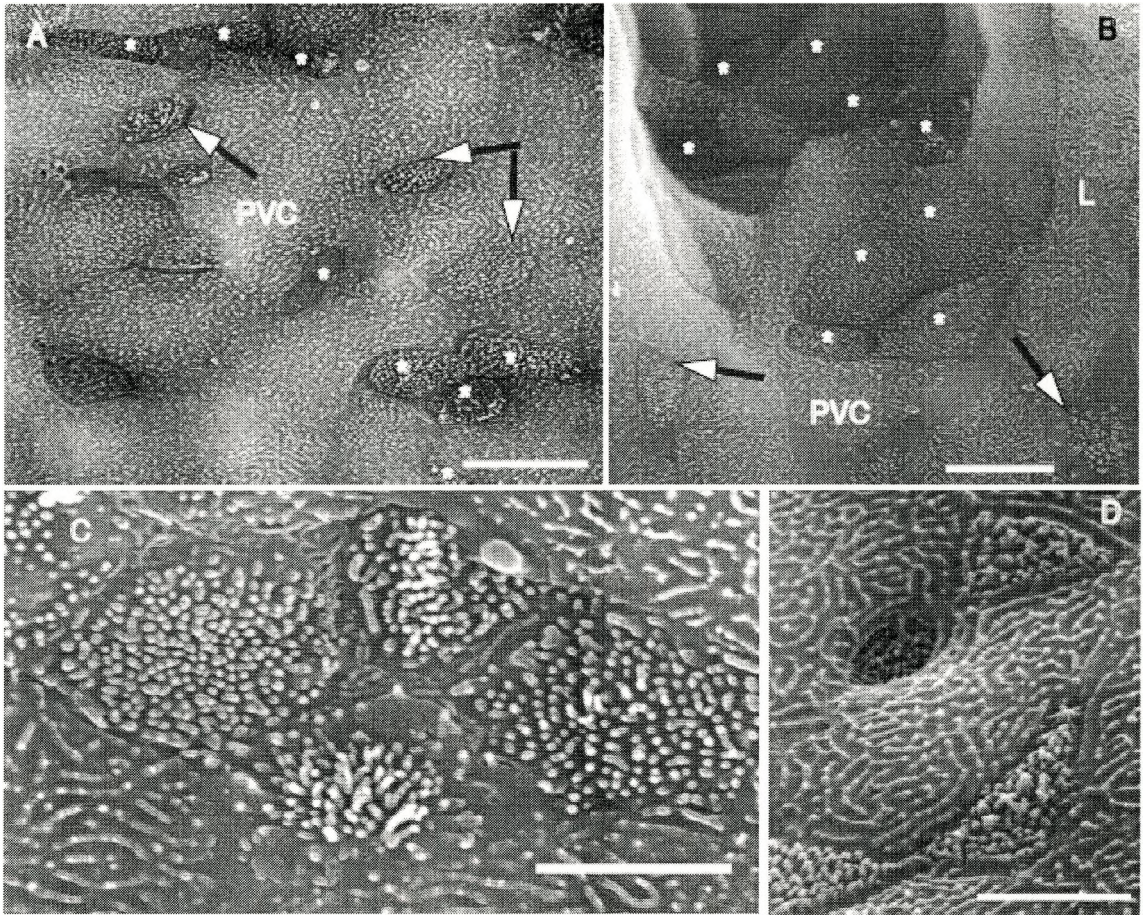


**Figure 10:** Surface structure of filament epithelium of the gills of adult rainbow trout exposed to 1 h hypoxia in experiment 5. Trailing edge of filament, SEM

- A.** Huge clusters of MRCs in the interlamellar regions (asterisks), 2-cell clusters of MRCs below this area (asterisks). Large solitary MRCs with convex apical surfaces with knob-like or completely reduced microvilli (blackhead arrows) and MRCs with “carpet-like” appearance due to highly interdigitated microvilli (white arrow)
  
- B.** MRCs indicated by blackhead arrow
  
- C.** Two MRCs indicated by white arrow

MC- mucous cell. Scale bars: A- 10  $\mu\text{m}$ ; B, C- 5  $\mu\text{m}$ .

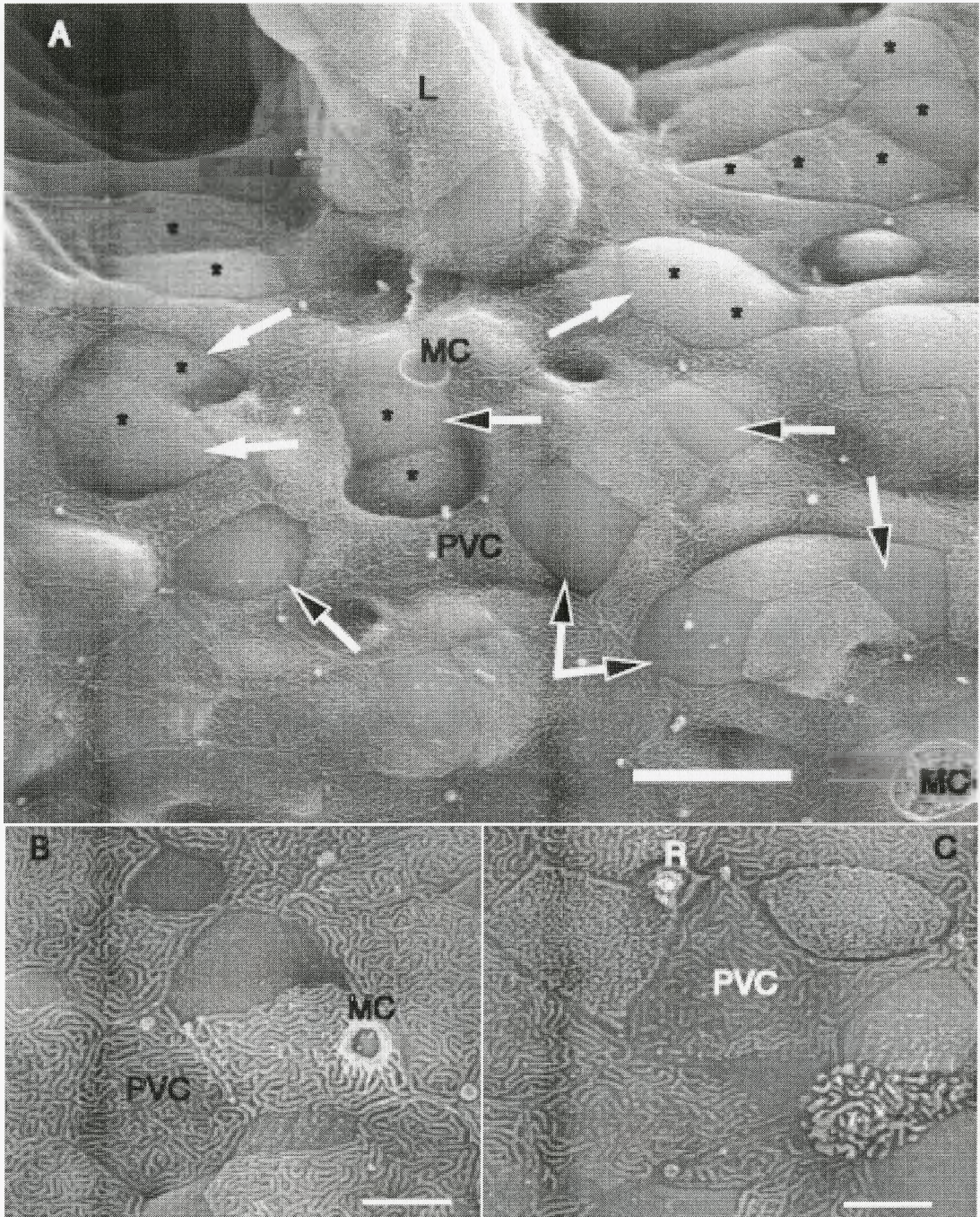


**Figure 11:** Surface structure of filament epithelium of the gills of adult rainbow trout exposed to 4h hypoxia in experiment 5. Trailing edge of filament, SEM

**A, B.** Lesser number of MRCs, no cell clusters. Solitary MRCs in the interlamellar area and below have either convex surfaces with knob-like microvilli (blackhead arrow) or flat carpet-like appearance (white arrows). Huge globs of mucus produced by MCs (B)

Scale bars: A, B – 10  $\mu\text{m}$ .

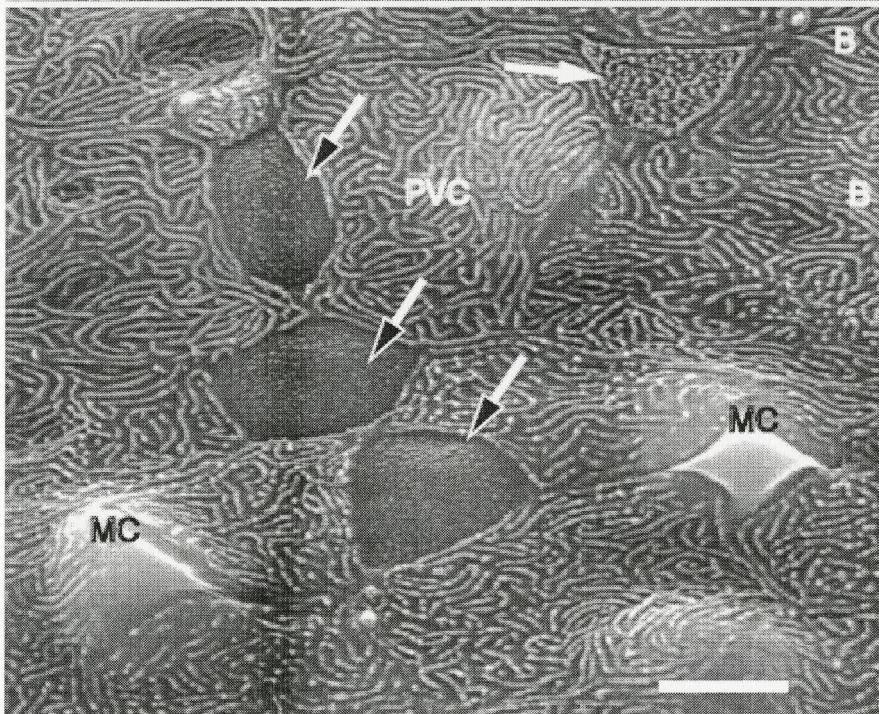
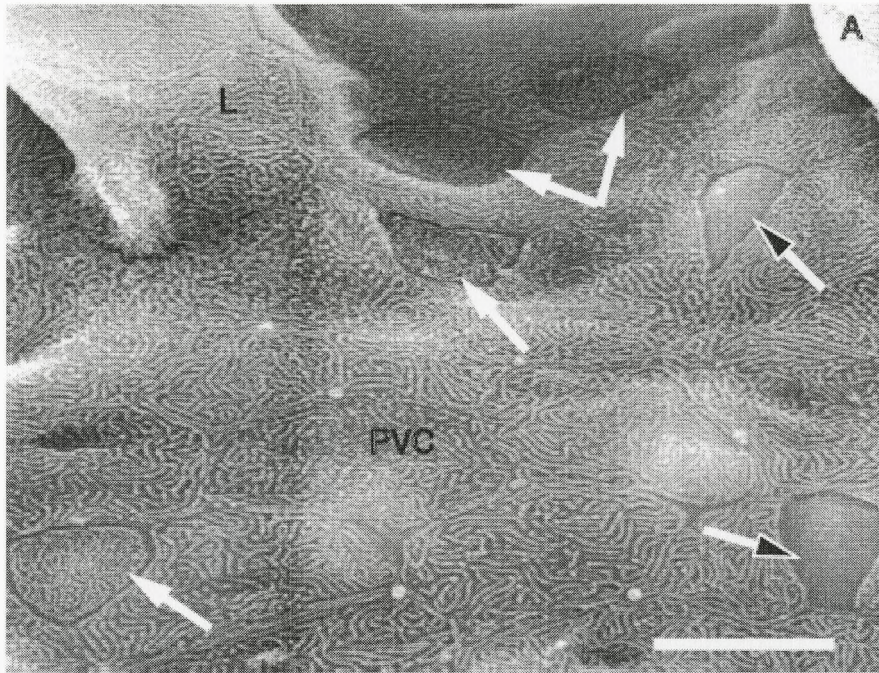


**Figure 12:** Surface structure of filament epithelium of the gills of adult rainbow trout exposed to hypoxia and a 6h recovery period in normoxic water in experiment 5. Trailing edge of filament, SEM:

- A.** Clusters of MRCs with extended microvilli (whitehead arrows). Solitary MRCs with convex surfaces and knob-like microvilli (blackhead arrows). Note presence of mucous cells.
- B.** Cluster of 3 MRCs. Note knob-like microvilli in middle and lower cells and longer microvilli in upper cell.
- C.** MRCs with carpet-like apical surface.

Scale bars: A- 10  $\mu\text{m}$ ; B, C- 5 $\mu\text{m}$ .

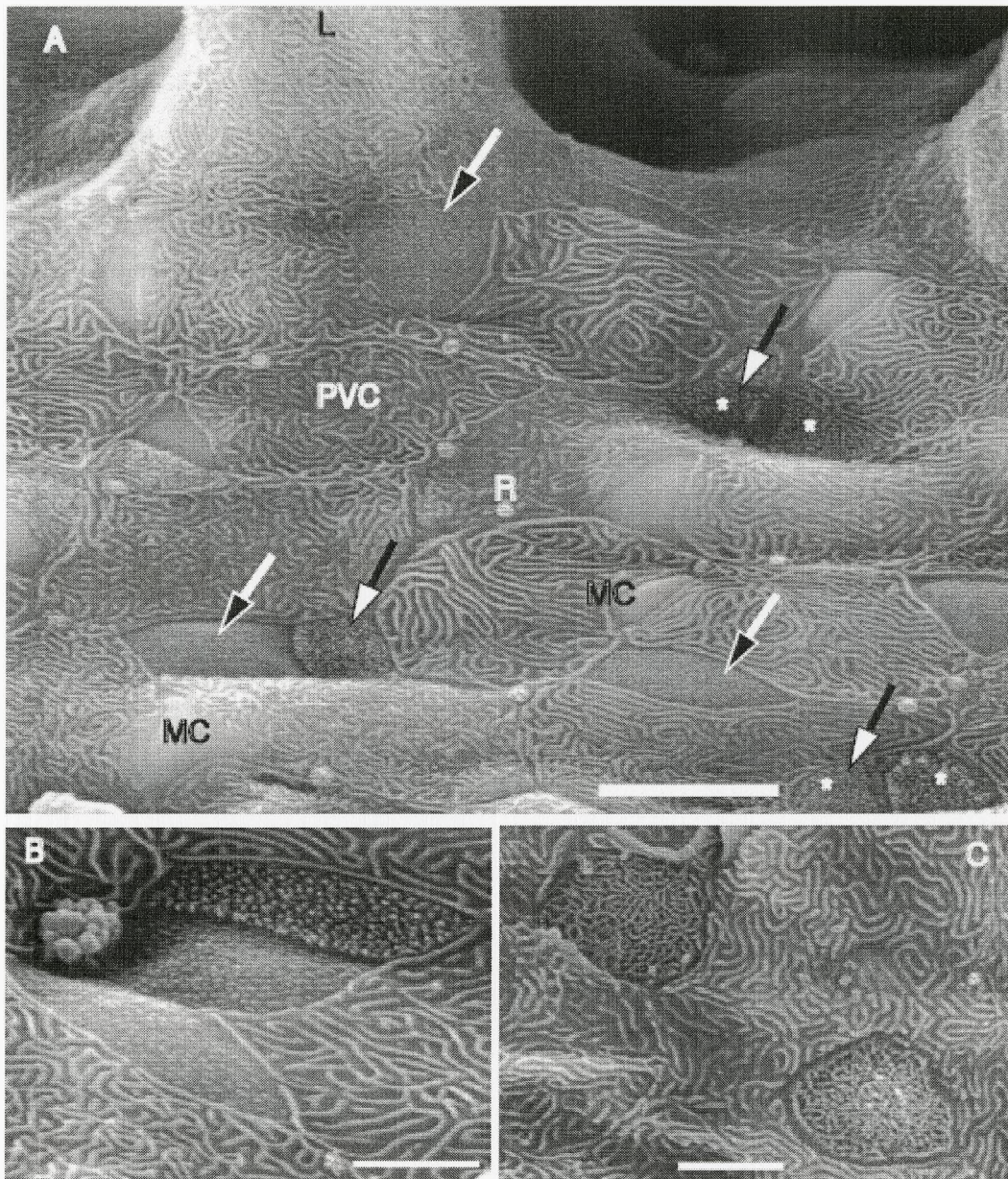
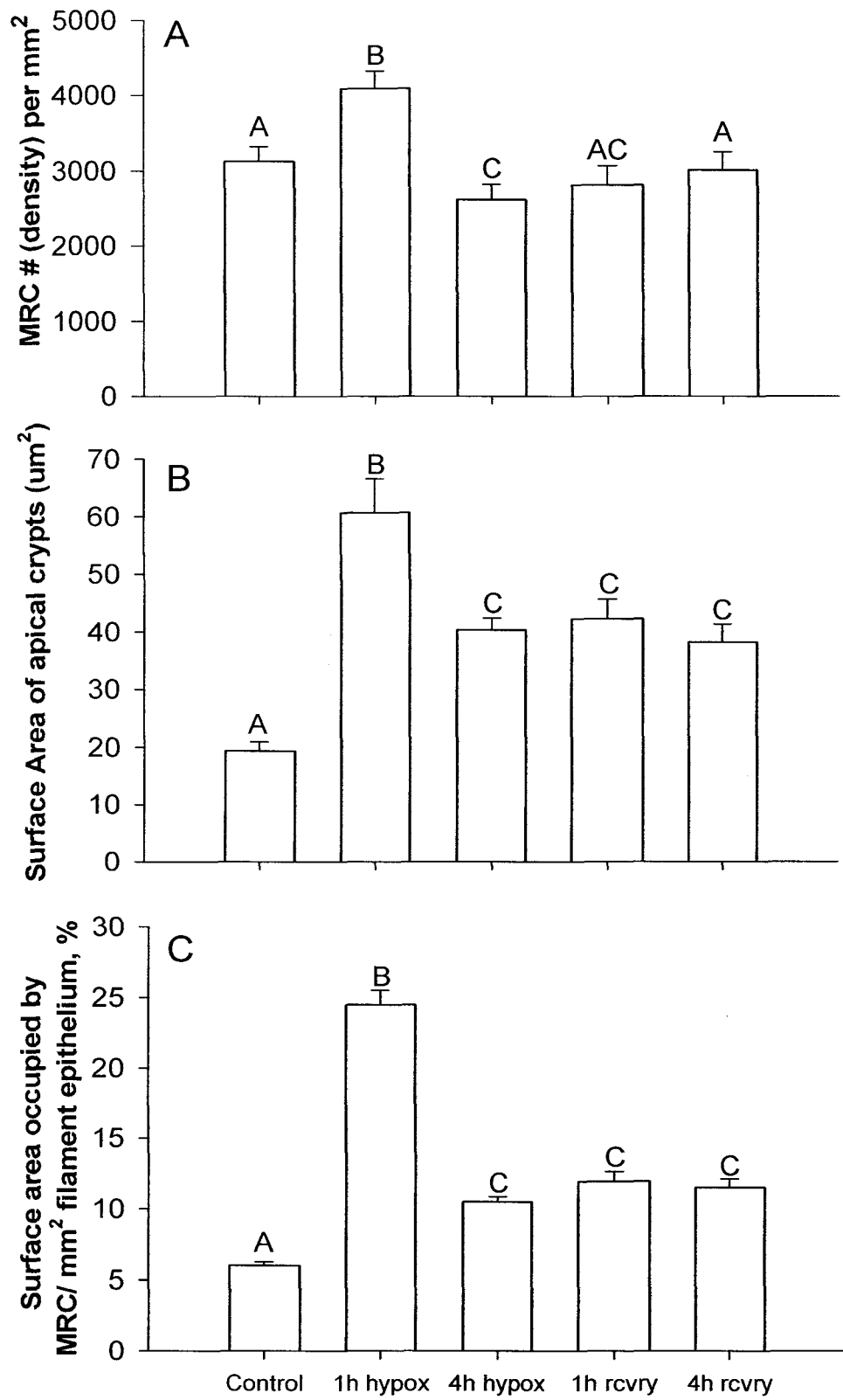


**Figure 13:** Quantitative morphometric analysis of changes in mitochondria rich cells (MRCs) of the gill filament epithelium in adult rainbow trout (N=8 per sampling time) of experiment 5 in response to acute induction of hypoxia (~80 mmHg) for 4 h followed by normoxic recovery in experiment 4. (A) MRC density in the filament epithelium, (B) Surface area of apical crypts ( $\mu\text{m}^2$ ) and (C) Surface area occupied by MRC/ $\text{mm}^2$  in the filament epithelium, %. Values are expressed as means  $\pm$  SEM. Means sharing the same letter are not significantly different from one another at  $P \geq 0.05$ .



### CHAPTER 3

#### **Investigating the effects of feeding on the osmorepiratory compromise during severe hypoxia in two hypoxia-tolerant freshwater species.**

##### **Abstract:**

We investigated the effects of feeding on the “osmorepiratory compromise” at the branchial epithelium during hypoxia in two hypoxia-tolerant species; the Amazonian oscar *Astronotus ocellatus* and the common goldfish *Carassius auratus*. Although both species exhibit the osmorepiratory compromise during severe hypoxia, the effects of feeding on this phenomenon differed between these species. Unidirectional flux measurements with  $^{22}\text{Na}$  indicated significantly greater rates of  $J_{\text{influx}}^{\text{Na}}$  and  $J_{\text{efflux}}^{\text{Na}}$  in fed goldfish versus starved goldfish during normoxia. Furthermore, fed goldfish also demonstrated greater ammonia excretion and  $\text{K}^+$  loss to the water compared to starved goldfish. Fed goldfish significantly depressed  $J_{\text{efflux}}^{\text{Na}}$  rates, ammonia excretion and  $\text{K}^+$  loss to the water with moderate ( $\sim 100$  mmHg) and severe ( $\sim 40$  mmHg) hypoxia.  $J_{\text{influx}}^{\text{Na}}$  rates did not change. In contrast, starved fish displayed no depression in unidirectional  $\text{Na}^+$  fluxes and  $\text{K}^+$  loss rates, and depressed ammonia excretion only with severe hypoxia. Differences between fed and starved oscar were generally opposite to those seen in goldfish, and changes during hypoxia were more apparent. During normoxia, fed oscars had lower  $J_{\text{influx}}^{\text{Na}}$  rates, ammonia excretion and  $\text{K}^+$  loss to the water compared to starved fish. With severe hypoxia ( $\sim 10$ - $20$  mmHg), although both fed and starved fish depressed their unidirectional  $\text{Na}^+$  fluxes, ammonia excretion and  $\text{K}^+$  loss to the water, relative changes were greater and occurred more rapidly in starved fish. In goldfish, branchial  $\text{Na}^+/\text{K}^+$ -ATPase and  $\text{H}^+$ -ATPase activity did not change with acute hypoxia (4-h at  $\text{PO}_2 \sim$

40 mmHg) and normoxic recovery. Additionally, oscars exhibited no changes in  $\text{Na}^+/\text{K}^+$ -ATPase and  $\text{H}^+$ -ATPase activity between fed and starved fish or between normoxic and severe hypoxic exposures. Examination of oscar gill filament morphology by scanning electron microscopy revealed a high density of single and clustered mitochondria-rich cells (MRCs) in both fed and starved fish under normoxia. Furthermore, starved oscars had significantly lower MRC density, average surface area and % surface of the filament occupied by the MRCs compared to fed fish. Acute hypoxia ( $\text{PO}_2 \sim 10\text{-}20$  mmHg for 3 h), caused a reduction in the number, average surface area and % surface area occupied by the apical crypts of MRCs exposed to ambient water in fed and starved oscars. Hypoxic exposure also affected the distribution of MRCs leaving them almost exclusively in the filament epithelium in these fish. Overall, our results indicate that feeding/ starvation induces opposite effects on the responses to hypoxia of oscars versus goldfish with respect to gill ionoregulatory function. However, there is a general reduction in gill permeability in response to severe hypoxia in both of these hypoxia-tolerant species regardless of feeding regime

**Introduction:**

Contrary to the investigations of the osmorepiratory compromise (Randall et al., 1972; Nilsson, 1986) during exercise in fish (Wood and Randall 1973a,b; Gonzalez and McDonald, 1992, 1994), recently there has been a rekindled interest in investigating its adaptation under hypoxic conditions in freshwater fish (Wood et al., 2007, Iftikar et al., 2008 submitted = chapter 2). The Amazonian oscar, *Astronotus ocellatus*, which is extremely tolerant of hypoxia (Almeida-Val and Hochachka, 1995; Muusze et al., 1998; Almeida-Val et al., 2000), exhibits rapid and profound reductions in unidirectional  $\text{Na}^+$  fluxes and ammonia excretion in response to acute severe hypoxia, indicating an overall occurrence of reduced gill permeability. This is an adaptive strategy employed by these freshwater fish to their environment, as they cannot escape the hypoxic conditions they face in the Amazon (Wood et al., 2007). However, when ionoregulatory responses to hypoxia were investigated in the rainbow trout, a hypoxia-intolerant freshwater fish often considered to be a “model” species, complex changes in gill ionoregulatory function were observed. In trout, it was found that the direction and magnitude of  $\text{Na}^+$  flux varied with the extent and duration of the hypoxia regime and were not as precise as those in the oscar (Iftikar et al., 2008 submitted = chapter 2).

These recent findings of diverse inter-specific patterns in the osmorepiratory compromise under hypoxia stimulated us to examine its regulation in two hypoxia-tolerant species to highlight possible intra-specific differences under a dual stress situation of hypoxia plus feeding. The gills are considered to be the major site of active ionic uptake in freshwater fish (Heisler, 1984). The diet is another principal route by

which freshwater teleosts can obtain salts (Smith et al., 1989), yet in order to avoid ‘complicating’ effects of feeding and the host of responses that this leads to in fish, many studies investigating osmoregulation deliberately withhold food (Taylor et al., 2007). Examining osmoregulation in unfed fish merely provides insight into the physiology of the fish under starvation – a situation only encountered during specific times in their life cycle such as cessation of feeding during migration, cold/frigid temperatures and nest guarding (Wood, 2001). However, what must be realized is that the effects of feeding and digestion on homeostatic processes, such as osmoregulation, highlight important physiological mechanisms that may not be as obvious in unfed animals. Consequently, our first goal was to examine the influence of feeding on the ‘osmorepiratory compromise’, specifically on ion regulation at the gill during hypoxia in two hypoxia-tolerant species, the Amazonian oscar and the common goldfish. We hypothesized that feeding status will influence ion-regulation by possibly reducing the amount of active ion uptake and increasing diffusive ion losses due to the extra salt available from food (Smith et al., 1989, 1995).

In this study, we chose to examine if feeding status affected ion regulation at the gill epithelium in the Amazonian oscar under severe hypoxic conditions. Oscars respond to severe hypoxia by suppressing their metabolic rate and thereby survive close to 16 h of severe hypoxia (Muusze et al., 1998). This depressed metabolic rate during severe hypoxia postpones anaerobic glycolysis and prevents early acidosis (Muusze et al., 1998). Oscars live in the Amazon basin which is subjected to periodic increases in water levels where extensive areas are flooded and covered by macrophytes (Muusze et al., 1998).

These flood plains, also known as varzeas are subjected to drastic oxygen fluctuations and comprise the habitat of oscars who migrate to feed here (Muusze et al., 1998). Therefore, these freshwater cichlids face a dual stress situation in their natural environment. Furthermore, since oscars live in ion-poor waters (Muusze et al., 1998; Almeida-Val et al., 2000) and may face a limited branchial  $\text{Na}^+$  uptake, dietary salt will probably play a significant role in ionoregulation (D'Cruz and Wood, 1998; Wood et al., 2002). Subsequently, we hypothesized that there will be a considerable difference between ion-regulation in fed and starved oscars in response to severe hypoxia. Specifically, we postulated that both fed and starved fish will suppress their unidirectional  $\text{Na}^+$  fluxes (based on Wood et al., 2007), however, overall fed fish will have a lower uptake of  $\text{Na}^+$  from the water due to the availability of supplementary salt from the diet.

We also chose to investigate feeding and its effects on the osmorepiratory compromise in the very-hypoxia tolerant common goldfish, *Carassius auratus*. Goldfish exhibit strong metabolic depression (to approximately 30% of normal) during anoxic conditions and survive close to 2 days of very limited oxygen availability and still remain active (Nilsson and Renshaw, 2004). These fish rely on large muscle and liver glycogen reserves, reduced metabolism, and avoidance of lactic acidosis (brought on by severe oxygen lack) by converting lactate to ethanol and  $\text{CO}_2$ . These end products can be excreted through the gills, helping goldfish to avoid the severe acid-base disturbances that would otherwise occur during hypoxia (Shoubridge and Hochachka, 1980). Goldfish further maintain, rather than suppress  $\text{Na}^+ - \text{K}^+$  ATPase activity in hepatocytes assisting

with the conversion of lactate to ethanol when faced with low environmental oxygen (Krumschnabel et al., 2000). Although there is a substantial background on goldfish physiology during anoxic conditions (e.g. Shoubridge and Hochachka, 1980; Nilsson and Renshaw, 2004), ionoregulatory functions under hypoxia have not been studied in detail in this common hypoxia-tolerant cyprinid species. Therefore, firstly, we wanted to investigate if goldfish exhibited a compromise between ion uptake and oxygen uptake during severe hypoxia similar to that which has previously been studied in the oscar (Wood et al., 2007) and the rainbow trout (Iftikar et al., 2008 submitted = chapter 2). Secondly, if such a compromise was made at the gill, we wished to test whether feeding status influenced this phenomenon. Unlike oscars, goldfish are primarily ornamental fish bred for aesthetic purposes and adapted to ion-rich waters of aquaria (Balon, 2004). Consequently, we hypothesized that although there will be differences between fed and starved goldfish in the uptake of ions, it would not be as significant as in the oscar due to the additional supply of ions they receive from the water, minimizing the importance of diet as a source for salts.

Secondly, we wanted to understand whether feeding status affected cellular function during hypoxia in oscar and in goldfish. Active  $\text{Na}^+$  uptake at the freshwater teleost gill epithelium is powered by  $\text{Na}^+/\text{K}^+$ -ATPase and  $\text{H}^+$ -ATPase in ionocytes (Avella and Bornancin, 1989; Evans et al., 2005). ATP production to power these pumps is maintained by oxidative phosphorylation of cellular glucose and glycogen reserves. Therefore, a tight coupling exists between oxygen consumption and energy demand (Evans et al., 2005). Fed fish have more cellular glycogen reserves due to dietary supply

of glucose (Driedzic and Short, 2007). However, actual oxidization of these glycogen reserves for ATP production is dependent on oxygen availability. So the two key indicators of severe oxygen deprivation are a rapid depletion of cellular ATP and a loss of intracellular  $K^+$  as the  $Na^+/K^+$  pump begins to fail (Boutilier and St-Pierre, 2000). We wanted to understand if severe oxygen deprivation was faced by oscar and goldfish at the level of the gill cells during hypoxia, by measuring the activity of gill  $Na^+/K^+$  ATPase and  $H^+$ -ATPase enzymes, and if feeding affected this activity. Although fed fish have higher glycogen reserves for phosphorylation, since oxygen supply is the limiting factor, we hypothesized that overall there will be a downregulation of  $Na^+,K^+$ -ATPase and  $H^+$ -ATPase activities in order to save metabolic costs, however, feeding status would not affect the rate of this downregulation. Coupled with these ideas, we also hypothesized that  $K^+$  leakage rates to the water would decrease during hypoxia as both these species are hypoxia-tolerant and are able to maintain cellular integrity.

In light of recent reports that severe hypoxic exposure can result in rapid, marked remodelling of the gills of hypoxia-tolerant species (Sollid and Nilsson, 2006; Nilsson, 2007; Matey et al., 2008), we further examined gill surface morphology using scanning electron microscopy in the Amazonian oscar. Our hypothesis in relation to cellular changes was that as oscar are hypoxia-tolerant, structural changes in branchial cells should be observed. Therefore we examined epithelial composition, cell distribution on the filament and lamellae, and surface structure of the cell composing the outermost layer of epithelia (directly contacts ambient water) under severe hypoxia for apparent alterations.

Our final objective was to examine nitrogenous-waste excretion in both these species in response to hypoxia, and the influence of feeding on this excretion. Fed teleosts, in comparison to starved fish, generally have a substantial excretion of nitrogenous waste (mainly in the form of ammonia) which is considered an excess fraction of nitrogen not retained for growth from the diet (Alsop and Wood, 1997; Wood, 2001). Therefore, with both oscar and goldfish, we hypothesized that fed fish will have a higher excretion of ammonia to the water compared to starved fish during normoxia and hypoxia, due to excess nitrogen provided by the diet not being retained and excreted instead. Secondly we hypothesized that both of these hypoxia-tolerant species will suppress their ammonia excretion to the water with hypoxic exposure, regardless of feeding status. For oscar, this was observed by Wood et al., (2007) and was attributed to overall reduction in gill permeability with hypoxia observed in this species.

**Methods and Materials:***Experimental Animals:*Goldfish:

Goldfish, *Carassius auratus*, were obtained from Big Al's pet store in Hamilton, ON and acclimated for at least 2 weeks to  $15 \pm 0.5^\circ\text{C}$  in flowing dechlorinated Hamilton tapwater ( $\text{Na}^+ = 0.6$ ;  $\text{Cl}^- = 0.7$ ;  $\text{K}^+ = 0.05$ ;  $\text{Ca}^{2+} = 1.0$ ,  $\text{Mg}^{2+} = 0.2 \text{ mmol L}^{-1}$ ; dissolved organic carbon,  $3.0 \text{ mg C. L}^{-1}$ ;  $\text{pH} = 8.0$ ) under a 12-h light photoperiod. Fish were fed commercial goldfish flakes (Big Al's flake food, Markham ON) every two days (ration = approximately 2% of body mass) until experiments, unless the pre-treatment required starvation as detailed below. Animals were cared for in accordance with the principles of the Canadian Council on Animal Care and protocols were approved by the McMaster Animal Care Committee.

Oscar:

Oscars, *Astronotus ocellatus*, were obtained from Sítio dos Rodrigues (Km 35, Rod. AM-010, Brazil), and were moved to the Ecophysiology and Molecular Evolution Laboratory of the Instituto Nacional de Pesquisas da Amazônia (INPA), in Manaus, Brazil. Fish were held for at least one month in 500 L tanks on a partially recirculating water filtration system at  $28 \pm 3^\circ\text{C}$ . The holding and experimental water was typical Amazonian soft water taken from a well on the INPA campus ( $\text{Na}^+ = 0.035$ ,  $\text{Cl}^- = 0.036$ ,  $\text{K}^+ = 0.016$ ,  $\text{Ca}^{2+} = 0.018$ ,  $\text{Mg}^{2+} = 0.004 \text{ mmol L}^{-1}$ ; dissolved organic carbon,  $0.6 \text{ mg C/l}$ ;  $\text{pH} 6.5$ ). Fish experienced a natural photoperiod and were fed daily with commercial

pellets (ration = approximately 1% of body mass), unless otherwise noted. All experimental procedures complied with Brazilian and INPA animal care regulations.

All protocols were designed to maximize the accuracy of branchial flux measurements over the critical exposure, and to ensure that the external to internal specific activity ratios remained high for greatest accuracy in radioisotopic flux determinations while ensuring that water ammonia levels remained low. Therefore different sizes of fish, container volumes, and experimental durations were used in different trials.

*Exposure Regimes:*

Goldfish:

***1. Unidirectional Na<sup>+</sup> uptake and net K<sup>+</sup> and ammonia fluxes in response to a range of acute (4 h) hypoxic exposures.***

In an initial range-finding study, goldfish (mass =  $3.64 \pm 0.16$  (60) g; mean  $\pm$  1 SEM (*n*)) were transferred in groups of 10 to small plastic aquaria (4 L) covered with duct tape for darkening, and left overnight. Experimental chambers were continuously supplied ( $0.5 \text{ L min}^{-1}$ ) with temperature-controlled ( $15 \pm 0.5^\circ\text{C}$ ) tapwater and submerged in an external water bath to maintain external temperature. The chambers were well aerated so as to maintain  $\text{PO}_2 \geq 140 \text{ mmHg}$  (normoxia). The experimental design consisted of 4-h exposures, where each randomly selected experimental group of fish were exposed to either normoxia or one of a range of  $\text{PO}_2$  levels of 120, 100, 80, 60 and 40 mmHg. Hypoxia was induced by a  $\text{N}_2$ /air mixture which was empirically adjusted

using a gas mixing pump (Wösthoff 301-af) to the desired severity of hypoxia. These fish were not starved prior to experimentation.

During the flux measurement, the aquaria were operated as closed systems at a volume of 2 L. Radioisotope ( $^{22}\text{Na}^+$  3.0 $\mu\text{Ci}/\text{tank}$ , PerkinElmer®, Boston MA) was added at 0 h. After an initial 10 min mixing period, a water sample (30 ml) was taken and subsequently at 1-h intervals until the end of the experiment for analysis of external  $[\text{Na}^+]$ , external  $[\text{K}^+]$ , total external ammonia ( $[\text{Amm}]$ ), and  $^{22}\text{Na}^+$  radioactivity (cpm). Water  $\text{PO}_2$  was monitored (1-ml samples) at the beginning of each 1-h flux during the 4-h exposure. At the end of the experiment, fish were rapidly anaesthetized with neutralized 0.0075 g.  $\text{L}^{-1}$  MS-222, killed via cephalic concussion, weighed and transferred to 15 ml plastic vials for gamma radioactivity counting to determine whole body uptake of  $^{22}\text{Na}^+$ .

***2. Unidirectional  $\text{Na}^+$  influxes, effluxes, net fluxes, net  $\text{K}^+$  and net ammonia fluxes in response to normoxia, 4-h moderate ( $\text{PO}_2 = 100 \text{ mmHg}$ ) and severe ( $\text{PO}_2 = 40 \text{ mmHg}$ ) hypoxia in fed and starved goldfish.***

Goldfish were separated into two groups ( $n=30$ ) where the first group were fed their regular 2% ration 24 h before experimental exposure (i.e. fed treatment). The second group was starved for 10 days prior to experimental exposure (i.e. starved treatment). Approximately 24 h prior to experiment, goldfish from each of the two pre-treatments ( $n = 10$  per sampling point, 60 in total, mean (SE) mass  $2.26 \pm 0.13$  g) were transferred to experimental chambers ( $n = 1/\text{chamber}$ ) which were 0.3 L sealable glass containers with flow-through water supply ( $0.1 \text{ L min}^{-1}$ ) and left overnight. Experimental containers were continuously supplied ( $0.5 \text{ L min}^{-1}$ ) with temperature-controlled ( $15 \pm 0.5^\circ\text{C}$ ) tapwater

and submerged in an external water bath to maintain external temperature. The chambers were well aerated so as to maintain  $PO_2 \geq 140$  mmHg (normoxia). The experimental design consisted of 4-h exposures, where each randomly selected experimental group of fed and starved fish ( $n=10$ ) were exposed to either normoxia or one of two hypoxia levels (100 or 40 mmHg). Hypoxia was induced by a  $N_2$ /air mixture which was empirically adjusted using a gas mixing pump (Wösthoff 301-af) to a desired level of hypoxia ( $PO_2 = 100$  or 40 mmHg).

During the experiment, experimental chambers were operated as closed systems at a volume of 0.225 L. The experiment was designed to measure  $Na^+$ ,  $K^+$  and ammonia fluxes over 4h during either normoxia or hypoxia exposures of  $PO_2$  100 or 40 mm Hg. Radioisotope ( $^{22}Na^+$ , 0.338 $\mu$ Ci/chamber) was added at 0 h of the exposure period. After an initial 10-min mixing period, a water sample (5 ml) was taken and subsequently at 1-h intervals till the end of the experiment for analysis of external [ $Na^+$ ], external [ $K^+$ ], total external ammonia ([Amm]), and  $^{22}Na^+$  radioactivity (cpm). Water  $PO_2$  was monitored (0.5-ml samples) at the beginning of each 1-h sample time to ensure  $PO_2$  remained at the desired level. At the end of the 4-h exposure, fish were rapidly anaesthetized with neutralized 0.0075 g. L<sup>-1</sup>MS-222, killed via cephalic concussion, weighed and transferred to 15 ml plastic vials for gamma radioactivity counting to determine whole body uptake of  $^{22}Na^+$ .

***3. The effect of acute hypoxia (4h) and normoxic recovery on branchial  $Na^+/K^+$  - ATPase and  $H^+$  - ATPase activities goldfish.***

Goldfish ( $n = 6$  per sampling point, 30 in total, mass  $4.01 \pm 0.17$  g) were transferred to the same flux boxes as used in experiment 1, with flow-through water supply ( $0.5 \text{ L min}^{-1}$ ), and left overnight. The experimental design consisted of a control normoxic period, 4-h hypoxia exposure and a subsequent 3-h normoxic recovery period. Hypoxia was induced by a  $\text{N}_2$ /air mixture which was empirically adjusted using a gas mixing pump (Wösthoff 301-af) to a desired level of hypoxia ( $\text{PO}_2 \text{ w} = \sim 40 \text{ mmHg}$ ). These fish were not starved prior to experimentation.

During the experiment, flux boxes were operated as closed systems at a volume of 2 L. Fish were rapidly killed with a lethal dose of anaesthetic ( $0.5 \text{ g L}^{-1}$  neutralized MS-222) during normoxia, after 1-h and 4-h of hypoxia, and after 1-h and 3-h of normoxic recovery. Water  $\text{PO}_2$  (1-ml samples) was also measured at each sampling time point. Samples of gill filaments were excised. Specifically, the 2<sup>nd</sup> gill arch was snap-frozen in liquid  $\text{N}_2$  and stored at  $-80^\circ\text{C}$  for later analysis for  $\text{Na}^+/\text{K}^+$  and  $\text{H}^+$  - ATPase activities.

#### Oscar:

1. ***Unidirectional  $\text{Na}^+$  influxes, effluxes, net fluxes, net  $\text{K}^+$  and net ammonia fluxes in response to normoxia and progressively (4-h) severe hypoxia in fed and starved oscar.***

Oscars were separated to two groups ( $n = 10$  per fed or starved group, 20 in total, mean (SE) mass  $112.9 \pm 7.1$  g) where the first group were fed their regular 1% ration 24 h before experimental exposure (i.e. fed treatment) and the second group was starved for 10 days prior to experimental exposure (i.e. starved treatment). Experimental chambers

for fish were 3.5-liter sealable Nalgene<sup>®</sup> containers where the horizontally flattened shape fitted the morphology of the fish. The chambers were shielded with black plastic to minimize visual disturbance and fitted with individual water lines for flushing, and air-stones for air or N<sub>2</sub> gassing. The chambers were 80% submerged in a flowing water bath to maintain the experimental temperature of  $26.9 \pm 0.2$  °C. Fish were placed in these individual containers the evening before the experiment and left overnight to settle. The containers were vigorously aerated to maintain air saturated conditions during the settling period and were supplied with a continuous water flow.

During the experiment, containers were operated as closed systems at a volume of approximately 1.7 L for the 3-h control normoxic period and the subsequent 4-h hypoxic exposure. During the experiment, the O<sub>2</sub> supply was manipulated by vigorous gassing with either air or N<sub>2</sub>, followed by more gentle gassing for maintenance. PO<sub>2</sub> was maintained above 130 mm Hg during the control normoxic period and between 10-20 mmHg during the 4-h hypoxic exposure and water PO<sub>2</sub> was monitored at the midpoint of each 1-h flux using an oxygen electrode (WTW Oxi 235 oxygen meter) to ensure that desired PO<sub>2</sub> levels were maintained. At the beginning of the experiment, radioisotope (<sup>22</sup>Na<sup>+</sup> 2.0μCi/container, manufactured by New England Nuclear-Dupont, Boston, MA, and supplied by REM, São Paulo, Brazil) was added immediately and allowed to mix for 10 minutes before the 0-h water sample was taken at the start of the control normoxic period. After an initial 10 min mixing period, a water sample (20 ml) was taken and subsequently at 1-h intervals till the end of the experiment for analysis of external [Na<sup>+</sup>],

external  $[K^+]$ , total external ammonia ( $[Amm]$ ), and  $^{22}Na^+$  radioactivity (cpm). At the end of 7 hours, the experiment was terminated and the animal was weighed.

2. *The effect of normoxia and acute severe hypoxia (3h) on branchial  $Na^+/K^+$  - ATPase and  $H^+$  - ATPase activities and gill morphology in fed and starved oscar.*

Oscar ( $n = 6$  per sampling point, 30 in total, mass  $69.3 \pm 5.4$  g) were transferred to the same flux containers as used in experiment 1, with flow-through water supply and left overnight. The experimental design consisted of exposing fed and starved ( $\sim 10$  days) oscars to a 3-h normoxic exposure and 3-h severe hypoxia exposure. During normoxia  $PO_2$  was maintained at  $> 130$  mm Hg, and hypoxia was induced by directly bubbling  $N_2$ , where  $PO_2$  was maintained between 10-20 mmHg.

During the experiment, flux boxes were operated as closed systems at a volume of  $\sim 1.7$  L. Fish were rapidly killed with a lethal dose of anaesthetic ( $0.5$  g.  $L^{-1}$  neutralized MS-222) at the end of 3-h normoxia and at the end 3-h of hypoxia. Water  $PO_2$  was monitored at the midpoint of each 1-h flux using an oxygen electrode (WTW Oxi 235 oxygen meter) to ensure that desired  $PO_2$  levels were maintained. Samples of gill filaments were excised. Specifically, the 2<sup>nd</sup> gill arch was snap-frozen in liquid  $N_2$  and stored at  $-80^\circ C$  for later analysis for  $Na^+/K^+$  and  $H^+$  - ATPase activities. The 3<sup>rd</sup> gill arch was dissected out, quickly rinsed in water and immediately fixed in cold Karnovsky's fixative (8% gluteraldehyde and 16% paraformaldehyde in a 0.4 M Sodium phosphate buffer; Karnovsky, 1965). These samples were later transported to San Diego State University, CA, USA for scanning electron microscopy (SEM).

*Analytical Methods for Fluxes and Flux Calculations:*

Water total ammonia (salicylate hypochlorite assay, Verdouw et al., 1978) was determined colorimetrically. Water total Na<sup>+</sup> and K<sup>+</sup> concentrations were measured using flame atomic absorption spectrophotometry (AAAnalyst 800, Perkin Elmer). In goldfish experiments (performed in Hamilton), both goldfish whole bodies and water samples were measured for <sup>22</sup>Na radioactivity using a gamma counter (Minaxi Auto-Gamma 5000 Series, Canberra-Packard, Meriden, CT) where absolute counts were calculated from counts per minute (cpm) values after background correction. In oscar experiments performed in Manaus, Brazil, <sup>22</sup>Na activities in water samples were measured via liquid scintillation counting (LS6500, Beckman Coulter, Fullerton, CA) on 5-ml water samples added to 5-ml of Packard Ultima Gold AB fluor (Perkin Elmer, Wellesley, MA). Again, absolute counts were calculated from counts per minute (cpm) values after background correction. Tests demonstrated that quenching was constant, so no correction was necessary.

In experiment 1 and 2 for goldfish, unidirectional Na<sup>+</sup> uptake ( $J_{influx}^{Na}$ , by convention positive) was measured based on the appearance of radioactivity in the whole body of the fish. Unidirectional Na<sup>+</sup> uptake for this experiment was calculated using the following equations based on Matsuo et al. (2004):

$$SA \text{ (average over 4 h)} = 0.2 \left( \frac{[R1]}{[ion1]} + \frac{[R2]}{[ion2]} + \frac{[R3]}{[ion3]} + \frac{[R4]}{[ion4]} + \frac{[R5]}{[ion5]} \right) \quad (1)$$

$$\text{Radioactivity in fish (R}_F\text{)} = \text{counts per minute} / W \quad (2)$$

$$J_{influx}^{Na} = R_F / SA \times T \quad (3)$$

where  $ionN$  are the  $Na^+$  concentrations in the water ( $\mu\text{mol L}^{-1}$ ) and  $RN$  are the radioactivity values ( $\text{cpm L}^{-1}$ ) of the  $^{22}\text{Na}$  at each of the 5 measurement times over the 4-h flux period,  $W$  is the weight of the fish (kg),  $T$  is the total flux period (4 h),  $SA$  is the mean specific activity of the isotope in  $\text{cpm}\cdot\mu\text{mol}^{-1}$  during the flux time.

In experiment 2 for goldfish and experiment 1 for oscar,  $Na^+$  flux calculations were performed based on equations presented by Wood and Randall (1973a), Kirschner (1970), and Wood (1992). Backflux correction was not needed during any of the experiments as the internal specific activity did not reach ~10 % of external specific activity. Therefore,  $Na^+$  influx rates ( $J_{\text{influx}}^{\text{Na}}$ , by convention positive) were calculated from the mean external specific activity over each 1-h flux period (equation analogous to equation 1 for averaging over 1 h), and the disappearance of counts from the external water (factored by time, volume, and fish mass):

$$J_{\text{influx}}^{\text{Na}} = \frac{([\text{CPM}_i] - [\text{CPM}_f]) \cdot V}{W \cdot T \cdot SA} \quad (4)$$

where  $[\text{CPM}_i]$  and  $[\text{CPM}_f]$  represent  $^{22}\text{Na}^+$  radioactivity ( $\text{cpm L}^{-1}$ ) in the external water at the start and end respectively of each 1-h flux period,  $V$  is the external water volume (L),  $W$  is the weight of the fish (kg), and  $T$  is the time (1 h).

Net  $Na^+$  flux rates ( $J_{\text{net}}^{\text{Na}}$ ) were calculated from the change in total  $Na^+$  concentration in the water (similarly factored):

$$J_{\text{net}}^{\text{Na}} = \frac{([X_i] - [X_f]) \cdot V}{W \cdot T} \quad (5)$$

where  $[X_i]$  and  $[X_f]$  are total  $\text{Na}^+$  concentrations ( $\mu\text{mol L}^{-1}$ ) in the external water at the start and end of each flux period.

Unidirectional  $\text{Na}^+$  efflux rates ( $J_{\text{efflux}}^{\text{Na}}$ , by convention negative) were calculated by difference:

$$J_{\text{efflux}}^{\text{Na}} = J_{\text{net}}^{\text{Na}} - J_{\text{influx}}^{\text{Na}} \quad (6)$$

Net flux rates of ammonia ( $J^{\text{Amm}}$ ) and  $\text{K}^+$  ( $J^{\text{K}}$ ) in all experiments were calculated as for  $J_{\text{net}}^{\text{Na}}$ .

*Calculation of dietary ion fluxes:*

Estimates of the intake rate of ions from the diet were calculated from measured concentrations of ions in the food and the daily ration:

$$\text{Dietary flux rate for [ion]} (\mu\text{M} \cdot \text{kg}^{-1} \cdot \text{h}^{-1}) = (r \times [\text{ion}] \text{ in food}) / T \quad (7)$$

Where  $r$  is the daily ration of food (kg food per kg fish, such that a 1% ration would be 0.010 kg food per kg fish),  $[\text{ion}]$  is the concentration of the calculated ion in mM. kg of food<sup>-1</sup>, and  $T$  is the relevant time (24 h in this case as it was per day).

*Gill  $\text{Na}^+/\text{K}^+$ -ATPase Enzyme Activity:*

Gill  $\text{Na}^+/\text{K}^+$ -ATPase activity was measured on crude gill homogenates using the methods outlined by McCormick (1993). This assay couples ouabain-sensitive ATP hydrolysis to the oxidation of NADH *via* pyruvate kinase and lactate dehydrogenase. For goldfish, on the day of the assay, a stock working solution was prepared from: 50  $\text{mmol} \cdot \text{l}^{-1}$  imidazole, 2.8  $\text{mmol} \cdot \text{l}^{-1}$  phosphoenol pyruvate (PEP), 0.23  $\text{mmol} \cdot \text{l}^{-1}$  NADH, 3.5  $\text{mmol} \cdot \text{l}^{-1}$  ATP, 4  $\text{U} \cdot \text{ml}^{-1}$  lactate dehydrogenase (LDH), 5  $\text{U} \cdot \text{ml}^{-1}$  pyruvate kinase (PK).

This solution was divided into two tubes, labelled A and B where each tube represented a treatment: A) control and B) ouabain. Ouabain ( $500 \mu\text{mol L}^{-1}$ ) was added to solution B. A salt solution ( $50 \text{ mmol}\cdot\text{l}^{-1}$  imidazole,  $189 \text{ mmol}\cdot\text{l}^{-1}$  NaCl,  $10.5 \text{ mmol}\cdot\text{l}^{-1}$   $\text{MgCl}_2$ ,  $84 \text{ mmol}\cdot\text{l}^{-1}$  KCl), was added to solution A, so that volume of salt solution: stock working solution had a ratio of 1:3. Salt was also added to solution B in the same manner; all solutions were well vortexed and kept on ice. For oscar, initially it was found that there was no inhibition with ouabain. Therefore, to distinguish  $\text{Na}^+/\text{K}^+$ -ATPase activity from total ATPase activity at the gill, samples were run in assay solutions (prepared as for goldfish) either with or without  $\text{K}^+$  (KCl) present, under the assumption that  $\text{K}^+$ -dependent ATPase activity is almost exclusively  $\text{Na}^+/\text{K}^+$ -ATPase activity. The KCl in the salt solution was replaced by an equal concentration of NaCl. All other procedures and solutions were identical to assay preparation as for goldfish.

Briefly, gill filaments ( $\sim 50 \text{ mg}$ ) were cut from the 2<sup>nd</sup> gill arch on ice and immediately homogenized in SEI buffer ( $250 \text{ mmol l}^{-1}$  sucrose,  $10 \text{ mmol l}^{-1}$  EGTA,  $50 \text{ mmol l}^{-1}$  imidazole, pH 7.3) with 0.1% sodium deoxycholate. Gill homogenates were then centrifuged at  $5000 \text{ g}$  for 30 s and the supernatant was separated. To determine  $\text{Na}^+/\text{K}^+$ -ATPase activity in goldfish,  $10 \mu\text{l}$ 's of homogenate was assayed for ATPase activity in the absence (solution A) or presence (solution B) of  $500 \mu\text{mol L}^{-1}$  ouabain. Each goldfish gill sample was run in triplicate and measured at 340 nm in a kinetic microplate reader (SpectraMAX Plus; Molecular Devices, Menlo Park, CA) at 15-s intervals for 30 min. For oscar,  $75 \mu\text{l}$  of homogenate (in cuvettes) was assayed for ATPase activity in the presence (solution A) or absence (solution B) of  $\text{K}^+$ . Oscar gill samples were also run in

triplicates and measured at 340 nm using a Shimadzu UV-240 spectrophotometer equipped with a thermostated cuvette holder at 25°C. The remaining homogenate was measured for [protein] using the Bradford assay method (Sigma-Aldrich) with bovine serum albumin standards.  $\text{Na}^+/\text{K}^+$ -ATPase activities were calculated as described below (Richards et al., 2003).

*Gill  $\text{H}^+$ -V-ATPase Enzyme Activity:*

Lin and Randall's methodology (1993) with some modifications was employed, using *N*-ethylmaleimide (NEM) as an  $\text{H}^+$ -ATPase inhibitor. Sodium azide was used to remove background activity of mitochondrial ATPases. Homogenate (10  $\mu\text{l}$ ) from goldfish gill samples (as prepared for the  $\text{Na}^+/\text{K}^+$ -ATPase activity above) was added to wells in a 96-well plate. Two treatments for each goldfish sample C and D [C: ouabain (500  $\mu\text{mol l}^{-1}$ ) + sodium azide, and D: ouabain (500  $\mu\text{mol l}^{-1}$ ) + sodium azide + NEM (50  $\text{nmol l}^{-1}$ )] with triplicate measurements of each treatment were performed. The plate was then measured at 340 nm in the same kinetic microplate reader at 15-s intervals for 30 min. For oscar samples, homogenate (75  $\mu\text{l}$ ) from gill samples (as prepared for the  $\text{Na}^+/\text{K}^+$ -ATPase activity above) was added to 1 ml cuvettes. Two treatments of solution C and D [C: sodium azide, and D: sodium azide + NEM (50  $\text{nmol l}^{-1}$ )] was also measured in triplicates for each treatment. Samples were measured at 15-s intervals for 30 min at 340 nm using a Shimadzu UV-240 spectrophotometer equipped with a thermostated cuvette holder at 25°C. The remaining homogenate was measured for [protein] using the Bradford assay as outlined below.  $\text{H}^+$ -ATPase activity was calculated as described below.

*Protein Measurement:*

Protein standards with concentrations ranging from 50 to 600  $\mu\text{g}$  protein/ml were prepared using  $1.0 \text{ mg}\cdot\text{ml}^{-1}$  BSA stock (BioChemika). 10  $\mu\text{l}$  of each protein standard was pipetted in a 96-well microplate in duplicates. 10  $\mu\text{l}$  of diluted homogenized sample (all dilutions in de-ionized water) were dispensed in triplicates into the same plate. To all standards and samples, 250  $\mu\text{l}$  of Bradford Assay Reagent (Sigma) was added, and the plate was read at 595 nm.

*Calculation of  $\text{Na}^+/\text{K}^+$ -ATPase and  $\text{H}^+$ -V-ATPase Enzyme Activities:*

Activities of the ATPase enzymes were measured using the linear disappearance of NADH over time. The average rate for each treatment was taken from the stable slope and calculated from an ADP standard curve generated just prior to the assay. ADP standard curves were run from 0 to 20  $\text{nmol ADP}\cdot\text{well}^{-1}$ . The rate of depletion in NADH stabilized around  $-0.012 \text{ OD unit}\cdot\text{nmol ADP}^{-1}\cdot\text{well}^{-1}$ .  $\text{Na}^+/\text{K}^+$ -ATPase activity was determined by subtracting the difference in ATP hydrolysis between the control wells and the inhibitor-treated ones (A vs. B).  $\text{H}^+$ -ATPase activity was obtained by calculating the difference in ATP hydrolysis between wells treated with ouabain + sodium azide and those treated with ouabain + sodium azide + NEM (C vs. D) (for oscar, solutions C and D did not contain ouabain). Calculated activity was then normalized to total protein content (measured as described above) and expressed in  $\mu\text{mol ADP}\cdot\text{mg}^{-1}\cdot\text{protein h}^{-1}$ .

*Analysis of Ion Levels in Goldfish and Oscar Diet:*

Goldfish flakes and oscar food pellets were weighed and digested in 1 N nitric acid for 48 h. After digestion, samples were analyzed for several ions. Total  $\text{Na}^+$ ,  $\text{K}^+$ ,

Ca<sup>2+</sup> and Mg<sup>2+</sup> concentrations were measured using flame atomic absorption spectrophotometry (AAAnalyst 800, Perkin Elmer). Total Cl<sup>-</sup> concentration was analyzed by the mercuric thiocyanate spectrophotometric method (Zall et al., 1956).

*Morphological Analyses of Oscar gills:*

Scanning electron microscopy:

At San Diego State University, the middle part of each fixed gill arch (~4 mm long) bearing up to 12 filaments in both anterior and posterior rows were used for scanning electron microscopy. Gill samples were rinsed in 0.1 M phosphate-buffered saline (PBS), and post-fixed in 1% osmium tetroxide for 1 h. Then samples were dehydrated in ascending concentrations of ethanol from 30% to 100%, critical-point dried with liquid CO<sub>2</sub>, mounted on stubs, sputter-coated with gold, and examined with a Hitachi S 2700 scanning electron microscope (Tokyo, Japan) at the accelerating voltage of 20 kV.

Morphometry:

Gill parameters measured in control and experimental fish included density of mitochondria-rich cells (number of MRCs per mm<sup>2</sup>) and surface area of individual MRCs. Quantification of MRCs density was performed on randomly selected areas of trailing edges of filaments located below respiratory lamellae. SEM microphotographs (magnification 2000x) of 4 randomly selected areas of filament epithelium of 6 fish (total number of measurements = 20) were analyzed and the number of apical crypts of MRCs was counted. The surface area of 30 individual MRCs (5 apical crypts for each of 6 fish examined in control and experimental treatments) was calculated on photographs at 6000x magnification accordingly to the shape of their crypts that varied from circular to oval, triangular and roughly trapezoid.

*Statistical Analyses:*

Data are reported as means  $\pm$  SE (N is the number of fish), unless otherwise stated. Data were normally distributed; therefore parametric statistics were used in all analyses. In experiment 1 and 2 for goldfish, statistical relationships were assessed by one-way ANOVA followed by Tukey's test for independent data. In experiments 1 for oscar, where repeated measurements were made on the same fish, differences within experimental exposures (e.g., fed or starved) at different time periods were evaluated with a repeated measures analysis of variance (ANOVA) followed by a post hoc test (Dunnett's multiple comparison test for paired data). Differences between fed and starved fish under normoxic conditions or specific hypoxic conditions were compared using an unpaired two-tailed Student's t-test. In experiment 3 for goldfish and experiment 2 for oscar, statistical relationships were assessed by one-way ANOVA followed by Tukey's test for independent data. The level of significance was set at  $P < 0.05$ . All statistical tests were run using SigmaStat<sup>®</sup> version 3.1 (Systat Software, Inc., San Jose, California).

**Results:****For goldfish:**

**1. *Unidirectional Na<sup>+</sup> uptake and net K<sup>+</sup> and ammonia fluxes in response to a range of acute (4 h) hypoxic exposures.***

To understand the overall effects of hypoxia on branchial ionoregulation, we initially surveyed gill ion fluxes at a range of acute (4 h) hypoxic exposures in goldfish (Fig. 1). There was no significant difference between  $J_{\text{influx}}^{\text{Na}}$  rates at normoxia or 120 mmHg, clearly indicating this level of hypoxia had no effect. However, there was a significant decrease of Na<sup>+</sup> uptake at around 100 mmHg (to approximately 42%) and at 40 mmHg (to approximately 32%), while at hypoxic exposures in between these levels (80, and 60 mmHg), flux rates were intermediate (Fig. 1).

Group net flux rates of K<sup>+</sup> and ammonia to the water were also measured in these experiments. Interestingly, with increasing severity of hypoxia, there was no clear trend in loss of K<sup>+</sup> to the water, but ammonia excretion appeared to be suppressed at 40 mmHg (Table 1).

**2. *Unidirectional Na<sup>+</sup> influxes, effluxes, net fluxes, net K<sup>+</sup> and net ammonia fluxes in response to normoxia, 4-h moderate (PO<sub>2</sub> = 100 mmHg) and severe (PO<sub>2</sub> = 40 mmHg) hypoxia in fed and starved goldfish***

Since we had observed a significant depression in  $J_{\text{influx}}^{\text{Na}}$  rates at 4 h of hypoxic exposure at 100 and 40 mmHg from experiment 1, we then chose to examine in a follow-up experiment with goldfish (N=10) if feeding status influenced sequential changes in flux rates during these specific hypoxic exposures (Figs. 2, 3 and 4).

Feeding alone had a significant effect on control  $J_{\text{influx}}^{\text{Na}}$  and  $J_{\text{efflux}}^{\text{Na}}$  rates, but not on  $J_{\text{net}}^{\text{Na}}$  flux rates (Fig. 2). Fed goldfish had both a significantly greater  $\text{Na}^+$  uptake from the water and a significantly greater efflux of  $\text{Na}^+$  to the water compared to starved fish during normoxia. With 4-h of moderate hypoxia (100 mmHg) or severe hypoxia (40mmHg) we did not observe significant changes in  $J_{\text{influx}}^{\text{Na}}$  in starved or fed goldfish (Fig. 2). However, there was an overall trend towards depressed  $J_{\text{influx}}^{\text{Na}}$  in starved goldfish with increasing severity of hypoxia. Changes in  $J_{\text{efflux}}^{\text{Na}}$  in starved goldfish mirrored those in  $J_{\text{influx}}^{\text{Na}}$ , but overall there were no significant changes in  $J_{\text{efflux}}^{\text{Na}}$  rates with increasing hypoxia compared to the control normoxic rates (Fig. 2). Changes in  $J_{\text{efflux}}^{\text{Na}}$  were more pronounced in fed goldfish. With increasing severity in hypoxia,  $J_{\text{efflux}}^{\text{Na}}$  rates were significantly depressed compared to normoxic goldfish. There was a 73% decrease in  $J_{\text{efflux}}^{\text{Na}}$  rates with moderate hypoxic exposure (100 mmHg) that was sustained at a comparable 68% inhibition with severe hypoxia (40 mmHg). For  $J_{\text{net}}^{\text{Na}}$  flux rates, negative  $\text{Na}^+$  balance was observed in starved and fed goldfish during the both normoxia and the subsequent hypoxic exposures with no significant changes overall (Fig. 2).

Feeding alone had a significant effect on control ammonia excretion rates where fed goldfish had a much greater excretion of ammonia to the water compared to starved fish during normoxia (Fig. 3). Fed goldfish maintained a greater excretion of ammonia to the water compared to starved goldfish during both moderate (100 mmHg) and severe hypoxia (40 mmHg) although the difference was significant only for the latter. Similar to unidirectional  $\text{Na}^+$  flux rates, reductions in mass specific ammonia excretion rates in

response to increasing severity in hypoxia were more pronounced in fed goldfish compared to starved goldfish (Fig. 3). In starved goldfish, there were no significant changes in mass-specific ammonia excretion rates in response to moderate hypoxic exposure (100 mmHg) compared to normoxic excretion rates. However, ammonia excretion was depressed by 50% with severe hypoxia (40 mmHg) in starved fish (Fig. 3). In fed goldfish, with moderate hypoxia (100 mmHg) there was a significant depression in ammonia excretion by 51% compared to levels at normoxia. This depression was more pronounced with severe hypoxia, where a 72% depression was observed (Fig. 3).

Feeding did not seem to affect  $K^+$  loss to the water during normoxia or moderate hypoxia but had a significant impact during severe hypoxia (Fig. 4). Starved goldfish had a significantly greater loss of  $K^+$  to the water compared to fed goldfish during severe hypoxia. There were no significant changes in  $K^+$  loss to the water during moderate and severe hypoxia in starved goldfish, though there was a trend for reduction in the fed goldfish (Fig. 4).

We also measured ion content in goldfish food in order to estimate dietary flux rates for ions which fed goldfish received via their daily ration (Table 2). Assuming fed goldfish consumed a daily ration of 2% wet body weight, they received  $547.5 \mu\text{M} \cdot \text{kg}^{-1} \cdot \text{h}^{-1}$  of  $[\text{Na}^+]$  from their food. This is a considerable potential uptake (~65%) relative to the unidirectional  $\text{Na}^+$  influx from the water which is  $846.8 \pm 93.1 \mu\text{M} \cdot \text{kg}^{-1} \cdot \text{h}^{-1}$  (Fig. 2). Fed fish further receive approximately  $277.5 \mu\text{M} \cdot \text{kg}^{-1} \cdot \text{h}^{-1}$  of  $[\text{K}^+]$  from their diet but only excrete (i.e. net negative flux)  $76.1 \pm 34.3 \mu\text{M} \cdot \text{kg}^{-1} \cdot \text{h}^{-1}$  (~27% of what they ingest) during normoxia (Fig. 4). Fed goldfish further received a considerable amount of  $[\text{Cl}^-]$

(381.0  $\mu\text{M} \cdot \text{kg}^{-1} \cdot \text{h}^{-1}$ ) and  $[\text{Ca}^{2+}]$  (348  $\mu\text{M} \cdot \text{kg}^{-1} \cdot \text{h}^{-1}$ ) supplement from their diet and additionally obtained some  $[\text{Mg}^{2+}]$  (125.0  $\mu\text{M} \cdot \text{kg}^{-1} \cdot \text{h}^{-1}$ ) (Table 2).

**3. *The effect of acute hypoxia (4h) and normoxic recovery on branchial  $\text{Na}^+/\text{K}^+$  - ATPase and  $\text{H}^+$  - ATPase activities in goldfish.***

The hypoxia exposure protocol in this terminal sampling experiment subjected goldfish (fed) to an acute exposure of either 1 h or 4 h of severe hypoxia (40 mmHg), followed by either 1 h or 3 h of normoxic recovery. Branchial  $\text{Na}^+/\text{K}^+$ -ATPase activity was not affected.  $\text{Na}^+/\text{K}^+$ -ATPase activity during normoxia was  $0.90 \pm 0.16 \mu\text{molADP} \cdot \text{mg protein}^{-1} \cdot \text{h}^{-1}$  and remained close to this level during the hypoxia exposure ( $\text{PO}_2 \sim 40$  mmHg; Fig. 5), and was maintained during normoxic recovery (Fig. 5).

Patterns in branchial  $\text{H}^+$ -ATPase activity were similar (Fig. 5). Gill  $\text{H}^+$ -ATPase activity during normoxia was  $0.13 \pm 0.05 \mu\text{molADP} \cdot \text{mg protein}^{-1} \cdot \text{h}^{-1}$ , and did not change with either 1 h or 4 h of hypoxic exposure or during normoxic recovery.

**For Oscars:**

**1. *Unidirectional  $\text{Na}^+$  influxes, effluxes, net fluxes, net  $\text{K}^+$  and net ammonia fluxes in response to normoxia and progressively (4-h) severe hypoxia in fed and starved oscar.***

In this paired design experimental series, we examined the sequential changes in both unidirectional influxes and effluxes of  $\text{Na}^+$  during normoxia and extreme hypoxia ( $\sim 10$ -20 mmHg) in starved ( $\sim 10$  days) and fed oscar (Fig. 6). During normoxia,  $J_{\text{influx}}^{\text{Na}}$  rates in starved fish were significantly higher than in fed fish. In starved fish, severe

hypoxia (4-h) led to a significant depression in mean  $J_{\text{influx}}^{\text{Na}}$  starting exactly at the onset of hypoxic exposure. In contrast, in fed oscars,  $J_{\text{influx}}^{\text{Na}}$  rates remained similar to those in normoxia during the first two hours of acute hypoxia, but were significantly depressed during the final two hours of hypoxic exposure. Thus they were less responsive to severe hypoxia, taking longer to turn down (Fig. 6).  $J_{\text{influx}}^{\text{Na}}$  was significantly lower in fed fish compared to starved fish during the final two hours of hypoxic exposure. In contrast to  $J_{\text{influx}}^{\text{Na}}$ ,  $J_{\text{efflux}}^{\text{Na}}$  values were similar during normoxia in fed versus starved fish. Changes in  $J_{\text{efflux}}^{\text{Na}}$  also tended to have similar patterns in both starved and fed oscars, where rates were depressed in the last 3-h of hypoxic exposure by both groups, though to a somewhat greater extent in the fed fish, though this difference was not significant (Fig. 6).  $J_{\text{net}}^{\text{Na}}$  flux rates in starved fish were in positive balance during normoxia and were in negative balance during the severe hypoxic exposure. In contrast, fed oscars displayed a continuous negative balance throughout normoxia and severe hypoxia (Fig. 6).

Similar to unidirectional  $\text{Na}^+$  flux rates, mass specific ammonia excretion rates also were depressed in both starved and fed oscars in response to severe hypoxia (Fig. 7). Interestingly, during normoxia, fed fish had a significantly lower ammonia excretion to the water compared to starved fish. However, both groups immediately depressed ammonia excretion to the water with the onset of severe hypoxia. The depressions became more severe with time, and the final levels in fed fish were not significantly different from those in starved fish, representing a more severe relative inhibition (Fig. 7).

Net  $K^+$  loss rates to the water during normoxia and severe hypoxia were also examined in starved and fed oscar (Fig. 8). Analogous to  $Na^+$  flux and ammonia excretion rates, starved fish lost more  $K^+$  to the water during normoxia and turned down excretion rates more effectively compared to fed fish during severe hypoxia. Fed oscars generally lost less  $K^+$  during normoxia and effectively depressed their excretion only during the last 2 h of severe hypoxic exposure (Fig. 8). The differences between fed and starved fish were significant in hours 2 and 4 of hypoxic exposure.

We also measured ion content in oscar food in order to obtain dietary flux rates for ions which fed fish received via their diet. Assuming fed fish consumed a feeding ration of 1% wet body weight, they received  $88.3 \mu M \cdot kg^{-1} \cdot h^{-1}$  of  $[Na^+]$  from their food (Table 3) which is comparable to normoxic  $Na^+$  uptake rates from the water which were  $106.3 \pm 11.9 \mu M Na^+ \cdot kg^{-1} \cdot h^{-1}$  (Fig. 6). They further received  $85.4 \mu M \cdot kg^{-1} \cdot h^{-1}$  of  $[K^+]$  from their diet but excreted only  $32.9 \pm 11.3 \mu M K^+ \cdot kg^{-1} \cdot h^{-1}$  during normoxia (Fig. 9). Oscars received large amounts of  $[Ca^{2+}]$  from the diet ( $277.5 \mu M \cdot kg^{-1} \cdot h^{-1}$ ) but modest amounts of  $[Mg^{2+}]$  ( $48 \mu M \cdot kg^{-1} \cdot h^{-1}$ ) and  $[Cl^-]$  ( $22.1 \mu M \cdot kg^{-1} \cdot h^{-1}$ ) (Table 3).

***2. The effect of normoxia and acute severe hypoxia (3h) on branchial  $Na^+/K^+$  - ATPase and  $H^+$  - ATPase in fed and starved oscar.***

The hypoxia exposure protocol in this terminal sampling experiment subjected fed and starved oscars to either 3 h of normoxia or 3 h of severe hypoxia (~10-20 mmHg). Branchial  $Na^+/K^+$ -ATPase activity did not change with severe hypoxia compared to normoxic exposure in both fed and starved groups (Fig. 9).  $Na^+/K^+$ -ATPase activity during normoxia in fed fish was  $0.093 \pm 0.012 \mu mol ADP \cdot mg \text{ protein}^{-1} \cdot h^{-1}$  and

comparable to activity in normoxic starved fish and remained close to this level after hypoxia in both groups. Although there was a trend towards increased gill  $\text{Na}^+/\text{K}^+$ -ATPase activity in starved fish during normoxia and hypoxia, this change was not significant (Fig. 9).

Patterns in branchial  $\text{H}^+$ -ATPase activity were similar to those observed for  $\text{Na}^+/\text{K}^+$ -ATPase (Fig. 9). Gill  $\text{H}^+$ -ATPase activity in normoxic fed ( $0.04 \pm 0.02 \mu\text{molADP} \cdot \text{mg protein}^{-1} \cdot \text{h}^{-1}$ ) and starved groups remained unchanged during the subsequent severe hypoxic exposure (Fig. 9).

### ***3. The effect of normoxia and acute severe hypoxia (3h) on gill morphology in fed and starved oscar.***

Gill morphology was studied in fed and starved oscar from experiment 2. SEM examination of the gills in fed oscar during normoxia revealed a morphology of epithelial tissues that is typical for fish that inhabit ion-poor and/or acidic waters (Fig. 10). There was a high density of mitochondria-rich cells (MRCs) present on both the gill filament and lamellar epithelia (Figs. 10 A, B). In the filament epithelium of the gill, single MRCs or MRCs gathered into clusters were mainly located on the trailing edge, in the interlamellar regions, and at the junctions between the filaments and lamellae (Fig. 10 A). Numerous MRCs were found to be further distributed on the whole lamellae including the outer margins (Figs. 10 A, B). Apical crypts of MRCs in both the filament and lamellar epithelia had similar surface structures. They were extensive (surface area  $8.09 \pm 0.22 \mu\text{m}^2$ , Table 4), roughly circular, flat or slightly concave, with an unusual fenestrated surface appearance composed of interdigitated and fused apical microplicae (Figs. 11 A-

D). Pavement cells (PVCs) in fed oscar had large polygonal surfaces ornamented by long microridges in a labyrinth-like pattern during normoxia (Fig. 11 A). Additionally, the filament epithelium contained a large population of mucous cells (MCs) releasing globs of secretion (Figs. 10 A, 11 A). Some MCs were also observed in the lower part of the lamellae bordering with filament epithelium. During normoxia, starved oscars (~10 days) displayed abundant MRCs in both the filament and lamellar epithelia, similar to the situation in fed fish (Figs. 10 C, D). However, the surface area of their apical crypts were significantly smaller ( $5.63 \pm 0.13 \mu\text{m}^2$ , Table 4), more concave, had an irregular shape and was composed of a reduced number of wide microplacae (Figs. 11 E, F). Microridges of the PVCs were found to be either dilated or fused (Fig. 11 E). Although a few MCs with small openings were located in the filament epithelium, they were not found on the lamellar surfaces (Figs 10 D, 11 E).

A 3 h exposure to severe hypoxia (~10-20 mmHg) led to dramatic changes in the cellular composition and surface structure of epithelial cells in fed and starved oscar. Specifically, in fed fish, no MRCs were found on the lamellae (Fig. 12 A). In the filament epithelium, the number of MRCs and their apical surface area decreased almost twofold (Table 4, Figs. 12 A, C). Apical crypts of MRCs displayed a highly concave and mostly oblong shape, and were found to be filled with mucus that completely or partially masked their fenestrated surface (Figs. 12 E, F). Comparatively, the surface pattern of PVCs remained similar to that observed during normoxia, however their cellular borders were more distinctive (Fig. 12 C). Only a few MCs were found on the filament epithelium and they did not appear to be present on the lamellae (Fig. 12 A). Starved fish displayed a

similar trend to fed fish during hypoxia where the MRCs in starved fish were only found in the filament epithelium (Fig. 12 B, C) and their number and apical surface area were significantly lower compared to fed fish (Table 4). Furthermore, the apical crypts of MRCs were deeply invaginated and had an irregular shape (Fig. 12 G). The surface structure of the PVCs did not exhibit any obvious alterations compared to those observed during normoxia (Fig. 12 D). A few MCs were found only on the filament epithelium, where they were located mainly in the distal parts of filaments (Fig. 12 B).

The magnitude of the above described gill morphological changes were then quantified to obtain changes in the percentage of surface area occupied by MRCs / mm<sup>2</sup> based on MRC density in the filament epithelium per mm<sup>2</sup> and the surface area of apical crypts (µm<sup>2</sup>, Table 4). During normoxia, fed and starved fish had a relative percentage of surface area occupied by MRCs/ mm<sup>2</sup> of  $1.41 \pm 0.06\%$  and  $0.94 \pm 0.03 \%$ , respectively. When comparing the same parameter in fed fish gills during hypoxia there was a significant decrease from 1.41% to 0.55%. A similar drastic decrease was observed in starved fish (from 0.94% to 0.18%) with hypoxic exposure (Table 4).

**Discussion:***Feeding and the osmorepiratory compromise in hypoxia-tolerant species:*

In the present study, the relationship between ion and gas exchange at the branchial epithelium of two hypoxia-tolerant species that were subjected to varying feeding regimes was examined. Teleosts in freshwater systems constantly face a threat of losing body ions such as sodium to the external medium mainly by diffusion at the gills (Smith et al., 1989) and this deficit of ions must be replaced. We wanted to understand the importance of the diet as a source of ions for goldfish and oscar under both normoxia and hypoxia, and to investigate how this affected the osmorepiratory compromise by mainly focusing on the exchange of  $\text{Na}^+$  across the gill epithelium. We also examined the loss of  $\text{K}^+$ , ammonia excretion and the cellular alterations of the gill in these species. The osmorepiratory compromise during hypoxia is already well established in oscar (Wood et al., 2007) and was confirmed by the present studies (e.g. Fig. 6). Through the initial range-finding experiment 1 with goldfish, we were able to demonstrate that the compromise does occur in this species as well, at least with respect to  $J_{\text{influx}}^{\text{Na}}$  (Fig. 1) therefore verifying our first goal in relation to goldfish. Overall, our results indicate that environmental hypoxia induces changes in gill ionoregulatory function in both the goldfish and oscar by suppressing both active ion uptake and passive ion efflux, while approximately maintaining net ion balance.

Although both these species exhibit the osmorepiratory compromise during severe hypoxia, the effects of feeding on this phenomenon differed between goldfish and oscar. Normoxic fed goldfish exhibited generally greater rates of unidirectional  $\text{Na}^+$

fluxes, ammonia excretion and  $K^+$  loss to the water compared to starved goldfish. With severe hypoxia, fed fish significantly depressed  $J_{\text{efflux}}^{\text{Na}}$  rates, ammonia excretion and  $K^+$  loss to the water with moderate and severe hypoxia.  $J_{\text{influx}}^{\text{Na}}$  rates were not significantly reduced. In contrast, starved goldfish displayed no depression in unidirectional  $\text{Na}^+$  fluxes and  $K^+$  loss, and depressed ammonia excretion only with severe hypoxia.

Differences between fed and starved oscar were generally opposite to those in goldfish, and changes during hypoxia were more apparent compared to goldfish. During normoxia, fed oscars had lower  $J_{\text{influx}}^{\text{Na}}$  rates, ammonia excretion and  $K^+$  loss to the water compared to starved fish. With severe hypoxia, although both fed and starved fish depress their unidirectional  $\text{Na}^+$  fluxes, ammonia excretion and  $K^+$  loss to the water, the reductions in starved fish were greater and occurred more rapidly.

*Unidirectional  $\text{Na}^+$  flux in response to hypoxia in fed vs. starved freshwater hypoxia-tolerant species:*

There was a significantly greater  $J_{\text{influx}}^{\text{Na}}$  from the water by fed goldfish compared to goldfish that were starved for 10 days during normoxia and severe hypoxia (Fig. 2). This observed trend was contrary to what we predicted in our hypothesis, as  $\text{Na}^+$  gain via branchial  $\text{Na}^+$  influx was expected to be lower in fed fish due to nutritional salt intake regulating  $\text{Na}^+$  homeostasis in these fish (Smith et al., 1989). In starved fish, lower  $J_{\text{influx}}^{\text{Na}}$  rates were observed during normoxia and the subsequent hypoxic exposures and it can be assumed that branchial uptake of  $\text{Na}^+$  was adequate for ionic balance in these fish even during hypoxia (Fig. 2). Therefore, it seems that starved goldfish maintain a stable blood sodium concentration even in the absence of dietary  $\text{Na}^+$  intake and with depressed

$J_{\text{influx}}^{\text{Na}}$  from the water (Heming & Paleczny, 1987; Nance et al., 1987). This is further illustrated in our results where with 4-h of moderate hypoxia (100 mmHg) or severe hypoxia (40mmHg) we did not observe significant changes in  $J_{\text{influx}}^{\text{Na}}$  in starved goldfish (Fig. 2). Further, starved goldfish did not exhibit significant changes in  $J_{\text{efflux}}^{\text{Na}}$  rates either with increasing hypoxia compared to the control normoxic rates. This lower rate of branchial ion turnover by starved goldfish especially during hypoxia may confer an advantage to the fish by reducing the metabolic costs associated with ion regulation (Smith et al., 1989). Changes in  $J_{\text{efflux}}^{\text{Na}}$  were more pronounced in fed goldfish where during normoxia there was a substantial net excretion of  $\text{Na}^+$  to the water (Fig. 2). Dietary  $\text{Na}^+$  uptake rates were found to be nearly 65% of unidirectional  $\text{Na}^+$  influx rates from the water (Table 2). In fed fish, the absorption of sodium content from the diet may depend on the ionic balance of the fish at the time of feeding. Furthermore, the rate of sodium uptake by the gut should also be taken into consideration (Smith et al., 1989). Therefore, in fed goldfish an over-compensatory  $\text{Na}^+$  intake from both the water and diet may have led to this significant  $J_{\text{efflux}}^{\text{Na}}$  to the water, where dietary salt uptake may have temporarily exceeded the requirements to maintain homeostasis and excess  $\text{Na}^+$  needed to be excreted at the gills. Additionally, with increasing severity in hypoxia, we observed a significant depression in  $J_{\text{efflux}}^{\text{Na}}$  compared to normoxic goldfish (Fig. 2). Since active  $\text{Na}^+$  uptake is maintained with severe hypoxia, a down-regulation of  $\text{Na}^+$  efflux, restores ionic balance under hypoxia (Wood et al., 2007). Therefore, agreeing with our hypothesis, results indicated that feeding does have an effect on the osmorepiratory compromise during normoxia where fed goldfish had greater unidirectional ion fluxes compared to

starved goldfish. Additionally, fed goldfish effectively turn down their passive efflux of ions to the water in response to severe hypoxia while starved goldfish did not exhibit this level of regulation.

A reverse pattern was observed when examining the regulation of ions in fed and starved oscar in response to severe hypoxia (Fig 6). During normoxia,  $J_{\text{influx}}^{\text{Na}}$  rates in starved oscars were nearly doubled to those observed in fed fish in agreement with our initial hypothesis. Since starved fish do not receive salt via their diet, they will compensate by increasing their intake of  $\text{Na}^+$  from the water (Smith et al., 1995). Furthermore, oscars live in very ion poor water (Muusze et al., 1998; Almeida-Val., 2000), and probably face a limited branchial  $\text{Na}^+$  uptake (D'Cruz and Wood, 1998; Wood et al., 2002). These environmental conditions may further contribute to the amplification of  $J_{\text{influx}}^{\text{Na}}$  rates in starved fish compared to fed fish. Dietary ingestion rates of  $\text{Na}^+$  to fed oscars were approximately equivalent to  $J_{\text{influx}}^{\text{Na}}$  rates from the water that were observed in fed fish (Table 3, Fig. 6), hence the importance of salt from the food was very important to fed oscars, as we had initially postulated. With severe hypoxia, there was a significant depression in mean  $J_{\text{influx}}^{\text{Na}}$ , but in fed fish, this depression was less responsive to severe hypoxia taking longer to turn down compared to starved oscars (Fig. 6). During normoxia  $J_{\text{efflux}}^{\text{Na}}$  rates were comparable in fed and starved oscars, and depressions in  $J_{\text{efflux}}^{\text{Na}}$  rates occurred over a similar time-course in both groups in response to hypoxia (Fig. 6). The effect of hypoxia on ionoregulation in oscar was originally documented by Wood et al. (2007) where fish of these species exhibited a rapid and profound reduction of both unidirectional  $\text{Na}^+$  uptake and unidirectional  $\text{Na}^+$

efflux during acute severe hypoxia, so that net  $\text{Na}^+$  flux was not altered. Although we confirmed these trends in our study, they were more apparent in starved fish compared to fed fish (Fig. 6). A possible reason for this difference is that since starved fish do not have the benefit of a dietary ion supply, they have to be more economical and effectively reduce gill permeability during hypoxia to prevent further ion loss (Wood et al., 2007). However, fed fish can afford to wait longer to turn down gill permeability as their dietary intake of ions is as large as their uptake rates from the water (Table 3, Fig. 6). An additional reason for different unidirectional flux rates observed in starved vs. fed oscars could be an imbalance between energy status and metabolic costs these fish individually face due to their feeding status. In general, with severe hypoxia, oscars depress their metabolic rate and face hypoglycemic conditions (Muusze et al., 1998). A faster depression of metabolic rate by starved fish would slow the need for activation of anaerobic glycolysis and detrimental hypoglycemia (due to not receiving glucose through diet). Therefore, it is advantageous to immediately reduce gill area and permeability during severe hypoxia by reducing lamellar perfusion, so that ionoregulatory costs under this already metabolically demanding situation are minimized (Wood et al., 2007). Although fed fish also face a compromise between ionic loss and oxygen uptake at the gill during hypoxia, due to stored energy (via glycogen stores, Nilsson, 1990), turning down gill permeability can be delayed until there is an actual compromise between metabolic demand and energy availability during severe hypoxia.

*The effect of hypoxia on gill ionocytes:*

In order to better understand the effects of hypoxia at the cellular level, our second goal was to examine the activity of  $\text{Na}^+/\text{K}^+$ -ATPase and  $\text{H}^+$ -ATPase pumps. In this study, *in vitro* measurements were made under optimal conditions where we were measuring capacity, in contrast to the situation *in vivo* where there may be a limiting ATP supply. Contrary to our hypothesis, branchial  $\text{Na}^+/\text{K}^+$ -ATPase activity in goldfish did not change with acute hypoxia ( $\text{PO}_2 \sim 40$  mmHg), and we found no further change in the activity of these pumps with normoxic recovery (Fig. 5). Patterns in branchial  $\text{H}^+$ -ATPase activity were also similar in these fish, where activity levels were maintained during normoxia, hypoxic exposure and normoxic recovery (Fig. 5). Comparatively, there were no apparent differences in branchial  $\text{Na}^+/\text{K}^+$ -ATPase and  $\text{H}^+$ -ATPase activity levels between fed and starved oscars, which was in accordance with our original prediction that feeding status would not affect ATPase activity as oxygen is a limiting factor equally in both fed and starved fish (Fig. 9). However, contrary to previous studies on the branchial  $\text{Na}^+/\text{K}^+$  ATPase activity in the oscar (Richards et al, 2007; Wood et al., 2007), we did not see a downregulation in the activity of these pumps with acute hypoxic exposure (3 h) in fed or starved fish. With hypoxia, a downregulation of these pump activities in order to conserve ATP due to reduced oxidative phosphorylation was expected in both these hypoxia-tolerant species (Boutilier and St. Pierre, 2000). When faced with oxygen depletion, in order to save energy, a reduction in  $\text{Na}^+$  pump activities is expected along with a decrease in cell membrane permeability (Boutilier, 2001). Although we did see reduced gill permeability in both these species (Fig. 2, goldfish; Fig. 6, oscar) the lack of

a depression  $\text{Na}^+/\text{K}^+$ -ATPase and  $\text{H}^+$ -ATPase activity with severe hypoxia in oscar cannot be readily explained, especially as hypoxic exposure conditions for this species were virtually identical to those used by Richards et al. (2007) and Wood et al. (2007).

Absolute activity levels of branchial  $\text{Na}^+/\text{K}^+$ -ATPase and  $\text{H}^+$ -ATPase in fed and starved oscar were considerably lower (by 10-fold) to activity levels that have been previously measured in this species (Richards et al, 2007; Wood et al., 2007). We believe this discrepancy is due to an over-estimation in protein content in gill homogenates. After considerable analysis, it was found that the concentration of sodium deoxycholate (in order to break down cell membranes) added to the SEI-EGTA homogenate had complex reactions with the Bradford assay reagent that was used to determine protein content, resulting in excess colour development, thereby confounding results by an over-representation of protein content in the sample. Since absolute ATPase activity was normalized to protein content, apparent activity levels were underestimated due to this artificially high protein content. In our previous study with trout ATPase assays (Chapter 2), and in the current study with goldfish ATPase assays, we were able to avoid this over-representation by determining the minimal concentration of sodium deoxycholate needed to break down gill cells that did not react with the Bradford assay reagent. However, on a relative basis, the oscar measurements still provided insight about ATPase activity levels and their lack of changes in fed and starved oscar during normoxia and severe hypoxic exposure.

We also examined net  $\text{K}^+$  loss rates to the water in starved and fed goldfish (Fig. 4) and oscar (Fig. 8) to understand if gill cells were facing cellular distress under hypoxia

(Boutilier, 2001). In goldfish, starved fish continuously excreted  $K^+$  to the water even under severe hypoxia at rates compared to normoxic levels (Fig. 4). We initially expected a depression in  $K^+$  loss in this species as goldfish are anoxia-tolerant, and would not face cellular distress regardless of their feeding status. However, we believe this constant loss of  $K^+$  to the water by starved goldfish (Fig. 4) are baseline levels of  $K^+$  loss that likely occur in starved fish due to the 'consumption' in body mass during starvation.  $K^+$  is very concentrated in the intracellular fluid of the cytoplasm and is the key intracellular ion (Lovell, 1998). Fed goldfish exhibited an increased  $K^+$  loss during normoxia (Fig. 4) and we attribute this higher loss rate due to the excess  $K^+$  they obtained from their diet (Table 2). The significant decrease observed in  $K^+$  loss in fed goldfish with severe hypoxia can be attributed to overall depression in gill permeability explained above. In comparison, starved oscars lost more  $K^+$  to the water than did fed fish during normoxia, but this loss was suppressed with hypoxia (Fig. 8), agreeing with our hypothesis. This initial normoxic increase in  $K^+$  loss by starved oscars could also be attributed to 'consumption' of body mass occurring in these fish. Starved oscars seem indifferent to hypoxic distress at gill ionocytes and this is further supported by a study by Scott et al., (2008) which found no evidence of  $O_2$  limitation in gill epithelial cells of oscars under hypoxia. Fed oscars had lower  $K^+$  loss to the water and this excretion was suppressed with hypoxia (Fig. 8). Potassium is the major cation of intracellular fluid, and is an essential nutrient to fish via diet. It is required for glycogen and protein synthesis, and further for metabolic breakdown of glucose (Lovell, 1998). Therefore, fed oscars could be utilizing the

considerable amount of  $K^+$  available from their food (Table 4) for growth and tissue synthesis instead of excreting it to the water.

*Nitrogenous waste excretion under hypoxia in starved and fed fish:*

In teleost fishes, the major waste product of nitrogen metabolism is ammonia which comprises 70 – 90% of the total N-waste and is excreted primarily at the gills (Van Waarde, 1983; Wood, 2001). The main internal source of ammonia in fish is through the catabolism of proteins (Ip et al., 2001). Mass specific ammonia excretion in starved and fed goldfish under moderate and severe hypoxia was examined, therefore addressing our final goal (Fig. 3). During normoxia and severe hypoxia, fed goldfish excreted significantly more ammonia to the water compared to starved goldfish (Fig. 3). This was expected as in general fed teleost fish have a much higher excretion of nitrogenous wastes compared with fasted fish (Wood, 2001). An increased excretion of ammonia by fed fish is attributed to increased ammonia production associated with the breakdown of ingested proteins (Ip et al., 2001), but ammonia production and excretion are sustained at low levels in starved fish (Brett and Zala, 1975). With severe hypoxia, both starved and fed goldfish depressed their ammonia excretion to the water (Fig. 3). Previous studies have found no change in ammonia production (therefore protein breakdown) in goldfish exposed to severe hypoxia (van Waversveld et al., 1989). In our study we might be seeing a situation where although ammonia production is not influenced, absolute ammonia excretion to the water may be suppressed with severe hypoxia. A similar situation was observed by Wood et al., (2007) in the Amazonian oscar where they saw an increase in plasma ammonia levels but at the same time a depression in overall ammonia excretion

rate to the water indicating a downregulation in gill permeability. It is quite possible that the same downregulation of gill permeability occurs in goldfish as we do see a general depression in  $\text{Na}^+$  efflux to the water with severe hypoxic exposure (Fig. 2). Goldfish, even under severe hypoxia (not anoxia) can still employ a secondary anaerobic pathway for waste excretion where they excrete ethanol as a waste product of glycogen metabolism (van Waversveld et al., 1989). In this study, since ammonia although suppressed was still excreted (Fig. 3) by goldfish, it can be inferred that goldfish were primarily employing an aerobic pathway for waste excretion.

In oscar, a different, albeit novel situation was observed. Contrary to our prediction, fed fish of this species excreted less ammonia to the water compared to starved fish during normoxia, and complete suppression of ammonia excretion was delayed during hypoxia (Fig. 7). It could be inferred that fed oscars probably still use protein as a metabolic fuel source to a limited extent, but allocate the majority of their protein intake for muscle growth and maintenance, thereby minimizing ammonia production and excretion (Wood, 2001; Kajimura et al., 2004; Iftikar et al., 2008). As observed in goldfish, both fed and starved oscar immediately depress their ammonia excretion to the water with the onset of severe hypoxia (Fig. 7). As explained above, we think this suppression is due to general reductions in gill permeability brought on by severe hypoxic exposure as reported previously for this species (Wood et al., 2007). In the oscar, the increase in plasma ammonia levels was believed not to be toxic to the fish as the absolute change in levels were not large and oscars still maintained internal homeostasis during severe  $\text{O}_2$  limitation (Wood et al., 2007).

*The impact of hypoxia on gill morphology in fed and starved oscars:*

The freshwater gill is known to alter its morphology in response to environmental variations, thereby adapting its structure and function to suit its environment (Wilson and Laurent, 2002; Sollid et al., 2003; Sollid and Nilsson, 2006; Matey et al., 2008). We investigated if gill morphology of the hypoxia-tolerant oscar changed under severe hypoxia and if feeding status influenced this change. This is the first studies to examine the gill morphology alterations of this interesting species under hypoxic conditions, and in agreement with our hypothesis, we did see gill morphological changes in oscar exposed to hypoxia. During normoxia, both fed and starved oscars had a high density of mitochondria-rich cells (MRCs) in both the gill filament and lamellae epithelia (Fig. 10 A, fed fish; Figs. 10 C, D, starved fish; Table 4). Comparatively, in the rainbow trout, normoxic MRC density in the trailing edge of the gill filament, surface area of apical crypts and % surface area occupied by MRCs in the filamental epithelium were all considerably higher than in the oscar (Figs. 13 A-C of Iftikar et al., 2008 submitted = Chapter 2). If MRCs are believed to facilitate both the active uptake (by ion pumps) and the diffusive effluxes of salts (via their leaky junctions; Daborn et al., 2001), then the much lower MRC density and surface area of apical crypts observed in oscar versus trout corresponds well to the lower gill ion fluxes observed in the oscar. Trout were found to have a higher MRC density and surface area of apical crypts (Figs. 13 A-B of Iftikar et al., 2008 submitted = Chapter 2) and had correspondingly greater unidirectional fluxes (Figs. 2 and 4 of Iftikar et al., 2008 submitted = Chapter 2) compared to oscar (Fig. 6). These changes could be attributed to the natural physiological differences between these

species, where trout are highly active salmonids while oscar tend to have lower activity. An additional reason for differences in MRC density in the gill filaments of these species could also be attributed to the environmental habitat these fish live in; specifically referring to ion content in water. Oscars are adapted to ion-poor waters of the Amazon (Muusze et al., 1998; Almeida-Val et al., 2000) while trout favour the hard waters of temperate regions. However, trout adapted to ion-poor waters were found to increase their total MRC surface area and to a lesser extent their density and a correlated increase in  $\text{Na}^+$  uptake from the water was also observed (Perry and Laurent, 1989; Laurent and Perry, 1990). Therefore, the discrepancy between MRC density and total crypt surface area (%) in oscar and trout cannot be attributed to their natural environments, and remains to be explained by their inherent physiology and behaviour.

Fed oscar displayed apical crypts that were circular, extensive, and larger in surface area compared to starved fish which displayed more concave, less regular shape crypts that had a small surface area (Fig. 11 A-D, fed fish; Fig. 11 E-F, starved fish; Table 4). This lower apical surface area of MRCs in starved fish compared to fed fish has also been observed in gill response of different fish species to hypoxia (Matey et al., 2008; Iftikar et al., 2008 submitted) and other environmental stresses such as high salinity (Sardella et al., 2004), low pH (Wendelaar Bonga et al., 1990), hypercapnia (Goss et al., 1994; 1998), and highly diluted water (Fernandes et al., 1998). A possible explanation for the reduced appearance of apical crypts is that the crypts may partially close and are covered over by pavement cells, providing a physical barrier to the diffusion of salts (Daborn et al., 2001). This idea seems to contrast with our physiological data, where we

saw an increased unidirectional  $\text{Na}^+$  flux, ammonia excretion and  $\text{K}^+$  loss to the water by starved fish compared to fed fish during normoxia (Fig. 6, 7, & 8). However, although starved fish display smaller apical crypts, it remains possible that these crypts may be underlain by a well-developed tubular network, with more mitochondria and a more abundant transporting tubular-vesicular system thereby making them functionally more active compared to fed fish. Although the latter may have larger apical crypts, they could be less active due to opposite reasons. These ideas are speculative, and in order to fully comprehend this phenomenon, MRCs will have to be studied by transmission electron microscopy and fluorescent microscopy; such studies are planned for the future.

With 3-h of severe hypoxic exposure, there was a reduction in the number, average surface area and % age of surface area of the filament occupied by the apical crypts of MRCs exposed to ambient water in fed and starved oscar (Fig. 12 A-F; Table 4). Furthermore, exposure to hypoxia affected the distribution of MRCs leaving them (exclusively) in the filament epithelium (Fig. 12 A-C). There have been previous observations of changes in the degree of exposure of MRCs focused on acid-base disturbances over periods of days (Perry and Goss, 1994). It has been suggested that increases in the fractional surface area of trout gill MRCs (in response to alkalization) could have been due to the retraction of pavement cells or the expansion of MRCs (Perry and Goss, 1994). In this study, the opposite reaction appears to occur in response to hypoxia. Probably in oscar, chloride cells shrink and are covered over by pavement cells, therefore reducing their exposure to the ambient hypoxic water and increasing the diffusion distances from water to blood of the gills, thereby accounting for overall

depressed fluxes we observed in ionoregulation data (Fig. 6, 7, & 8). This can be confirmed by further TEM analysis. Oscars could be utilizing a host of mechanisms to alter their MRC structure during severe hypoxia such as alteration of gill MRCs by stress hormones (eg. cortisol) (Perry and Laurent, 1989; Laurent and Perry, 1990). However, Muusze et al., (1998) reported that cortisol levels in oscars did not change significantly with hypoxia. Therefore, it can be speculated that other mechanistic influences such as HIF1 $\alpha$  (if stabilised with severe hypoxia in this species) could be involved in hypoxic-induced MRC density and surface area change (Sollid et al., 2006). Overall, our results indicate that the effects of hypoxia on modifications to gill morphology exhibit a very different pattern in the oscar compared to the trout, possibly attributing the importance of adaption (or lack thereof) to low environmental oxygen conditions in these two species.

By examining the osmo-respiratory compromise in two hypoxia-tolerant species, we attempted to understand possible mechanisms taking place at the gill epithelium during hypoxia and additional changes brought on by feeding. Overall, fed goldfish had significantly greater  $J^{\text{Na}}_{\text{efflux}}$ , ammonia excretion and  $\text{K}^+$  loss rates to the water that were effectively turned down during hypoxia. Starved goldfish only exhibited a depressed ammonia excretion at severe hypoxia and seem to have unidirectional  $\text{Na}^+$  fluxes and  $\text{K}^+$  loss similar to rates during normoxia. Comparatively, fed oscars had lower  $\text{Na}^+$  uptake, ammonia excretion and  $\text{K}^+$  loss to the water compared to starved fish. Both fed and starved fish suppressed their ion loss to the water with severe hypoxia, however starved fish responded immediately while fed fish took longer to turn down fluxes. In conclusion,

feeding did seem to affect the osmorepiratory compromise in both these species but exerted opposite influences in goldfish versus oscar.

**Literature Cited:**

Almeida-Val, V. M. F. and Hochachka, P. W. 1995. Air-breathing fishes: metabolic biochemistry of the first diving vertebrates. In Environmental and Ecological Biochemistry. Eds. P.W. Hochachka and T. Mommsen, pp 45-55. Amsterdam: Elsevier Science.

Almeida-Val, V. M. F., Val, A. L., Duncan, W. P., Souza, F. C. A., Paula-Silva, M. N. and Land, S. 2000. Scaling effects on hypoxia tolerance in the Amazonian fish *Astronotus ocellatus* (Perciformes: Cichlidae): contribution of tissue enzyme levels. *Comp. Biochem. Physiol. B.* 125: 219-226.

Alsop, D. H. and Wood, C. M. 1997. The interactive effects of feeding and exercise on oxygen consumption, swimming performance and protein usage in juvenile rainbow trout. *J. Biol. Chem.* 200: 2337 -2346.

Avella, M. and Bornancin, M. 1989. A new analysis of ammonia and sodium transport through the gills of the freshwater rainbow trout (*Salmo gairdneri*). *J. Exp. Biol.* 142: 155 -175.

Balon, E. K. 2004. About the oldest domestication among fishes. *J. Fish. Biol.* 65: 1-27.

Boutilier, R. G. and St-Pierre, J. 2000. Surviving hypoxia without really dying. *Comp. Biochem. Physiol.* 126: 481-490.

Boutilier, R. G. 2001. Mechanisms of cell survival in hypoxia and hypothermia. *J. Exp. Biol.* 204: 3171-3181.

Bradford, M. M. 1976. A rapid and sensitive method for the quantitation of microgram quantities of protein utilizing the principle of protein-dye binding. *Anal. Biochem.* 72: 248-54.

Brett, J. R. and Zala, C. A. 1975. Daily pattern of nitrogen excretion and oxygen consumption of sockeye salmon (*Oncorhynchus nerka*) under controlled conditions. *J. Fish. Res. Bd. Can.* 32: 2479-2486.

Daborn, K., Cozzi, R. R. F. and Marshall, W. S. 2001. Dynamics of pavement cell-chloride cell interactions during abrupt salinity change in *Fundulus heteroclitus*. *J. Exp. Biol.* 204: 1889-1899.

D'Cruz, L. M. and Wood, C. M. 1998. The influence of dietary salt and energy on the response to low pH in juvenile rainbow trout. *Physiol. Zool.* 71: 642-657.

Driedzic, W. R. and Short, C. E. 2007. Relationship between food availability, glycerol and glycogen levels in low-temperature challenged rainbow smelt *Osmerus mordax*. *J. Exp. Biol.* 210: 2866-2872.

Evans, D. H., Piermarini, P. M. and Choe, K. P. 2005. The multifunctional fish gill: dominant site of gas exchange, osmoregulation, acid-base regulation, and excretion of nitrogenous waste. *Physiol. Rev.* 85: 97-177.

Fernandes, M. N., Perna, S. A. and Moron, S. F. 1998. Chloride cell apical surface changes in gill epithelia of the armoured catfish *Hypostomus plecostomus* during exposure to distilled water. *J. Fish. Biol.* 52: 844-849.

Gonzalez, R. J. and McDonald, D. G. 1992. The relationship between oxygen consumption and ion loss in a freshwater fish. *J. Exp. Biol.* 163: 317-332.

Gonzalez, R. J. and McDonald, D. G. 1994. The relationship between oxygen uptake and ion loss in fish from diverse habitats. *J. Exp. Biol.* 190: 95-108.

Goss, G. G., Laurent, P. and Perry, S. F. 1994. Gill morphology during hypercapnia in brown bullhead (*Ichthylurus nebulosus*): role of chloride cells and pavement cells in acid-base regulation. *J. Fish. Biol.* 45: 705-718.

Goss, G. G., Perry, S. F., Fryer, J. N. and Laurent, P. 1998. Gill morphology and acid-base regulation in freshwater fishes. *Comp. Biochem. Physiol. A.* 119: 107-115.

Heisler, N. 1984. Acid-base regulation in fish. In *Fish Physiology*. Eds. W. S. Hoar and D. J. Randall, Vol. XA, pp. 315-401. New York: Academic Press.

Heming, A. T. and Paleczny, E. J. 1987. Compositional changes in skin mucus and blood serum during starvation of trout. *Aquaculture*. 66: 265-273.

Hochachka, P. W. 1986. Defence strategies against hypoxia and hypothermia. *Science*. 231: 234–241.

Hochachka, P. W. and Lutz, P. L. 2001. Mechanism, origin, and evolution of anoxia tolerance in animals. *Comp. Biochem. Physiol. B*. 130: 435–459.

Iftikar, F. I., Matey, V. and Wood, C. M. 2008. The osmorepiratory compromise during hypoxia in the freshwater rainbow trout *Oncorhynchus mykiss*. Submitted to *Physiol. Biochem. Zool*.

Iftikar, F.I., Patel, M., Ip, Y.K., Wood, C.M. 2008. The influence of feeding on aerial and aquatic oxygen consumption, nitrogenous waste excretion, and metabolic fuel usage in the African lungfish *Protopterus annectens*. *Can. J. Zool*. 86: 790-800.

Ip, Y.K., Chew, S. F. and Randall, D. J. 2001. Ammonia Toxicity, Tolerance, and Excretion. In *Fish Physiology*. Eds. P. A. Anderson and P. A. Wright, Vol. XX, pp. 109-140. Academic Press: Orlando.

Karnovsky, M. J. 1965. A formaldehyde-glutaraldehyde fixative for high osmolarity for use in electron microscopy. *J. Cell. Biol. A*. 27:137.

Kajimura, M., Croke, S. J., Glover, C. N., and Wood, C. M. 2004. Dogmas and controversies in the handling of nitrogenous wastes: The effect of feeding and fasting on the excretion of ammonia, urea and other nitrogenous waste products in rainbow trout. *J. Exp. Biol.* 207: 1993-2000.

Kirschner, L. 2004. The mechanism of sodium chloride uptake in hyper-regulating aquatic animals. *J. Exp. Biol.* 207: 1439-1452.

Krumschnabel, G., Schwarzbaum, P. J., Lisch, J., Biasi, C. and Wieser, W. 2000. Oxygen-dependent energetics of anoxia-tolerant and anoxia-intolerant hepatocytes. *J. Exp. Biol.* 203: 951-59.

Laurent, P. and Perry, S. F. 1990. Effects of cortisol on gill chloride cell morphology and ionic uptake on the freshwater trout, *Salmo gairdneri*. *Cell. Tiss. Res.* 259: 429-442.

Lovell, T. 1998. Digestion and Metabolism. In *Nutrition and Feeding of Fish*. Eds. T.

Lovell, pp 71-89. Springer: New York.

Lin, H. and Randall, D. J. 1993. H<sup>+</sup>-ATPase activity in crude homogenates of fish gill tissue: inhibitor sensitivity and environmental and hormonal regulation. *J. Exp. Biol.* 180: 163-174.

Matey, V., Richards, J. G., Wang, Y., Wood, C. M., Rogers, J., Davies, R., Murray, B. W., Chen, X. Q., Du, J. and Brauner, C. J. 2008. The effect of hypoxia on gill morphology and ionoregulatory status in the Lake Qinghai scaleless carp, *Gymnocypris przewalskii*. *J. Exp. Biol.* 211: 1063-1074.

Matsuo, A. Y., Playle, R. C., Val, A. L. and Wood, C.M. 2004. Physiological action of dissolved organic matter in rainbow trout in the presence and absence of copper: Sodium uptake kinetics and unidirectional flux rates in hard and SW. *Aquat. Toxicol.* 70: 63-81.

McCormick, S. D. 1993. Methods for nonlethal gill biopsy and measurement of Na<sup>+</sup>, K<sup>+</sup>-ATPase activity. *Can. J. Fish. Aquat. Sci.* 50: 656-658.

Muusze, B., Marcon, J., van den Thillart, G. and Almeida-Val, V. M. F. 1998. Hypoxia tolerance of Amazon fish. Respirometry and energy metabolism of the cichlid *Astronotus ocellatus*. *Comp. Biochem. Physiol. A.* 120:151-156.

Nance, J. M., Masoni, A., Sola, F. and Bornancin, M. 1987. The effects of starvation and sexual maturation on Na<sup>+</sup> transbranchial fluxes following direct transfer from freshwater to sea-water in rainbow trout (*Salmo-gairdneri*). *Comp. Biochem. Physiol. A.* 87: 613-622.

Nikinmaa, M. and Rees, B. B. 2005. Oxygen-dependent gene expression in fishes. *Am. J. Physiol. Regul. Integr. Comp. Physiol.* 288: R1079-R1090.

Nilsson, S. 1986. Control of gill blood flow. In *Fish Physiology: Recent Advances*. Eds. S. Nilsson and S. Holmgren, pp 87-101. London: Croom Helm.

Nilsson, G. E. 1990. Long term anoxia in crucian carp: changes in the levels of amino acid and monoamine neurotransmitters in the brain, catecholamines in chromaffin tissue, and liver glycogen. *J. Exp. Biol.* 150: 295-320.

Nilsson G. E. and Renshaw, G. M. 2004. Hypoxic survival strategies in two fishes: extreme anoxia tolerance in the North European crucian carp and natural hypoxic preconditioning in a coral-reef shark. *J. Exp. Biol.* 207: 3131–39.

Nilsson, G. E. 2007. Gill remodeling in fish – a new fashion or an ancient secret? *J. Exp. Biol.* 210: 2403–2409.

Perry, S. F. and Laurent, P. 1990. The role of carbonic anhydrase in carbon dioxide excretion, acid-base balance and ionic regulation in aquatic gill breathers. In *Animal*

*Nutrition and Transport Processes. 2. Transport, Respiration and Excretion.* Eds. J-P.

Truchot, and B. Lahlou, pp. 39–57. Basel: Karger.

Perry S. F. and Goss G. G. 1994. The effects of experimentally altered gill chloride cell surface area on acid-base regulation in rainbow trout during metabolic alkalosis. *J. Comp. Physiol. A.* 164: 327– 36.

Randall, D. J., Baumgarten, D. and Malyusz, M. 1972. The relationship between gas and ion transfer across the gills of fishes. *Comp. Biochem. Physiol. A.* 41: 629-637.

Richards, J. G., Semple, J. W., Bystriansky, J. S. and Schulte, P. M. 2003. Na<sup>+</sup>/K<sup>+</sup>-ATPase  $\alpha$ -isoform switching in gills of rainbow trout (*Oncorhynchus mykiss*) during salinity transfer. *J. Exp. Biol.* 206: 4475-4486.

Richards, J. G., Wang, Y. S., Brauner, C. J., Gonzalez, R. J., Patrick, M. L., Schulte, P. M., Chippari-Gomes, V. M., Almeida-Val, V. M. F. and Val, A. L. 2007. Metabolic and ionoregulatory responses of the Amazonian cichlid, *Astronotus ocellatus*, to severe hypoxia. *J. Comp. Physiol. B.* 177: 361-374.

Sardella, B. A., Matey, V., Cooper, J., Gonzalez, R. J. and Brauner, C. J. 2004. Physiological, biochemical and morphological indicators of osmoregulatory stress in 'California' Mozambique tilapia (*Oreochromis mossambicus* x *O. urolepis hornorum*) exposed to hypersaline water. *J. Exp. Biol.* 207: 1399-1413.

Scott, G. R., Wood, C. M., Sloman, K. A., Iftikar, F. I. De Boeck, G., Almeida-Val, V. M. and Val, A. L. 2008. Respiratory responses to progressive hypoxia in the Amazonian oscar, *Astronotus ocellatus*. *Respir. Physiol. Neurobiol.* 162: 109-116.

Shoubridge, E. A. and Hochachka, P. W. 1980. Ethanol: novel end product of vertebrate anaerobic metabolism. *Science.* 209: 308–9.

Smith, N. F., Talbot, C. and Eddy, F. B. 1989. Dietary salt intake and its relevance to ionic regulation in freshwater salmonids. *J. Fish. Biol.* 35: 749-753.

Smith, N. F., Eddy, F. B. and Talbot, C. 1995. Effect of dietary salt load on transepithelial Na<sup>+</sup> exchange in freshwater rainbow trout (*Oncorhynchus mykiss*). *J. Exp. Biol.* 198: 2359-2364.

Sollid, J. and Nilsson, G. E. 2006. Plasticity of respiratory structures – adaptive remodeling of fish gills induced by ambient oxygen and temperature. *Respir. Physiol. Neurobiol.* 154: 241-251.

Sollid, J., Rissanen, E., Numminen, H., Thorstensen, T., Vuori, K. A. M., Nikinmaa, M. and Nilsson, G. E. 2006. HIF-1 $\alpha$  and iNOS in crucian carp gills during hypoxia induced transformation. *J. Comp. Physiol. B.* 176: 359 -369.

Taylor, J. R., Whittamore, J. M., Wilson, R. W. and Grosell, M. 2007. Postprandial acid-base balance and ion regulation in freshwater and seawater-acclimated European flounder, *Platichthys flesus*. *J. Comp. Phys. B.* 177: 597-608.

van den Thillart, G. and Kesbeke, F. 1978. Anaerobic production of carbon dioxide and ammonia by goldfish *Carassius auratus (L.)*. *Comp. Biochem. Physiol. A.* 59: 393-400.

van Waarde, A. 1983. Aerobic and anaerobic ammonia production by fish. *Comp. Biochem. Physiol. B.* 74: 675-684.

van Waversveld, J., Addink, A. D. F. and van den Thillart, G. 1989. The anaerobic energy metabolism of goldfish determined by simultaneous direct and indirect calorimetry during anoxia and hypoxia. *J. Comp. Physiol. B.* 159: 263-268.

Verdouw, H., van Echteld, C. J. A. and Dekkers, E. M. J. 1978. Ammonia determination based on indophenol formation with sodium salicylate. *Water. Res.* 12: 399-402.

Wendelaar Bonga, S. F., Flik, G., Balm, P. H. M. and van der Meij, J. C. A. 1990. The ultrastructure of chloride cells in the gills of the teleost *Oreochromis mossambicus* during exposure to acidified water. *Cell. Tiss. Research.* 259: 575-585.

Wilson, J. M. and Laurent, P. 2002. Fish gill morphology: inside out. *J. Exp. Zool.* 293: 192-213.

Wood, C. M. and Randall, D. J. 1973*a*. The influence of swimming activity on sodium balance in the rainbow trout (*Salmo gairdneri*). *J. Comp. Physiol.* 82: 207-233.

Wood, C. M. and Randall, D. J. 1973*b*. Sodium balance in the rainbow trout (*Salmo gairdneri*) during extended exercise. *J. Comp. Physiol.* 82: 235-256.

Wood, C. M. and Randall, D. J. 1973*c*. The influence of swimming activity on water balance in the rainbow trout (*Salmo gairdneri*). *J. Comp. Physiol.* 82: 257-276.

Wood, C. M. 1992. Flux measurements as indices of H<sup>+</sup> and metal effects on freshwater fish. *Aquat. Toxicol.* 22: 239–264.

Wood, C. M. 2001. The influence of feeding, exercise, and temperature on nitrogen metabolism and excretion. In *Fish Physiology*. Eds. P. A. Anderson and P. A. Wright, Vol XX, pp 201-238. Academic Press: Orlando.

Wood, C. M., Matsuo, A. Y. O., Gonzalez, R. J., Wilson, R. W., Patrick, M. L., and Val, A. L. 2002. Mechanisms of ion transport in *Potamotrygon*, a stenohaline freshwater

elasmobranch native to the ion-poor blackwaters of the Rio Negro. *J. Exp. Biol.* 205; 3039-3054.

Wood, C. M., Kajimura, M., Sloman, K. A., Scott, G. R., Walsh, P.J., Almeida-Val, V. M. F. and Val, A. L. 2007. Rapid regulation of Na<sup>+</sup> fluxes and ammonia excretion in response to acute environmental hypoxia in the Amazonian oscar, *Astronotus ocellatus*. *Am. J. Physiol. Regul. Integr. Comp. Physiol.* 292: 2048-2058.

Zall, D. M., Fisher, M. D. and Garner, Q. M. 1956. Photometric determination of chlorides in water. *Anal. Chem.* 28: 1665–1678.

For Goldfish:

**Table 1:**

Group net flux rates of  $K^+$  and ammonia (n = 10 fish per group) to the water by goldfish acutely exposed to various levels of hypoxia for 4 h in experiment 1.

---

Exposure	K <sup>+</sup> excretion ( $\mu\text{mol. kg}^{-1} \cdot \text{h}^{-1}$ )	Ammonia excretion ( $\mu\text{mol. kg}^{-1} \cdot \text{h}^{-1}$ )
Normoxic Control (n=10)	- 23	- 141
PO <sub>2</sub> = 120 mmHg (n=10)	- 49	- 123
PO <sub>2</sub> = 100 mmHg (n=10)	- 97	- 112
PO <sub>2</sub> = 80 mmHg (n=10)	- 9	- 123
PO <sub>2</sub> = 60 mmHg (n=10)	- 20	- 124
PO <sub>2</sub> = 40 mmHg (n=10)	- 19	- 20

---

**Table 2:**

Ion levels found in goldfish food (mM/kg) and estimated dietary uptake rates based on a 2% daily ration.

---

Ion	Content (mM/kg)	Dietary flux rate ( $\mu\text{M} \cdot \text{kg}^{-1} \cdot \text{h}^{-1}$ )
Calcium [ $\text{Ca}^{2+}$ ]	418	348.0
Sodium [ $\text{Na}^+$ ]	657	547.5
Potassium [ $\text{K}^+$ ]	333	277.5
Magnesium [ $\text{Mg}^{2+}$ ]	150	125.0
Chloride [ $\text{Cl}^-$ ]	457	381.0

---

For Oscar:

**Table 3:**

Ion levels found in oscar food (mM/kg) and estimated dietary uptake rates based on a 1% daily ration.

---

Ion	Content (mM/kg)	Dietary flux rate ( $\mu\text{M} \cdot \text{kg}^{-1} \cdot \text{h}^{-1}$ )
Calcium [ $\text{Ca}^{2+}$ ]	666	277.5
Sodium [ $\text{Na}^+$ ]	212	88.3
Potassium [ $\text{K}^+$ ]	205	85.4
Magnesium [ $\text{Mg}^{2+}$ ]	115	48.0
Chloride [ $\text{Cl}^-$ ]	53	22.1

---

**Table 4:** Density and apical surface area of the mitochondria-rich cells in fed and starved oscar gills in during normoxia and severe hypoxia (10-20 mmHg).

	Fed fish		Starved fish	
	Normoxia	Hypoxia 3 hrs	Normoxia	Hypoxia 3hrs
MRC number (density) per mm <sup>2</sup> , Filament epithelium, trailing edge	1785 ± 30 a	1112 ± 19 b	1691 ± 24 a	897 ± 15 c
Surface area of apical crypts in filament epithelium, µm <sup>2</sup>	8.09 ± 0.22 a	4.95 ± 0.18 b	5.63 ± 0.13 b	1.98 ± 0.16 c
Surface area occupied by MRC / mm <sup>2</sup> in filament epithelium, %	1.41 ± 0.06 a	0.55 ± 0.03 b	0.94 ± 0.03 a	0.18 ± 0.02 c

- N (number of measurements) for all groups = 20.
- Data represented as means ± s.e.m.
- Means for each category sharing the same letter are not significantly different from one another ( $P \geq 0.05$ ).

For Goldfish:

**Figure 1:** Mean Na<sup>+</sup> uptake rates ( $J_{\text{influx}}^{\text{Na}}$ ) in separate groups of goldfish (n=10) subjected to different levels of hypoxia for 4 h in experiment 1. Values are expressed as means  $\pm$  SEM. Means sharing the same letter are not significantly different from one another at  $P \geq 0.05$ .

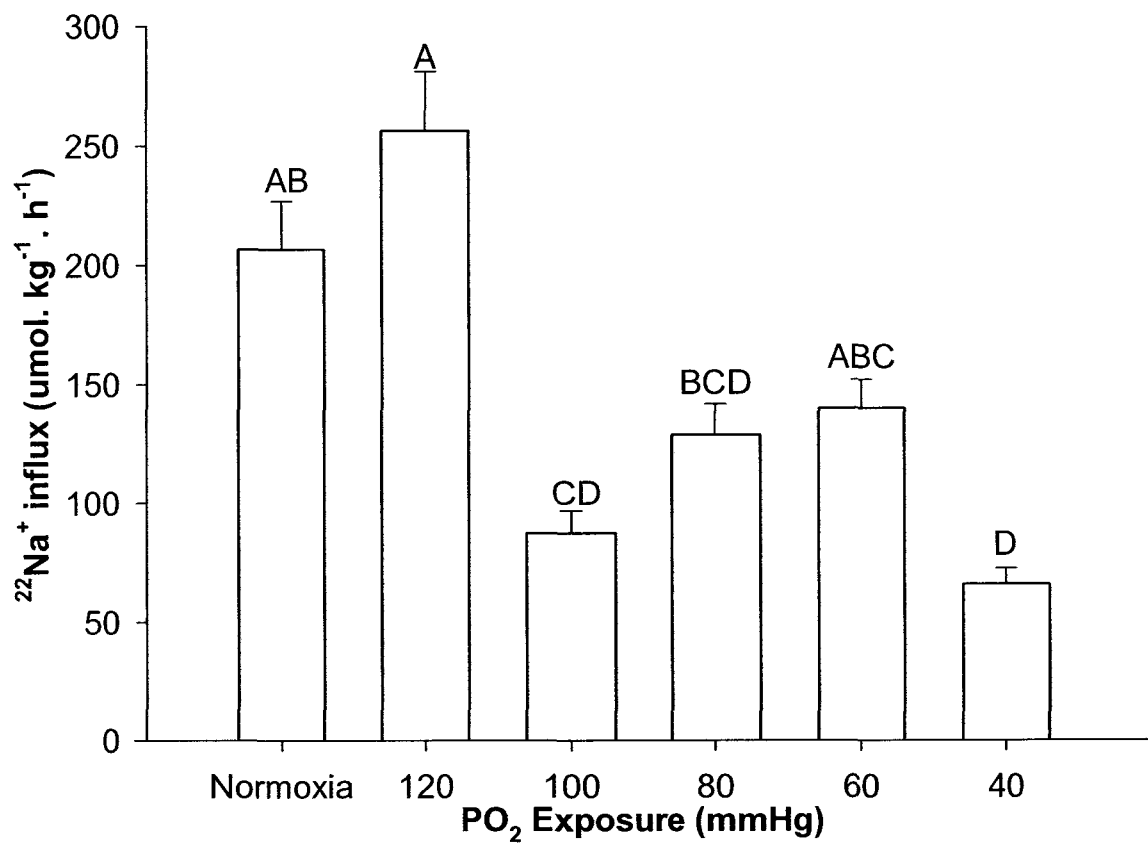


**Figure 2:** Mean Na<sup>+</sup> flux rates of goldfish (N=10 for fed and starved groups) in normoxia or when subjected to an acute induction of either moderate hypoxia (~100 mmHg) or severe hypoxia (~40 mmHg) for 4 h in experiment 2; Na<sup>+</sup> unidirectional influx ( $J_{influx}^{Na}$ , upward bars, clear bars; starved fish, gray bars; fed fish), Na<sup>+</sup> efflux ( $J_{efflux}^{Na}$ , downward bars, clear bars; starved fish, gray bars; fed fish), and Na<sup>+</sup> net flux rates ( $J_{net}^{Na}$ , black bars; starved fish, striped bars; fed fish). Values are expressed as means  $\pm$  SEM. Means sharing the same letter are not significantly different from one another at  $P \geq 0.05$ . The plus sign (+) denotes a significant difference between Na<sup>+</sup> influx/efflux/netflux values for fed and starved fish in a given PO<sub>2</sub> exposure at  $P \leq 0.05$ .

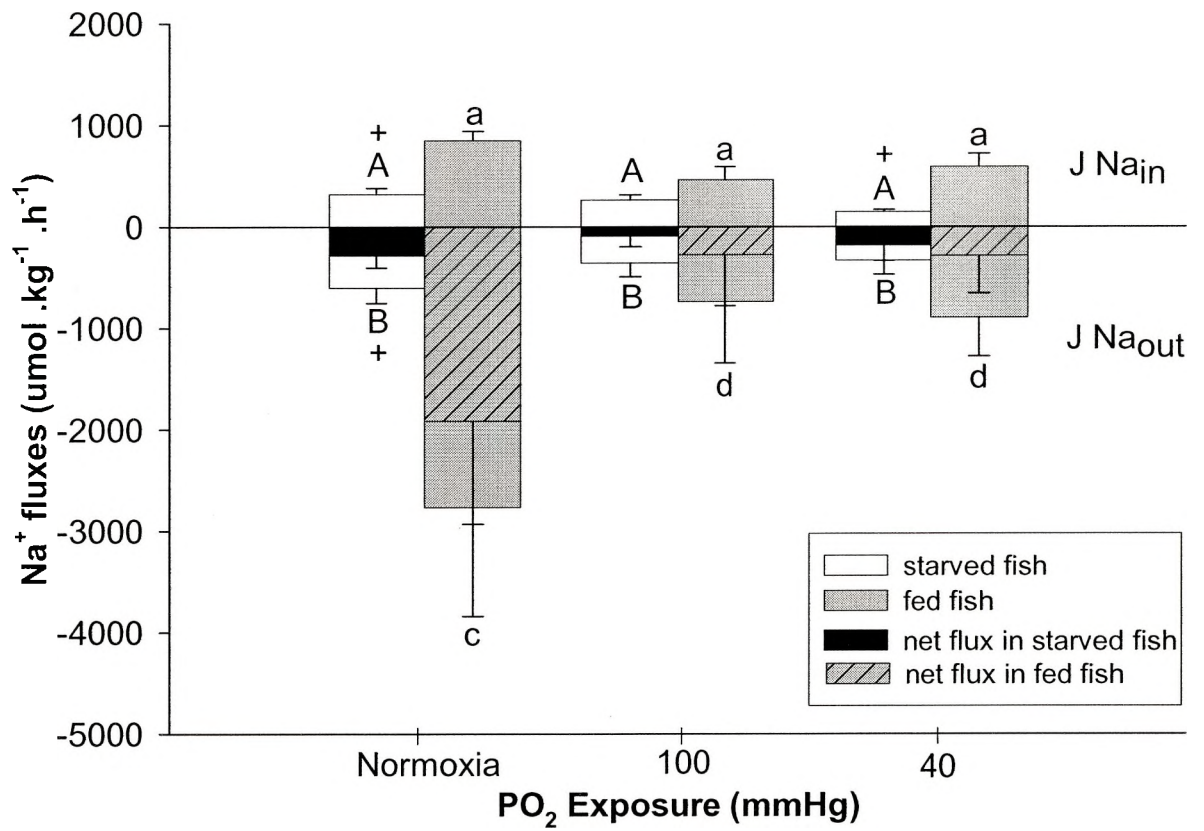


**Figure 3:** Mean ammonia excretion rates of goldfish (N=10) in normoxia or when subjected to an acute induction of either moderate hypoxia (~100 mmHg) or severe hypoxia (~40 mmHg) for 4 h in experiment 2; Starved fish, clear bars; Fed fish, gray bars. Values are expressed as means  $\pm$  SEM. Means sharing the same letter are not significantly different from one another at  $P \geq 0.05$ . The plus sign (+) denotes a significant difference between ammonia excretion values for fed and starved fish in a given PO<sub>2</sub> exposure at  $P \leq 0.05$ .

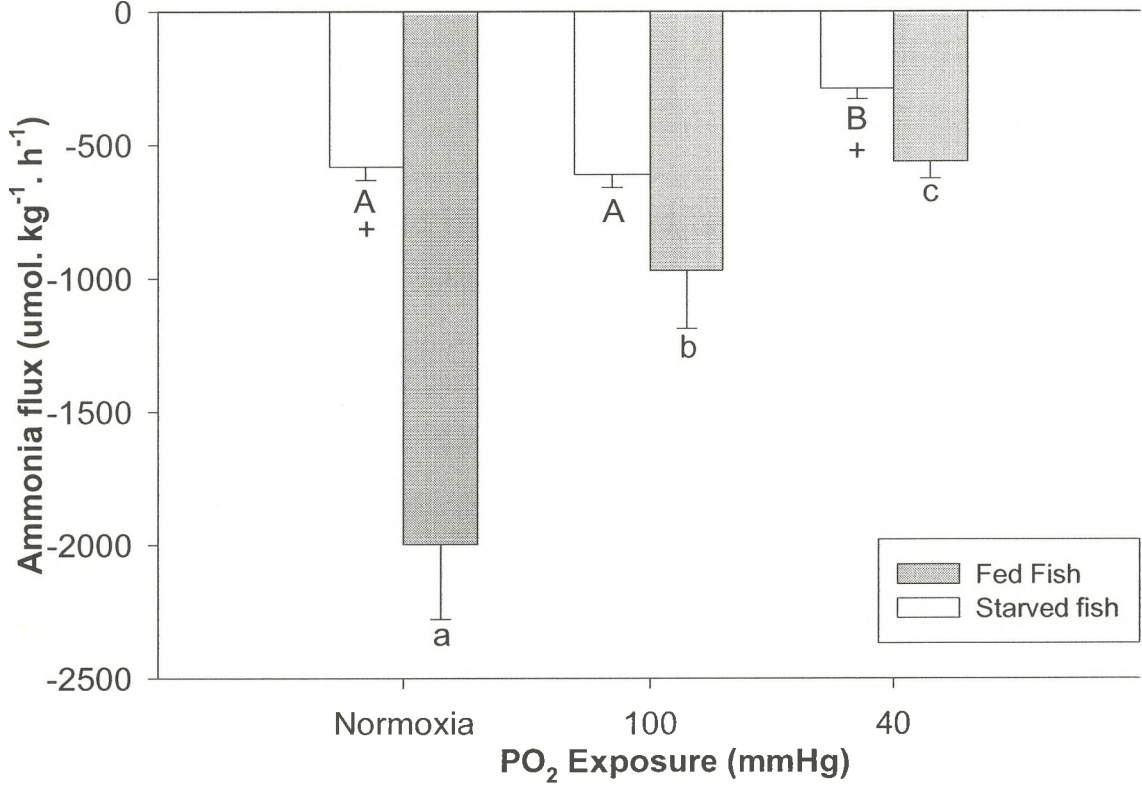


**Figure 4:** Mean potassium ( $K^+$ ) net flux rates of goldfish (N=10) in normoxia or when subjected to an acute induction of either moderate hypoxia (~100 mmHg) or severe hypoxia (~40 mmHg) for 4 h in experiment 2; Starved fish, clear bars; Fed fish, gray bars. Values are expressed as means  $\pm$  SEM. Means sharing the same letter are not significantly different from one another at  $P \geq 0.05$ . The plus sign (+) denotes a significant difference between ammonia excretion values for fed and starved fish in a given  $PO_2$  exposure at  $P \leq 0.05$ .

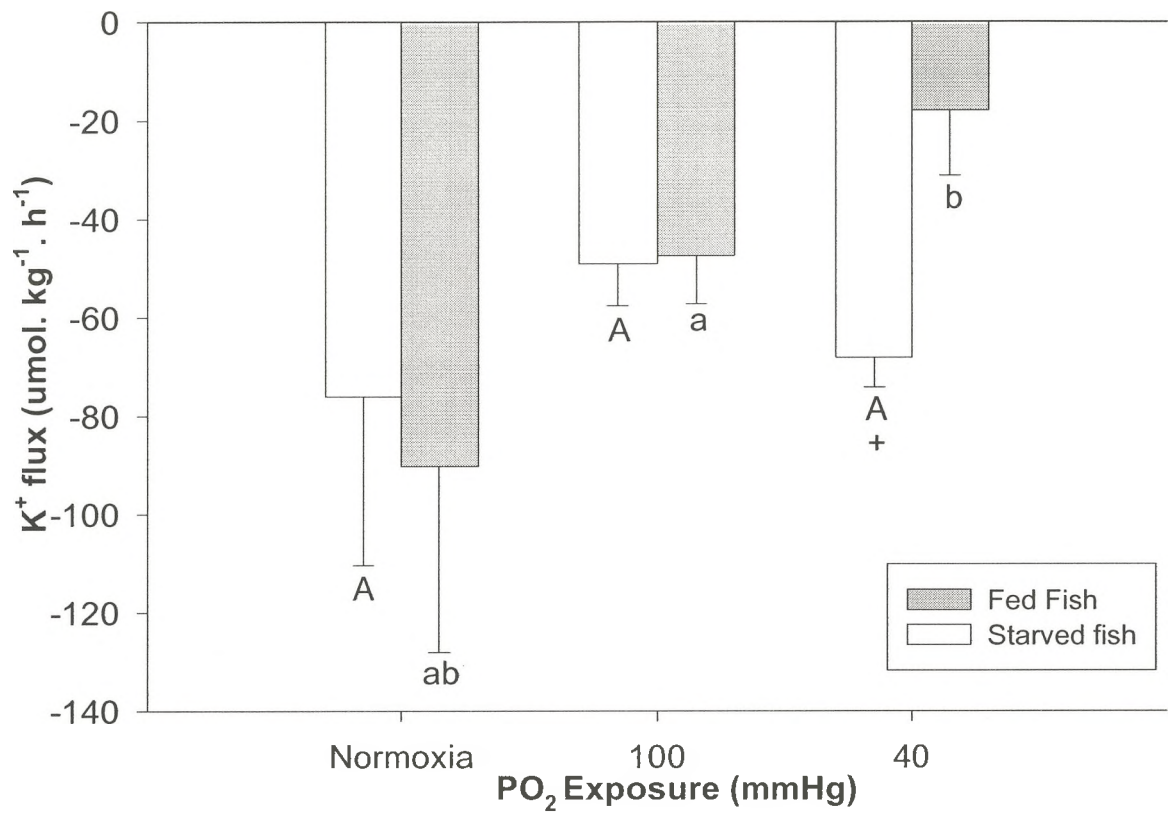
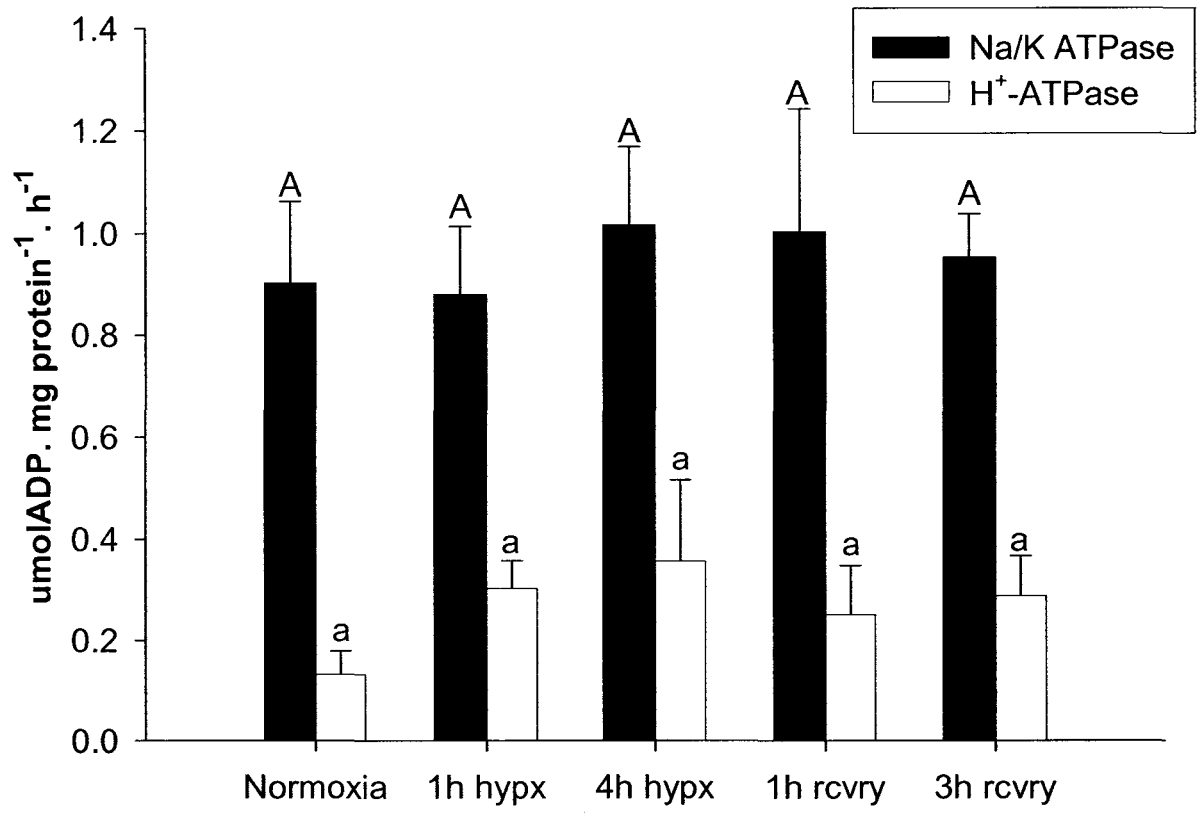


**Figure 5:** Gill Na<sup>+</sup>, K<sup>+</sup>-ATPase and H<sup>+</sup>-ATPase activity changes in goldfish (N=6 per sampling time) in response to acute induction of hypoxia (~40 mmHg) for either 1 h or 4 h followed by normoxic recovery for either 1 h or 3 h in experiment 3. Values are expressed as means ± SEM. Means sharing the same letter of the same case are not significantly different from one another at  $P \geq 0.05$ .



For Oscar:

**Figure 6:** Mean Na<sup>+</sup> flux rates of Amazonian oscar (N=10) subjected to an acute induction of hypoxia (~10-20 mmHg) prolonged for 4 h subsequent to a 3-h normoxic control period in experiment 1 for oscar; Na<sup>+</sup> unidirectional influx ( $J_{influx}^{Na}$ , upward bars, clear bars; starved fish, gray bars; fed fish), Na<sup>+</sup> efflux ( $J_{efflux}^{Na}$ , downward bars, clear bars; starved fish, gray bars; fed fish), and Na<sup>+</sup> net flux rates ( $J_{net}^{Na}$ , black bars; starved fish, striped bars; fed fish) . Values are expressed as means  $\pm$  SEM. Means sharing the same letter are not significantly different from one another and the plus sign (+) denote a significant difference between overall mean values of fed and starved treatments at  $P \leq 0.05$ .

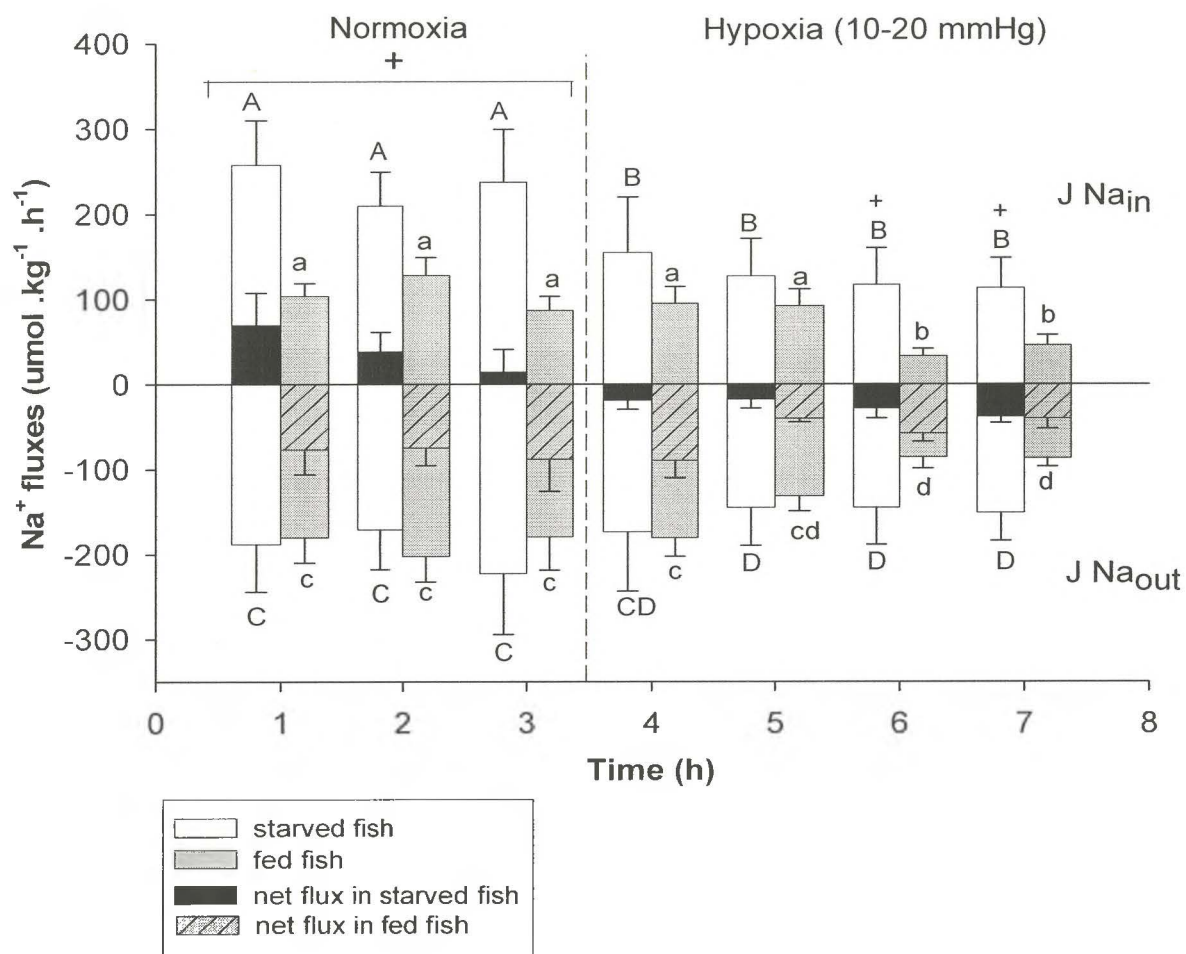


**Figure 7:** Mean ammonia excretion rates of Amazonian oscar (N=10) subjected to acute induction of hypoxia (~10-20 mmHg) prolonged for 4 h subsequent to a 3-h normoxic control period in experiment 1 for oscar; Starved fish, clear bars; Fed fish, gray bars. Values are expressed as means  $\pm$  SEM. Means sharing the same letter are not significantly different from one another and the plus sign (+) denote a significant difference between overall mean values of fed and starved treatments under normoxia at  $P \leq 0.05$ .

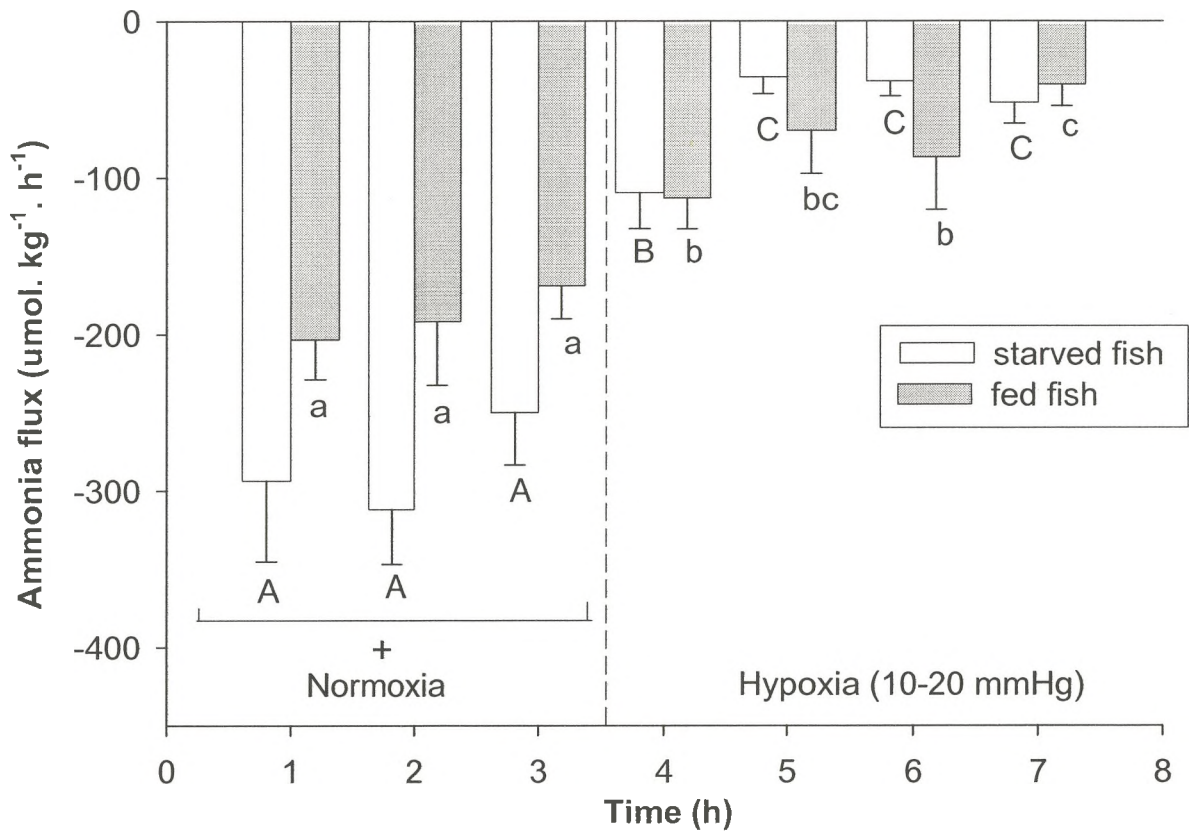


**Figure 8:** Mean potassium ( $K^+$ ) net flux rates of Amazonian oscar (N=10) subjected to acute induction of hypoxia (~10-20 mmHg) prolonged for 4 h subsequent to a 3-h normoxic control period in experiment 1 for oscar; Starved fish, clear bars; Fed fish, gray bars. Values are expressed as means  $\pm$  SEM. Means sharing the same letter are not significantly different from one another and the plus sign (+) denote a significant difference between overall mean values of fed and starved treatments at  $P \leq 0.05$ .

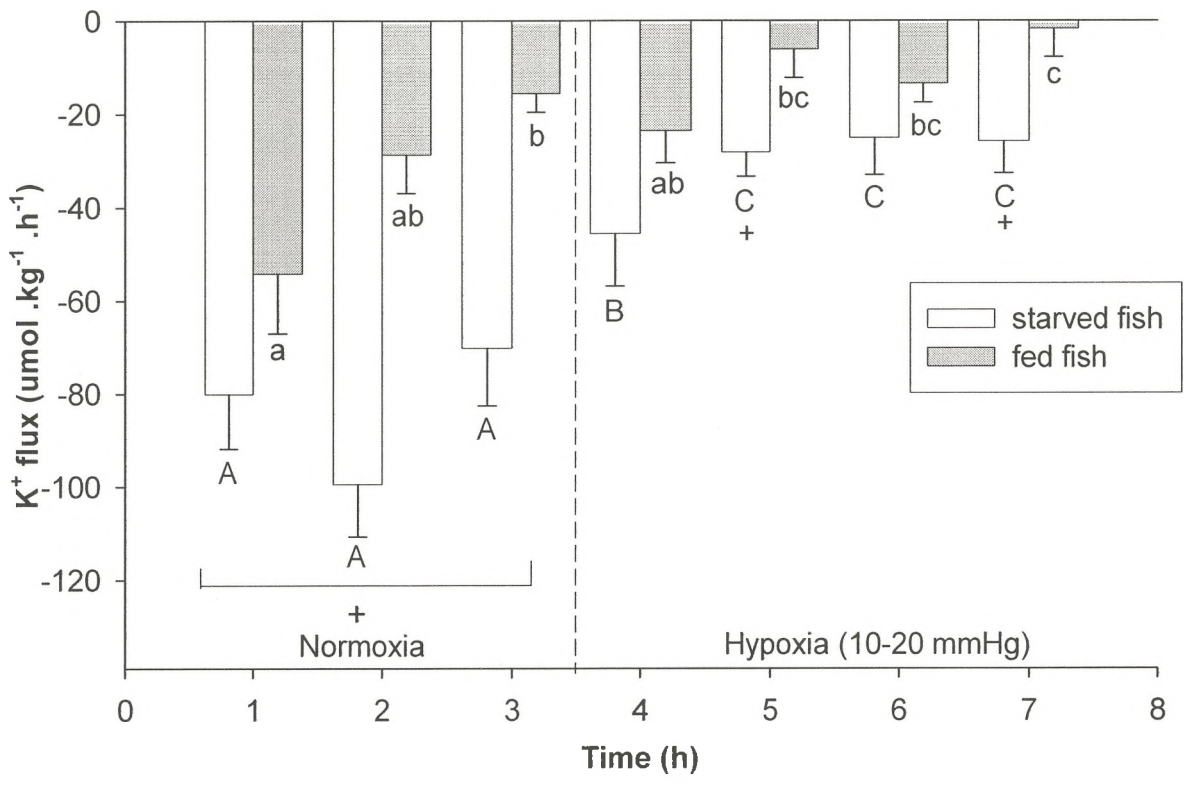


**Figure 9:** Gill Na<sup>+</sup>, K<sup>+</sup>-ATPase and H<sup>+</sup>-ATPase activity changes in fed and starved oscar (N=6 per sampling time) in response to normoxia and acute induction of severe hypoxia (~10-20 mmHg) for 3h in experiment 2 for oscar. Values are expressed as means ± SEM. Means sharing the same letter of the same case are not significantly different from one another at  $P \geq 0.05$ .

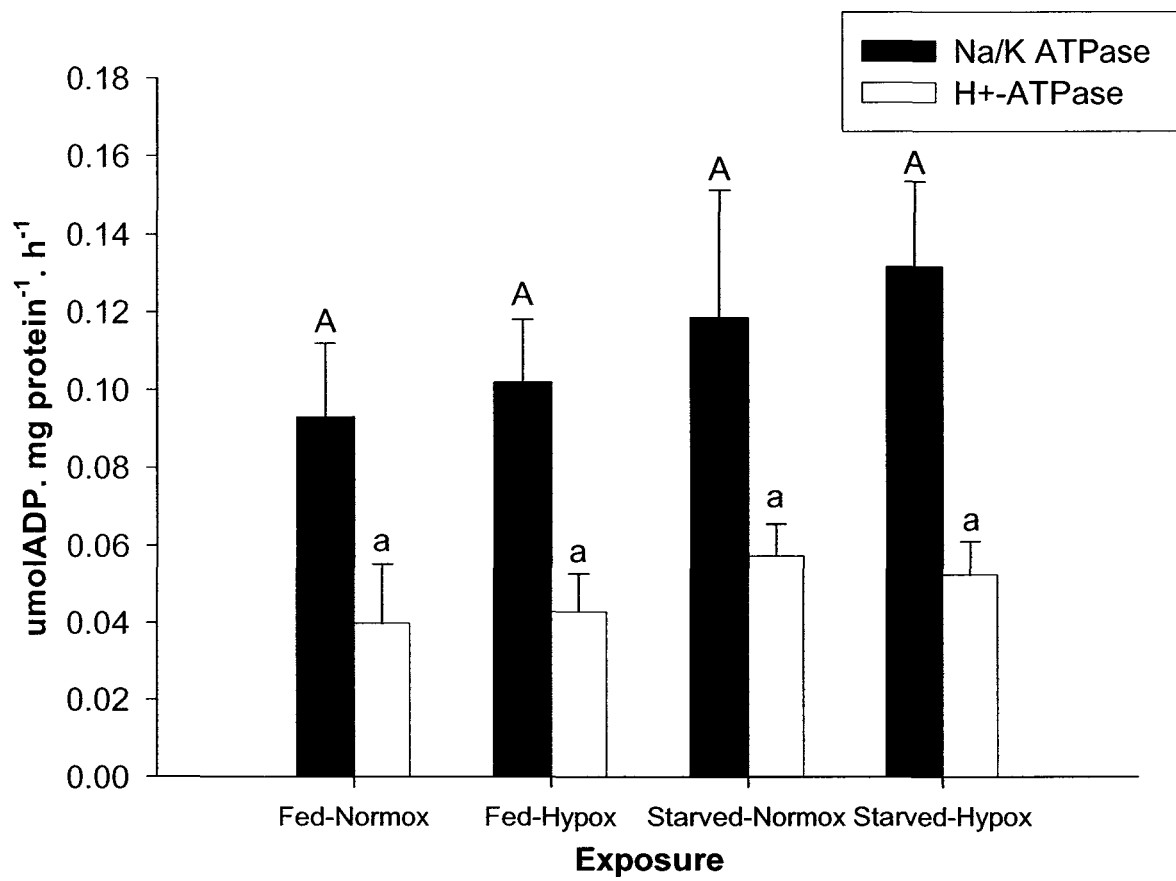


**Figure 10:** Scanning electron micrographs of oscar gills exposed to normoxic conditions.

A- Fed fish: Low resolution of the gill filament and lamellae. Note numerous crypts of mitochondria-rich cells in the filament epithelium and lamellar epithelium.

B- Fed fish. Higher resolution of lamellae displays a large population of mitochondria rich cells with huge apical crypts (arrows) distributed along lamellae and few mucous cells

C- Starved fish (10 d of starvation). Low resolution of the filament and lamellae.

Filament epithelium shows few apical crypts of mitochondria-rich cells (arrows) that remain abundant in the lamellae surface.

D- Starved fish (10 d of starvation). Higher resolution of lamellae shows small apical crypts of mitochondria-rich cells on the surface of lamellar epithelium.

MC-mucous cell. Scale bars: A, C- 50  $\mu\text{m}$ ; B, D- 30  $\mu\text{m}$ .

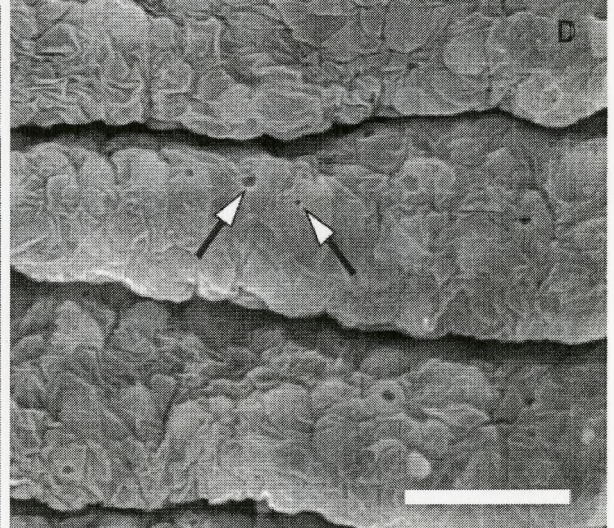
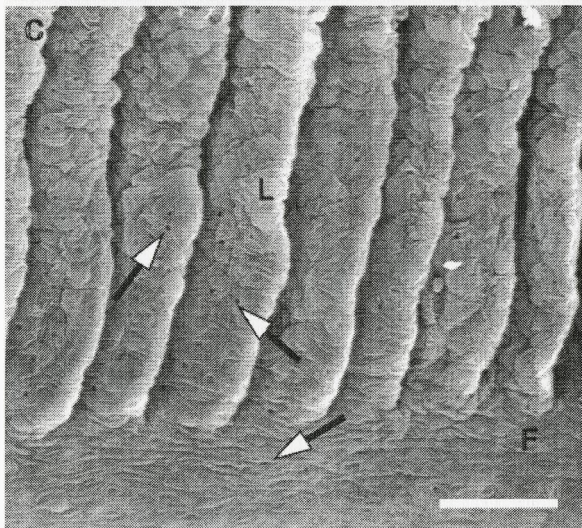
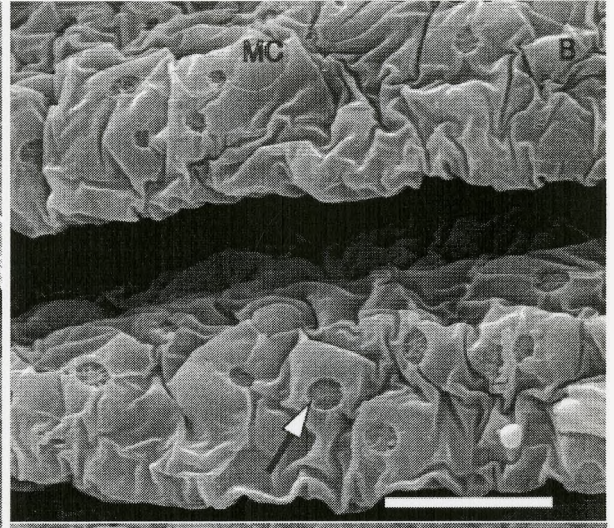
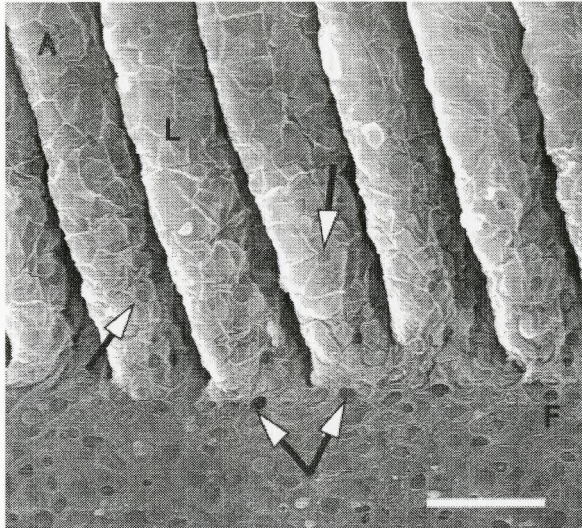


**Figure 11:** Scanning electron micrographs of filament epithelium in fed oscars (A-D) and starved oscars (E-F) exposed to normoxic conditions, control.

A- Fed fish. Trailing edge of filament. Large pavement cells, mucous cells releasing huge globs of secretion and mitochondria-rich cells (arrows) with large apical crypts present in filament epithelium surface.

B, C- Fed fish. Large roughly circular and flat apical crypts of MRCs with a fence-like surface structure composing of interdigitated and fused microplacae.

D- Cluster of MRCs, common in the interlamellar areas of filament epithelium.

E- Starved fish. Trailing edge of filament. Note alterations in the PVCs surface pattern, small crypts of MRCs and few MCs.

F- Starved fish. Slightly concave apical crypt of the MRC. Note its irregular shape, smaller size compare to C-D, and more simple arrangement of "fence"-like surface structure.

PVC- pavement cells. Scale bars: A, E- 10  $\mu\text{m}$ ; B-D,F- 2  $\mu\text{m}$ .

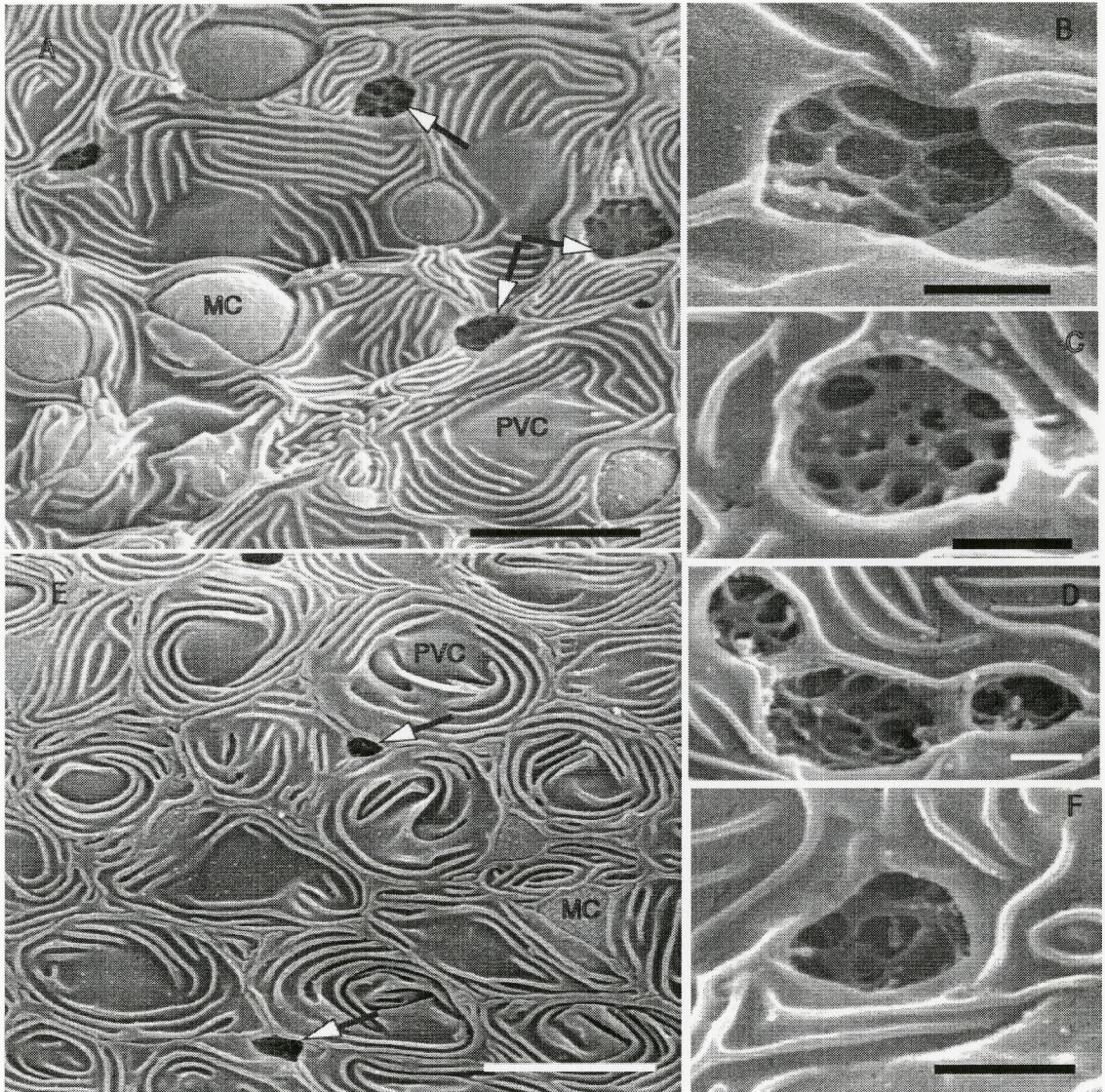


**Figure 12:** Scanning electron micrographs of oscar gills exposed to 3h hypoxia.

A- Fed fish. Low resolution of filament and lamellae. Note small apical crypts of MRCs in filament epithelium surface and no visible MRCs in the lamellar epithelium.

B- Starved fish. Trailing edge of filament. Low resolution of filament and lamellae. Few small MRC apical crypts in filament epithelium, mostly at the lamellae base. No MRCs found on the surface of lamellar epithelium.

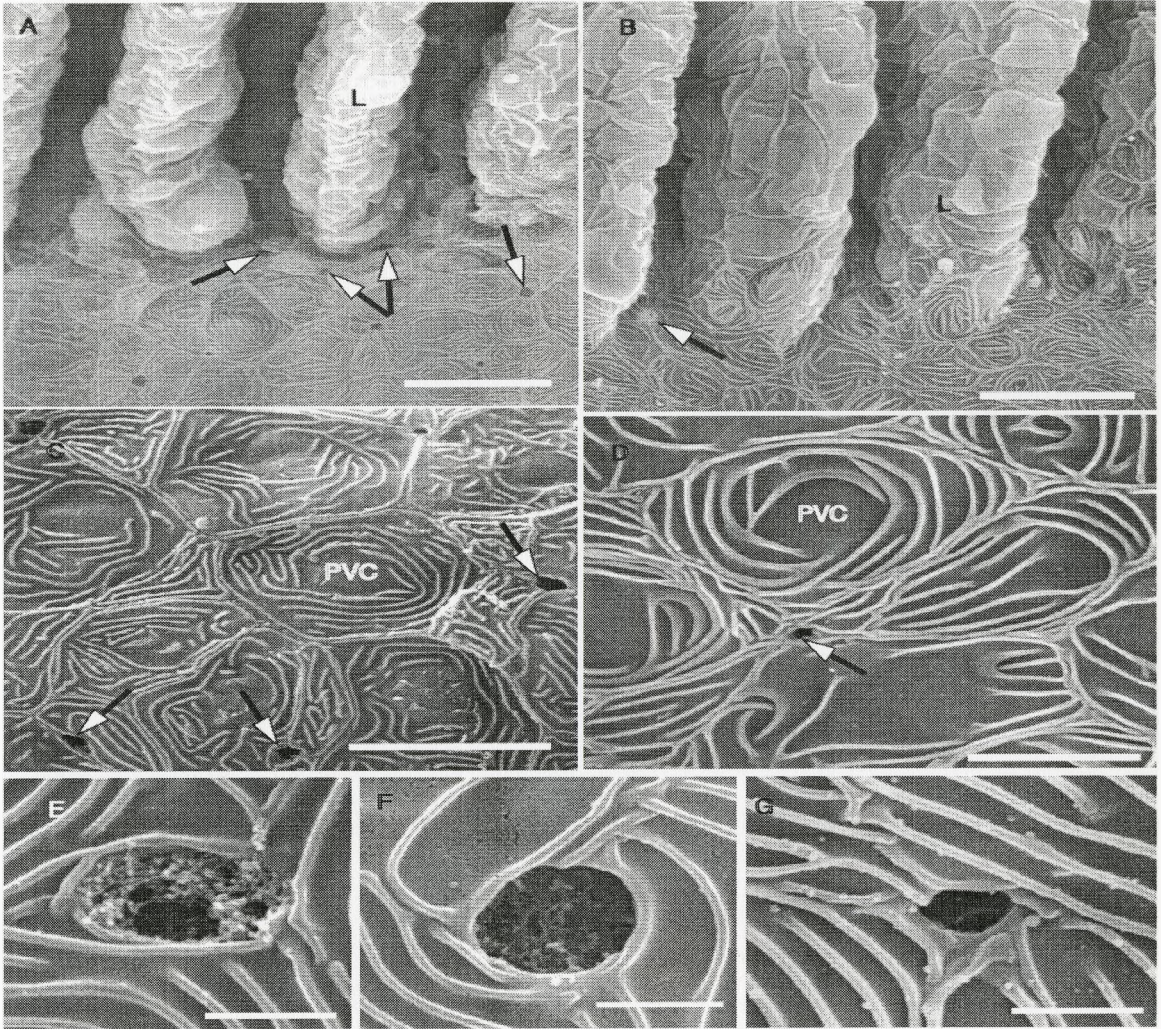
C, D- High magnification of filament epithelium in fed and starved fish, respectively.

Note characteristic topology of PVCs and shape and size of apical crypts of MRCs.

E, F- Fed fish. Highly concave MRC apical crypt masked by mucus. Note reduction of MRC surface area compare to control.

G- Starved fish. Deeply invaginated apical crypt of MRC. Note irregular shape of the crypt and dramatic reduction of its surface compare to control.

Scale bars: A, B- 25  $\mu\text{m}$ ; C, D- 10  $\mu\text{m}$ ; E- G- 2  $\mu\text{m}$ .



## **CHAPTER 4**

### **General Summary and Conclusions**

The focus of this thesis was to examine the relationship between ion and gas exchange at the branchial epithelium of freshwater fish and its regulatory adaptation under hypoxia. A species-specific approach was utilized where general ionoregulatory responses to hypoxia were examined in rainbow trout (*Oncorhynchus mykiss*, a hypoxia-intolerant freshwater fish), as well as their regulation in two hypoxia-tolerant species (the goldfish *Carassius auratus* and the Amazonian oscar *Astronotus ocellatus*) to understand possible intra-specific differences. We measured fluxes across the whole animal assuming the gills to be the predominant site of exchange in freshwater fish. We mainly focused on the exchange of  $\text{Na}^+$  across the gill epithelium, but further examined the loss of  $\text{K}^+$ , ammonia excretion and the cellular and morphological alterations of the gill to fully comprehend the osmorepiratory compromise during hypoxia. In addition, in the latter two species, the dual stress situation of hypoxia plus feeding was explored.

#### *The Osmorepiratory Compromise during Hypoxia:*

In chapter 2, an initial experiment with juvenile trout served to demonstrate that the compromise does occur in this species (Fig. 1 of Chapter 2). However, in light of well-known differences in hypoxia tolerance between juvenile and adult teleosts (see Sloman et al., 2006 for discussion), our further detailed analyses were largely restricted to the latter. Our results indicated that environmental hypoxia induces changes in gill ionoregulatory function in the freshwater adult rainbow trout, the direction and magnitude of which vary with both the extent and duration of the hypoxia regime. The

tridirectional nature of the changes over time suggested a more complex set of responses in this hypoxia-intolerant species, compared to those previously reported in the hypoxia-tolerant Amazonian oscar (Wood et al., 2007). In chapter 3, we were able to confirm these previously-documented responses in the oscar. We were also able to demonstrate that the compromise occurs in a similar fashion in the goldfish as in the oscar, therefore verifying our first goal with respect to goldfish. Overall, our results indicate that environmental hypoxia induces changes in gill ionoregulatory function in both the goldfish and oscar by suppressing both active ion uptake and passive ion efflux, while allowing approximate maintenance of net ion balance.

*The effects of feeding on the osmorepiratory compromise during hypoxia:*

Although both the goldfish and oscar clearly exhibit the osmorepiratory compromise during severe hypoxia, the effects of feeding on this phenomenon differed between goldfish and oscar (Chapter 3). Normoxic fed goldfish generally exhibited greater rates of unidirectional  $\text{Na}^+$  fluxes, compared to starved goldfish. With moderate and severe hypoxia, fed fish significantly depressed  $J_{\text{efflux}}^{\text{Na}}$  rates, however  $J_{\text{influx}}^{\text{Na}}$  rates were not significantly reduced. In contrast, starved goldfish displayed no depression in unidirectional  $\text{Na}^+$  fluxes with severe hypoxia. Differences between fed and starved oscar were generally opposite to those in goldfish, and changes during hypoxia were more apparent compared to goldfish. During normoxia, fed oscars had lower  $J_{\text{influx}}^{\text{Na}}$  rates compared to starved fish. With severe hypoxia, although both fed and starved fish depressed their unidirectional  $\text{Na}^+$  fluxes, the reductions in starved fish were greater and occurred more rapidly. The lower availability of ions in the ion-poor Amazonian

softwater of the oscar, relative to ion-rich hardwater normally inhabited by the goldfish, may explain this difference. Starved oscars must rely more on the waterborne source during normoxia, and are under greater pressure to conserve ions by turning down gill permeability during hypoxia.

*The Impact of Hypoxia at the Gill Ionocytes:*

To understand hypoxic effects at the cellular level, we examined the activity of  $\text{Na}^+/\text{K}^+$ -ATPase and  $\text{H}^+$ -ATPase pumps in all three species. We expected a downregulation of these pump activities so as to conserve ATP in a situation where oxidative phosphorylation is slowed down by oxygen limitation during hypoxia (Boutilier and St. Pierre, 2000). Indeed, many previous reviews indicate that absolute downregulation of ATP pumps occurs when animals are subjected to anoxic conditions and/or face very severe oxygen lack (Hochachka, 1986; Boutilier and St. Pierre, 2000; Hochachka and Lutz, 2001). In contrast to our prediction, we found no change in the activity of these pumps with 4 h of hypoxic exposure in rainbow trout (Fig. 8 of Chapter 2). However, our measurements were of enzyme capacities under optimal conditions *in vitro* where ATP was not limiting, in contrast to the situation during hypoxia *in vivo*.

Branchial  $\text{Na}^+/\text{K}^+$ -ATPase and  $\text{H}^+$ -ATPase activity in goldfish also did not change with acute hypoxia (4 h), and we found no further change in the activity of these pumps with normoxic recovery (Fig. 5 of Chapter 3). Furthermore, there were no apparent changes in branchial  $\text{Na}^+/\text{K}^+$ -ATPase and  $\text{H}^+$ -ATPase activity levels of either fed or starved oscars in response to acute (3 h) hypoxic exposure (Fig X? of Chapter 3).

This was in contrast to previous studies on the branchial  $\text{Na}^+/\text{K}^+$  ATPase activity in the oscar (Richards et al, 2007; Wood et al., 2007), where there was a downregulation in absolute activity of this enzyme with 3-4h of similar hypoxic exposure. The reason for this difference, at least in the oscar, remains unexplained.

We also examined net  $\text{K}^+$  loss rates to the water in trout (Fig. 6 of Chapter 2), starved and fed goldfish (Fig. 4 of Chapter 3) and starved and fed oscar (Fig. 8 of Chapter 3) to understand if gill cells were facing cellular distress under hypoxia (Boutilier, 2001). Interestingly, net  $\text{K}^+$  loss rates to the water approximately doubled in trout with prolonged hypoxia, a significant increase compared to normoxic levels (Fig. 6 of Chapter 2). Cells are believed to lose intracellular  $\text{K}^+$  when the  $\text{Na}^+/\text{K}^+$ -ATPase pump begins to fail with oxygen deprivation (Boutilier and St. Pierre, 2000). This suggests that *in vivo*, ATP limitation may impact  $\text{Na}^+/\text{K}^+$ -ATPase activity during moderate hypoxia in trout, even though there was no change in enzymatic capacity (Fig. 8 of Chapter 2).

In goldfish, starved fish continuously excreted  $\text{K}^+$  to the water even under severe hypoxia at rates comparable to normoxic levels (Fig. 4 of Chapter 3). We believe this constant loss of  $\text{K}^+$  to the water by starved goldfish (Fig. 4) are baseline levels of  $\text{K}^+$  loss that likely occur in starved fish due to the ‘consumption’ of body mass during starvation. Fed goldfish exhibited a greater  $\text{K}^+$  loss than starved fish during normoxia (Fig. 4 of Chapter 3) and we attribute this higher loss rate due to the excess  $\text{K}^+$  they obtained from their diet (Table 2 of Chapter 3). The significant decrease observed in  $\text{K}^+$  loss in fed goldfish with severe hypoxia can be attributed to overall depression in gill permeability. In comparison, starved oscars lost more  $\text{K}^+$  to the water than did fed fish during

normoxia, but this loss was suppressed with hypoxia (Fig. 8 of Chapter 3). This greater  $K^+$  loss by starved oscars under normoxia could also be attributed to ‘consumption’ of body mass occurring in these fish. Potassium is the major cation of intracellular fluid, and is an essential nutrient to fish via diet. It is required for glycogen and protein synthesis, and further for metabolic breakdown of glucose (Lovell, 1998). Therefore, fed oscars could be utilizing the considerable amount of  $K^+$  available from their food (Table 4 of Chapter 3) for growth and tissue synthesis instead of excreting it to the water. Fed oscars had lower  $K^+$  loss rates to the water and this excretion was suppressed with hypoxia (Fig. 8 of Chapter 3). Starved oscars were also effective in conserving  $K^+$  during acute hypoxia by rapidly turning down branchial loss rates. In this respect, both fed and starved oscars appeared to be indifferent to hypoxic distress at gill ionocytes, and this is further supported by a study by Scott et al., (2008) which found no evidence of  $O_2$  limitation in gill epithelial cells of oscars under comparable levels of severe hypoxia..

#### *Hypoxia-induced Changes in Gill Morphology:*

We examined morphological changes in the trout gill epithelium during hypoxia utilizing SEM (Fig. 9-13 of Chapter 2). With 1 h hypoxic exposure, there were immediate alterations in the cellular composition of the surface of filament epithelium. Density and surface area of MRCs increased (Fig. 13 A-B of Chapter 2), correlating with increased unidirectional  $Na^+$  fluxes at this time (Fig. 4 of Chapter 2). It is known that in teleost fishes, some MRCs are located just beneath the leaf-like PVCs (Wilson and Laurent, 2002) and are usually not visible by SEM. With hypoxic exposure it was thought that the “hidden” MRCs covered by PVCs become dilated and push out the PVCs that covered

them, exposing their apical openings to the environment. After a 4 h hypoxic exposure, MRCs became less numerous and displayed smaller surface areas (Fig. 13 A, B of Chapter 2), though percentage of the filament surface occupied by exposed MRCs was still greater than under normoxia (Fig 13C). This may correlate with the fact that  $\text{Na}^+$  fluxes were not reduced (Fig. 4 of Chapter 2), in contrast to the situation in oscars (Fig. 6 of Chapter 3). We propose that when MRCs decrease their volume and their apical exposures display a flatter appearance, the PVCs become more protracted and are able to cover part of the MRCs on the epithelial surface. During normoxic recovery, we see the re-emergence of MRC clusters that still have an enlarged apical surface (Fig. 12 and of Chapter 2).

We further investigated if gill morphology of the hypoxia-tolerant oscar changed under severe hypoxia and if feeding status influenced this change. During normoxia, both fed and starved oscars had a high density of MRCs in both the gill filament and lamellar epithelia (Fig. 10 A, fed fish; Figs. 10 C, D, starved fish; Table 4 of Chapter 3). Comparatively, in the rainbow trout, normoxic MRC density on the trailing edge of the gill filament, surface area of apical crypts and percentage of surface area occupied by MRCs in the filamental epithelium were all considerably higher than in the oscar (Fig. 13 A-C of Chapter 2). Fed oscar displayed apical crypts with larger individual surface areas compared to starved fish (Fig. 11 A-D, fed fish; Fig. 11 E-F, starved fish; Table 4 of Chapter 3). With 3-h of severe hypoxic exposure, there were substantial reductions in the number, average surface area and percentage of surface area of the filament occupied by the apical crypts of MRCs exposed to ambient water in both fed and starved oscar (Fig.

12 A-F; Table 3 of Chapter 3). This correlated well with the observed reductions in gill ion fluxes at this time (Fig. 6 of Chapter 3). We suggest that this change occurred in oscar because with severe hypoxia MRCs must shrink and are covered over by pavement cells, therefore reducing their exposure to the ambient hypoxic water. This serves as an important mechanism for the conservation of valuable ions.

*Ammonia Excretion during Hypoxia:*

Waste excretion in fish are mainly composed of two nitrogenous end products; ammonia-N and urea-N, where ammonia is the major end product composing ~70% of total waste in freshwater species and is excreted mainly at the gills (Van Waarde, 1983; Wood, 2001). We observed no significant changes in mass-specific ammonia excretion rates in trout in response to acute 4-h hypoxic conditions (Fig. 3 of Chapter 2).

Contrastingly, during times of stress (eg; exercise) trout are shown to increase ammonia production and efflux rates (Wood, 2001). Compared to the initial 4 h hypoxic exposure, an 8-h prolonged and slightly more severe hypoxia was anticipated to be more stressful and was predicted to elevate ammonia excretion, although this observed elevation was not significant (Fig. 5 of Chapter 2).

Mass-specific ammonia excretion rates in starved and fed goldfish under moderate and severe hypoxia were examined (Fig. 3 of Chapter 3). During normoxia and severe hypoxia, fed goldfish excreted significantly more ammonia to the water compared to starved goldfish (Fig. 3). This was expected as in general fed teleost fish have a much higher excretion of nitrogenous wastes compared with fasted fish (Wood, 2001). With

severe hypoxia, both starved and fed goldfish depressed their ammonia excretion to the water (Fig. 3 of Chapter 3). Previous studies have found no change in ammonia production (therefore protein breakdown) in goldfish exposed to severe hypoxia (van Waversveld et al., 1989). In our study we might be seeing a situation where although ammonia production is not influenced, absolute ammonia excretion to the water may be suppressed with severe hypoxia due to reduced gill permeability. In oscar, a different, albeit novel situation was observed. Fed fish of this species excreted less ammonia to the water compared to starved fish during normoxia (Fig. 7 of Chapter 3). It could be inferred that fed oscars probably still use protein as a metabolic fuel source to a limited extent, but allocate the majority of their protein intake for muscle growth and maintenance, thereby minimizing ammonia production and excretion (Wood, 2001; Kajimura et al., 2004; Iftikar et al., 2008). As observed in goldfish, both fed and starved oscar immediately depressed their ammonia excretion to the water with the onset of severe hypoxia due to general reductions in gill permeability brought on by severe hypoxic exposure as reported previously for this species (Fig. 7 of Chapter 3; Wood et al., 2007).

*Conclusion:*

In the rainbow trout (Chapter 2), we suggest that the osmorepiratory compromise has a different manifestation during hypoxia than during exercise. There seems to be a host of factors that have complex influences on the osmorepiratory compromise during hypoxia where several competing aspects such as alterations in blood flow patterns, exchange diffusion, acid-base status, and branchial ionocyte morphology take place during hypoxia in this species, all influencing effective gill permeability and ion

exchange rates. In both goldfish and oscar, there were clear reductions in gill permeability, ion exchange rates, and ammonia excretion rates in response to severe hypoxia regardless of feeding regime, rather different from the complex patterns seen in the hypoxia-intolerant trout. However, the effects of feeding on this phenomenon differed between these two hypoxia-tolerant species. Differences in ion concentrations in the waters (ion-poor Amazonian water versus ion-rich hardwater) normally inhabited by these species may account for these differences due to feeding/starvation between oscars and goldfish.

**Literature Cited (For Chapters' 1 and 4):**

Ali, M. A. 1980. Introduction. In *Environmental Physiology of Fishes*. Eds. M. A. Ali, pp 3-7. Plenum Press: New York.

Almeida-Val, V. M. F., Val, A. L., Duncan, W. P., Souza, F. C. A., Paula-Silva, M. N. and Land, S. 2000. Scaling effects on hypoxia tolerance in the Amazonian fish *Astronotus ocellatus* (Perciformes: Cichlidae): contribution of tissue enzyme levels. *Comp. Biochem. Physiol. B.* 125: 219-226.

Booth, J.H. 1979. The effect of oxygen supply, epinephrine, and acetylcholine on the distribution of blood flow in trout gills. *J Exp Biol* 83:31-39.

Boutilier, R. G. and St-Pierre, J. 2000. Surviving hypoxia without really dying. *Comp. Biochem. Physiol.* 126: 481-490.

Boutilier, R. G. 2001. Mechanisms of cell survival in hypoxia and hypothermia. *J. Exp. Biol.* 204: 3171-3181.

Evans, D. H., Piermarini, P. M. and Choe, K. P. 2005. The multifunctional fish gill: dominant site of gas exchange, osmoregulation, acid-base regulation, and excretion of nitrogenous waste. *Physiol. Rev.* 85: 97-177.

Farrel, A. P., Sobin, S. S., Randall, D. J. and Crosby, S. 1980. Intralamellar blood flow in fish gills. *Am. J. Physiol.* 239: 428-436.

Gonzalez, R. J. and McDonald, D. G. 1992. The relationship between oxygen consumption and ion loss in a freshwater fish. *J. Exp. Biol.* 163: 317-332.

Gonzalez, R. J. and McDonald, D. G. 1994. The relationship between oxygen uptake and ion loss in fish from diverse habitats. *J. Exp. Biol.* 190: 95-108.

Graham, J. B. 2006. Aquatic and Aerial Respiration. In *The Physiology of Fishes*. Eds. D. H. Evans and J. B. Claireborne, pp 85-119. CRC Press: Florida.

Hochachka, P. W. 1986. Defence strategies against hypoxia and hypothermia. *Science*. 231: 234-241.

Hochachka, P. W. and Lutz, P. L. 2001. Mechanism, origin, and evolution of anoxia tolerance in animals. *Comp Biochem Physiol B* 130:435–459.

Holeton, G. F. and Randall, D. J. 1967*a*. Changes in blood pressure in the rainbow trout during hypoxia. *J. Exp. Biol.* 46: 297-305.

Holeton, G. F. and Randall, D. J. 1967*b*. The effect of hypoxia on the partial pressures of gases in the blood and water afferent and efferent to the gills of rainbow trout. *J. Exp. Biol.* 46: 317-327.

Iftikar, F.I., Patel, M., Ip, Y.K., Wood, C.M. 2008. The influence of feeding on aerial and aquatic oxygen consumption, nitrogenous waste excretion, and metabolic fuel usage in the African lungfish *Protopterus annectens*. *Can. J. Zool.* 86: 790-800.

Isaia, J. 1984. Water and Nonelectrolyte Permeation. In *Fish Physiology*. Eds. W. S. Hoar and D. J. Randall, Vol X, pp1-31. Academic Press: Orlando.

Kajimura, M., Croke, S. J., Glover, C. N., and Wood, C. M. 2004. Dogmas and controversies in the handling of nitrogenous wastes: The effect of feeding and fasting on

the excretion of ammonia, urea and other nitrogenous waste products in rainbow trout. *J. Exp. Biol.* 207: 1993-2000.

Lovell, T. 1998. Digestion and Metabolism. In *Nutrition and Feeding of Fish*. Eds. T. Lovell, pp 71-89. Springer: New York.

Muusze, B., Marcon, J., van den Thillart, G. and Almeida-Val, V. M. F. 1998. Hypoxia tolerance of Amazon fish. Respirometry and energy metabolism of the cichlid *Astronotus ocellatus*. *Comp. Biochem. Physiol. A.* 120:151-156.

Nikinmaa, M. AND Soivio, A. 1982. Blood oxygen transport of hypoxic *Salmo gairdneri*. *J. Exp. Biol.* 219:173-178.

Nikinmaa, M. and Rees, B. B. 2005. Oxygen-dependent gene expression in fishes. *Am. J. Physiol. Regul. Integr. Comp. Physiol.* 288: R1079-R1090.

Nilsson, S. 1986. Control of gill blood flow. In *Fish Physiology: Recent Advances*. Eds. S. Nilsson and S. Holmgren, pp 87-101. London: Croom Helm.

Perry, S. F. and Reid, S. G. 1992. Relationships between blood oxygen content and catecholamine levels during hypoxia in rainbow trout and American eel. *Am J Physiol* 263:R240–249.

Randall, D. J., Baumgarten, D. and Malyusz, M. 1972. The relationship between gas and ion transfer across the gills of fishes. *Comp. Biochem. Physiol. A.* 41: 629-637.

Reid, S. G. and Perry, S. F. 2003. Peripheral O<sub>2</sub> chemoreceptors mediate humoral catecholamine secretion from fish chromaffin cells. *Am J Physiol Regul Integr Comp Physiol* 284: R990–R999.

Richards, J. G., Semple, J. W., Bystriansky, J. S. and Schulte, P. M. 2003. Na<sup>+</sup>/K<sup>+</sup>-ATPase  $\alpha$ -isoform switching in gills of rainbow trout (*Oncorhynchus mykiss*) during salinity transfer. *J. Exp. Biol.* 206: 4475-4486.

Sloman, K. A., Wood, C. M., Scott, G. R. Wood, S., Kajimura, K., Johannsson, O. E., Almeida-Val, V. M. F. and Val, A. L. 2006. Tribute to R.G. Boutilier: The effect of size on the physiological and behavioural responses of oscar, *Astronotus ocellatus*, to hypoxia. *J Exp Biol* 209:1197-1205.

Smith, H. W. 1932. Water regulation and its evolution in the fishes. *Q. Rev. Biol.* 7: 1-26.

Smith, N. F., Talbot, C. and Eddy, F. B. 1989. Dietary salt intake and its relevance to ionic regulation in freshwater salmonids. *J. Fish. Biol.* 35: 749-753.

Soivio, A. and Tuurula, H. 1981. Structural and circulatory responses to hypoxia in the secondary lamellae of *Salmo gairdneri* gills at two temperatures. *J. Comp. Phys.* 145:37-43.

Sundin, L. and Nilsson, G. E. 1997. Neurochemical mechanisms behind gill microcirculatory responses to hypoxia in trout: in vivo microscopy study. *Am. J. Physiol.* 272: 576-585.

Thomas, S., Fievet, B. and Motais, R. 1986. Effect of deep hypoxia on acid-base balance in trout: role of ion transfer processes. *Am J Physiol Regul Integr Comp Physiol* 250:R319-R327.

van Waarde, A. 1983. Aerobic and anaerobic ammonia production by fish. *Comp. Biochem. Physiol. B.* 74: 675-684.

van Waversveld, J., Addink, A. D. F. and van den Thillart, G. 1989. The anaerobic energy metabolism of goldfish determined by simultaneous direct and indirect calorimetry during anoxia and hypoxia. *J. Comp. Physiol. B.* 159: 263-268.

Wilson, J. M. and Laurent, P. 2002. Fish gill morphology: inside out. *J. Exp. Zool.* 293: 192-213.

Wood, C. M. and Randall, D. J. 1973a. The influence of swimming activity on sodium balance in the rainbow trout (*Salmo gairdneri*). *J. Comp. Physiol.* 82: 207-233.

Wood, C. M. and Randall, D. J. 1973b. Sodium balance in the rainbow trout (*Salmo gairdneri*) during extended exercise. *J. Comp. Physiol.* 82: 235-256.

Wood, C. M. and Randall, D. J. 1973c. The influence of swimming activity on water balance in the rainbow trout (*Salmo gairdneri*). *J. Comp. Physiol.* 82: 257-276.

Wood, C. M. 2001. The influence of feeding, exercise, and temperature on nitrogen metabolism and excretion. In *Fish Physiology*. Eds. P. A. Anderson and P. A. Wright, Vol XX, pp 201-238. Academic Press: Orlando.

Wood, C. M., Kajimura, M., Sloman, K. A., Scott, G. R., Walsh, P.J., Almeida-Val, V. M. F. and Val, A. L. 2007. Rapid regulation of Na<sup>+</sup> fluxes and ammonia excretion in response to acute environmental hypoxia in the Amazonian oscar, *Astronotus ocellatus*. *Am. J. Physiol. Regul. Integr. Comp. Physiol.* 292: 2048-2058.

Wood, S. C. and Johansen, K. 1973 b. Organic phosphate metabolism in nucleated red cells: Influence of hypoxia on the HbO affinity. *Neth. J. Sea. Res.* 7:328-338.